THE ELECTROCHEMICAL SOCIETY

ENLARGED ABSTRACTS
of Papers Presented by the
ELECTRONICS DIVISION

Spring Meeting — Cincinnati
May 1 to 5, 1955

$2.00

THE ELECTROCHEMICAL SOCIETY, INC.

Spring Meeting, May 1-5, 1955

Cincinnati, Ohio

ENLARGED ABSTRACTS

of Papers Presented by the

ELECTRONICS DIVISION

Subjects:

Luminescence

Oxide Cathodes

Phosphor Application

Semiconductors

Abstracts duplicated photographically from
copy as furnished by authors

Printed, but not published

CONTENTS

Luminescence

ABSTRACT NUMBER		PAGE
29	"The Theoretical Basis for Photoluminescence, Electroluminescence, and Photoelectroluminescence" by Ferd. E. Williams	1
30	"Influence of Electric Fields on Ultraviolet-Excited Phosphors" by Frank Matossi and Sol Nudelman	3
31	"Dielectric Behavior of Electroluminescent Zinc Sulfide" by Willi Lehmann	5
32	"Electroluminescence in ZnS Single Crystals" by D. R. Frankl	10
33	"The Effect of Electron Traps on Electroluminescence" by P. D. Johnson, W. W. Piper and F. E. Williams	14
34	"Infra-Red Quenching of Cadmium Sulphide" by S. H. Liebson	19
35	"Recombination Processes in Cadmium Sulfide" by John Lambe	22
36	"Sensitized Luminescence in NaCl:Ag + Cu" by Esther W. Claffy and C. C. Klick	24
37	"Fluorescence of Thallium Activated Halide Phosphors: I Spectra of NH_4Br:Tl" by Keith H. Butler	27
38	"Fluorescence of Thallium Activated Halide Phosphors: II Spectra of KCl:Tl" by Keith H. Butler	28
39	"Some General Considerations on the Preparation of Oxygen-Dominated Phosphors" by J. L. Ouweltjes and W. L. Wanmaker	29
40	"The Activator Systems in Zinc Sulfide and Halophosphate Phosphors" by J. S. Prener and F. E. Williams	31
41	"Controlled Preparation and X-Ray Investigations of CdS" by F. Schossberger	*
42	"Retention of Chloride in Fired Zinc Sulfide" by P. Goldberg, D. J. Bracco and A. Kremheller	34

*No Abstract available

ABSTRACT NUMBER		PAGE
43	"Particle Size and Structure of Fired Zinc Sulfide Powders" by A. Kremheller, D. J. Bracco and P. Goldberg	37
44	"The Oxidation of Zinc Sulfide Precipitates to Zinc Sulfate" by Dominic T. Palumbo and Albert K. Levine	40
45	"Lead and Manganese Activated Cadmium Fluorophosphates" by R. W. Wollentin	43
46	"Calcium Halophosphate Phosphors: II Optical Properties of the Particle Surface" by M. J. Bergin, K. H. Butler and H. H. Homer	46
47	"A Blue Emitting Phosphor with Manganese Activator" by E. L. Lind	48
48	"Magnesium Fluosilicate Phosphors" by P. W. Ranby and S. T. Henderson	50
49	"Preliminary Studies of the Perowskite-Type Ternary Oxides as Luminophors" by S. Terol and Roland Ward	52
50	"Two Arsenate Phosphors and the Significance of Their Emission" by Gorton R. Fonda	53
51	"The System, CdO:B_2O_3" by E. C. Subbaro and F. A. Hummel	56
52	"Luminescent Screens Made by Vapor Reaction" by D. A. Cusano and F. J. Studer	63
53	"Cathodoluminescent Lamps" by L. R. Koller	74
54	"Color Shifts in Zn-Cd-S (Ag) Phosphors" by Vanja Srepel	78
	Oxide Cathodes	
55	"Fundamental Phenomena of Thermionic Emission" by W. B. Nottingham	*
56	"A New Sintered Tungsten Matrix Cathode" by E. A. Thurber	82
57	"Some Studies on Problems Associated with the Molded Nickel Cathode" by Irving J. Bell and George R. Brewer	83
58	"Some Applications of L Cathodes" by J. Babakian, A. Matthewson and J. Bloom	84

* No Abstract available

ABSTRACT NUMBER		PAGE
59	"Manufacturing Advantages of Philips Impregnated Cathode used in Magnetron Applications" by Markus Nowogrodski	87
60	"Emission from Molybdenum Activated with Barium" by R. H. Ahlert and E. S. Rittner	89
61	"An Investigation of the Impregnated Cathode" by W. C. Rutledge, E. S. Rittner and R. H. Ahlert	90
62	"Improved Philips 'Impregnated Cathode'" by Roberto Levi	93
63	"Chemical Processes in Thin-Film Dispenser Cathodes" by R. C. Hughes and P. P. Coppola	95
64	"A New Pressed Dispenser Cathode" by P. P. Coppola and R. C. Hughes	98
65	"Thermionic Emission Evaluation of Single Constituent Additives in Pure Nickel Cathodes" by Frederick T. Hill	103
66	"Application of Automatic Recording Instruments to the Measurement of Emission" by C. D. Richard, Jr. and R. D. Yeaton	107
67	"A Simplified Gas Adsorption Method for the Determination of the Surface Area of Fine Powders" by Dominic T. Palumbo, Forest M. Starkweather and D. J. Bracco	110
68	"The Electrical Properties of the Oxide Cathode Coating" by Ralph Forman	114
69	"Activation of an Oxide Cathode by Ba, Sr, Ca and Mg Deposited via a Mass Spectrometer" by R. M. Matheson and R. d. Plumlee	117
70	"Mass Spectrometric Study of the Field Dependent Evolution of Constituents of a BaO Cathode" by R. H. Plumlee	119
71	"Factors Influencing the Particle Size in the Preparation of Alkaline Earth Carbonates" by D. T. Palumbo, D. J. Bracco and A. K. Levine	121
	Phosphor Application	
72	"Particle Size Measurements of Television Phosphors" by J. G. Rabatin, E. S. Palik and R. H. Gale	122
73	"Polyvinyl Alcohol for Preparation of Color Television Screens" by C. W. Saltonstall	124

ABSTRACT NUMBER		PAGE
74	"Screen Potential Measurements in Cathode-Ray Tubes" by J. R. Young	125
75	"Positive Ion Production, Ion-Focussing Fields and X-Burn in Commercial Cathode-Ray Tubes" by W. A. Thornton	126
76	"Secondary Electron Emission in Cathode-Ray Tubes" by A. B. Laponsky	128
	Semiconductors	
77	"Properties of Germanium and Silicon" by E. M. Conwell	*
78	"Injection and Extraction" by R. Bray	130
79	"Germanium-Oxygen System" by D. Tuomi and E. S. Candidus	133
80	"Donor-Acceptor Balance in Selenium Rectifiers" by H. W. Henkels	137
81	"Correlation of Electrical Properties of Selenium Rectifiers with Fundamental Bulk Properties" by H. W. Henkels	139
82	"State of Semiconductor Surfaces" by R. H. Kingston	143
83	"Ultra-High Vacuum Studies on Germanium Surfaces" by F. G. Allen	146
84	"Theory of Surface Barrier Electrodes" by W. E. Bradley	149
85	"Holes and Electrons in Germanium Electrodes" by C. G. B. Garrett and W. H. Brattain	*
86	"Effects of Surface Treatments in Low Pressure Gas Atmospheres Upon Characteristics of Evaporated Surface Barrier Rectifiers" by P. A. Hartig	153
87	"Effect of Water on Germanium and Silicon Junctions" by J. T. Law and P. S. Meigs	159
88	"Observations of Channel Formation on N and P Type Semiconductors" by R. N. Noyce	164
89	"Oxidation of Clean Surfaces of Germanium Below 25°C" by M. Green and J. A. Kafalas	169
90	"Etches for Imperfections in Silicon and Germanium" by J. W. Faust	172

*No Abstract available

ABSTRACT NUMBER		PAGE
91	"Jet Etching" by W. E. Bradley	174
92	"The Purification of Germanium - The $GeCl_4$-$AsCl_3$ System" by M. Green and J. A. Kafalas	176
93	"A New Method for Producing High Purity Silicon" by G. Szekely	*
94	"Depth of Surface Damage on Germanium by Abrasion" by T. M. Buck and F. S. McKim	181
95	"The Electrochemical Preparation of Germane" by M. Green and P. H. Robinson	185
96	"The Present Status of Intermetallic Semiconductors" by R. G. Breckenridge	191
97	"Effect of Zone-Refining Variables on the Segregation of Impurities in InSb" by T. C. Harman, R. K. Willardson, H. L. Goering and A. C. Beer	194
98	"Photoeffects in InSb" by S. W. Kurnick, A. E. Goldberg, G. M. Mitchell and R. N. Zitter	199
99	"Effects of Impurities on Photoconductive CdS, CdSe, and PbS" by W. B. Hugle	207
100	"Anode Films on InSb" by J. Dewald	210

* No Abstract available

Abstract Number 29

THE THEORETICAL BASIS FOR PHOTOLUMINESCENCE, ELECTROLUMINESCENCE AND PHOTOELECTROLUMINESCENCE

Ferd E. Williams

General Electric Research Laboratory
Schenectady, New York

The luminescent emission of phosphors is determined by impurities known as activators. The activator plus neighboring atoms involved in the lattice rearrangements accompanying photoluminescent excitation and emission constitute the activator system. The characteristics of activator systems in simple ionic phosphors are now understood in considerable detail. In KCl:Tl the excitation and emission spectra are adequately accounted for by the interaction energies of Tl^+ with the KCl lattice calculated from Hartree free ion wave functions for the ground and excited states.[1] The transition probabilities are in accord with free ion spectra. In KCl:Mn, however, since transitions between states of the same electron configuration are responsible for excitation and emission, Hartree-Fock wave functions are necessary, the angular dependence of the excited state acquires unexpected significance, and interaction with the lattice markedly affects the transition probabilities. In covalent phosphors such as ZnS:Cu, the energy levels responsible for photoluminescent excitation and emission are recognized as perturbed bond orbitals of the unactivated crystals. The spectra, however, are still determined by the properties of the localized activator system.[2]

Electroluminescence—the conversion in a solid of an applied electrical potential into luminescent emission—is feasible theoretically in suitable phosphors by three general mechanisms. 1) Direct field ionization of the activator system is feasible with local fields of the order of 10^7 v/cm. In thin films of dielectrics with large band gaps and with activator systems near the conduction band, this mechanism is expected but has not yet been reported experimentally. 2) Fields of 10^5 v/cm are adequate to accelerate charge carriers to kinetic energies sufficient for excitation or ionization of the activator system by inelastic collisions. In electroluminescent ZnS:Cu crystals, conduction electrons are formed by field ionization of deep donors in an exhaustion layer resulting from ionization of shallow donors.[3] 3) Injected minority carriers in a semiconducting phosphor can be captured by the activator system. The ionized activator emits radiation following capture of the majority charge carrier. There is no threshold field for the carrier injection mechanism of electroluminescence. The electroluminescence of SiC is believed to occur by this mechanism.[4] In addition, direct

optical recombination of injected carriers in Ge and Si to yield infrared emission is well known.[5]

Photoelectroluminescence is the conversion initiated by radiation of an applied electrical potential into luminescent emission. This phenomenon was predicted from theoretical studies on the impact excitation mechanism of electroluminescence. In this case, charge carriers are not formed by field ionization of deep donors but rather are created by an internal photoelectric effect. Either the incident radiation creates electron-positive hole pairs by absorption in the fundamental band or the incident radiation is absorbed in an impurity system which is subsequently ionized. The charge carriers are then accelerated and inelastic collisions occur with the activator systems to yield luminescent emission dependent on the intensity of the incident radiation. If the field is sufficient for more than one impact ionization to occur per incident photon, either by sequential ionizations by the same charge carrier or by small avalanche formation, light amplification results. This phenomenon has been observed experimentally by Cusano[6] in vapor-deposited ZnS:Mn films.

References

1. F. E. Williams, J. Chem. Phys. 19, 457 (1951).
2. F. E. Williams, Brit. J. Appl. Phys. Supplement 4 on Luminescence (1955).
3. W. W. Piper and F. E. Williams, Phys. Rev. 87, 151 (1952), Brit. J. Appl. Phys. Supplement 4 on Luminescence (1955).
4. K. Lehovec, C. A. Accardo and E. Jamgochian, Phys. Rev. 83, 603 (1951).
5. J. R. Haynes and H. B. Briggs, Phys. Rev. 86, 647 (1952).
6. D. A. Cusano, Bull. Am. Phys. Soc. (New York Meeting 1955).

Abstract Number 30

INFLUENCE OF ELECTRIC FIELDS ON ULTRAVIOLET-EXCITED PHOSPHORS

Frank Matossi and Sol Nudelman

U. S. Naval Ordnance Laboratory
White Oak, Maryland

If a ZnS-phosphor (electroluminescent or non-electroluminescent) is first excited by ultraviolet and then, while ultraviolet excitation continues, is subjected to a periodic electric field, sudden intensity increases (stimulations) are observed at the instants of field application or removal. During the field application, a quenching is obtained that is strong in the beginning but attains a much smaller steady value after some time.

The stimulation at "field on" generally decreases with increasing frequency up to about 20 kcps. At higher frequencies, it either remains constant or increases slightly. The stimulation at "field off" generally increases with frequency. For some phosphors, the quenching behaves irregularly at the low frequencies. The amplitude of the periodic ripple superimposed on the quenching reaches a maximum at several hundred cps. The quantitative details vary appreciably from phosphor to phosphor.

For a few phosphors, the brightness waves of electroluminescence change their aspect if ultraviolet excitation is superimposed. Some lose the "C peaks" (secondary peaks occurring whenever the field begins to decrease). These peaks appear again after removal of ultraviolet radiation, but only after times in the order of minutes. The ratio of the C peak intensity to that of the main peaks ("B peaks" in phase with the field) depends on frequency, the C peaks becoming more prominent at about 1000 cps. In other phosphors, the amplitudes of the brightness waves in the two half-periods of the field become unequal with ultraviolet imposed.

The peaks of the ripple pattern during the quenching of an electroluminescent phosphor with weak sinusoidal fields lag behind the field. If the field is increased, a new peak begins to appear at a certain critical field that is identical with the field necessary to obtain electroluminescence. These peaks grow further with increasing field strength, finally becoming the B peaks of electroluminescence. They precede the field. The phase shift from the ripple pattern to the brightness waves is, therefore, not the gradual shifting of one peak, but the result of different relative intensities of two independent peaks which demonstrates that quenching and electroluminescence effects have different origins. A similar transition is observed with square wave fields. This can be

understood on the basis of the influence of polarization effects on the phase of the brightness waves while the quenching ripple pattern is principally determined by a change in the number of electrons in the conduction band and not by the internal field.

Also, some of the other observations reported farther above can be understood as the consequence of polarization effects if the particle balance between valence band and conduction band is considered. The treatment is analogous to that of Jaffe (Phys. Rev. 85, 354, 1952) and McDonald (Phys. Rev. 92, 4, 1953) and takes into account steady and periodic excitation, recombination, motion of electrons in a field obeying Poisson's equation, and diffusion of space charges.

Abstract Number 31

DIELECTRIC BEHAVIOR OF ELECTROLUMINESCENT ZINC SULFIDE

Willi Lehmann

Westinghouse Electric Corporation
Bloomfield, New Jersey

A sinusoidal electric field was applied to several powdered electroluminescent zinc sulfides activated with copper. The phosphors were embedded in castor oil between two plane electrodes, one of which was transparent, with an electrode distance of 50 to 60 microns. The applied voltage could be varied between zero and 600 volts r.m.s. and the frequency between 20 cycles and several tens of kilocycles per second. Measurements were made of the dependency upon frequency f and voltage V of

a. the electroluminescent brightness L of the phosphor.
b. the capacitance C of the cell with and without phosphor.
c. the phase angle ϕ of the cell with and without phosphor.

Under the assumption of a special geometrical arrangement of the phosphor particles in the castor oil of the cell it is possible to determine from these measurements the electrical properties of the phosphor itself. These may be represented by the complex dielectric constant $k = k' + ik''$ with $i = (-1)^{\frac{1}{2}}$. Both the real part k' and the imaginary part k'' of the dielectric constant of the phosphors are practically constant for applied voltages below the level of measurable electroluminescence. With higher voltage both parts increase, slowly for low and more rapidly for high voltages. The amount of increase is greatest for the lowest frequency (Figure 1).

The imaginary part k'' of the dielectric constant of the phosphor is connected with the conductivity of the phosphor which can be expressed in the usual way by the concentrations and the mobilities of electrons and holes. On the other hand, the electroluminescent brightness L can be assumed to be proportional to the number of free electrons and the number of ionized activator centers. By assuming that the influence of the frequency f on the relation between the number of holes, n_p, in the valence band and the number of ionized activators A^+ is

$$n_p \propto f \cdot A^+ \qquad (1)$$

a relation can be obtained between the electroluminescent brightness L, the frequency f, the average a.c. mobility μ and the imaginary dielectric constant k_0'' for very low and k'' for higher voltages

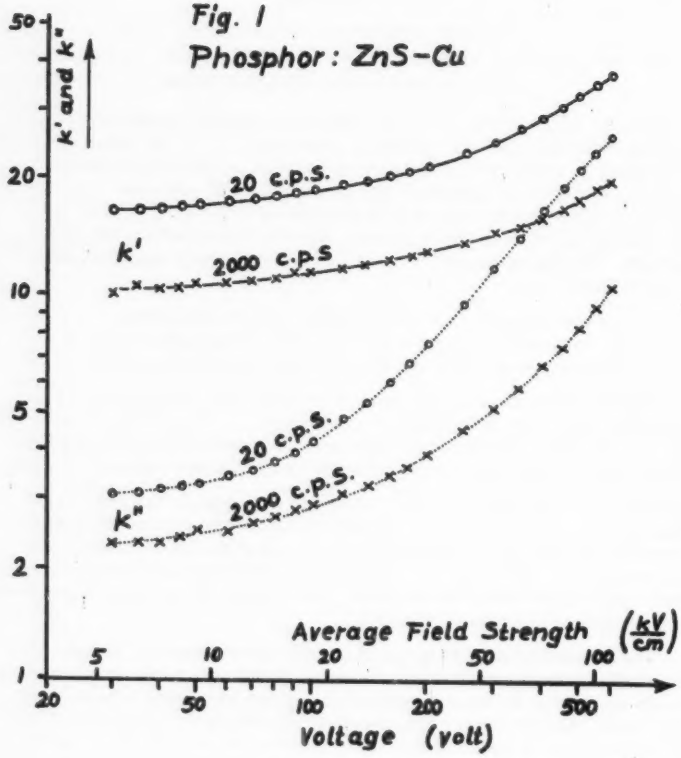
Fig. 1
Phosphor : ZnS–Cu
k' and k"
50
20
10
5
2
1
20 c.p.s.
2000 c.p.s
k'
20 c.p.s.
2000 c.p.s.
k"
Average Field Strength (kV/cm)
5
10
20
50
100
20
50
100
200
500
Voltage (volt)

$$L/f = C(k'' - k_o'')^2/\mu^2 \qquad (2)$$

with C as a constant of proportionality.

Equation (2) is checked graphically by plotting L/f versus $(k'' - k_o'')$. As can be seen in Figure 2, the fit is good for not too high values of L/f (i.e. for not too high applied voltages). In this region of low and moderate voltage the mobility μ is found to be constant and therefore L/f is proportional to $(k'' - k_o'')^2$. However, a strong deviation from the straight line in Figure 2 is observed for high values of L/f. This deviation can be explained with equation (2) by a variation of the mobility μ with high field strength. In Figure 3, an example, the variation of the mobility μ with the a.c. field strength is shown. The mobility μ is constant up to a field strength of about 30 kV/cm and increases rapidly for higher field strengths. It cannot be determined by these experiments whether this increase in mobility is due to the free electrons, or to the holes, or to both.

The behavior of the real part of the dielectric constant, k', as a function of L/f is about the same as that of the imaginary part, as can be seen in Figure 4, but a theoretical explanation for this behavior of k' has not yet been obtained.

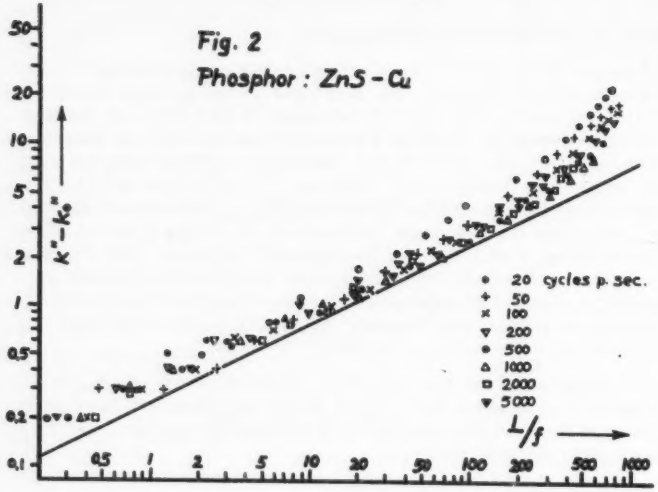
Fig. 2
Phosphor : ZnS - Cu
$k''-k_0''$
20 cycles p. sec.
50
100
200
500
1000
2000
5000
L/f
50
20
10
5
2
1
0.5
0.2
0.1
0.5
1
2
5
10
20
50
100
200
500
1000

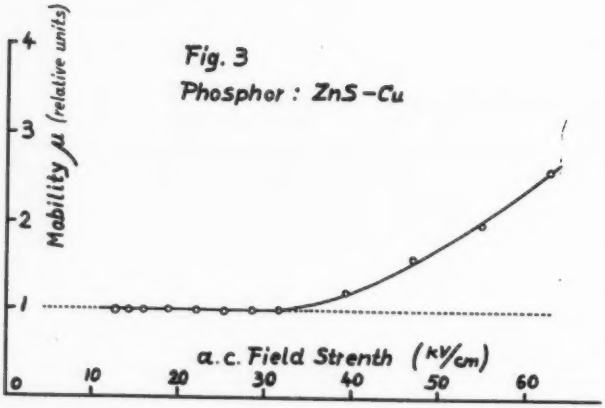
Fig. 3
Phosphor : ZnS - Cu
Mobility μ (relative units)
4
3
2
1
a.c. Field Strenth (kV/cm)
0
10
20
30
40
50
60

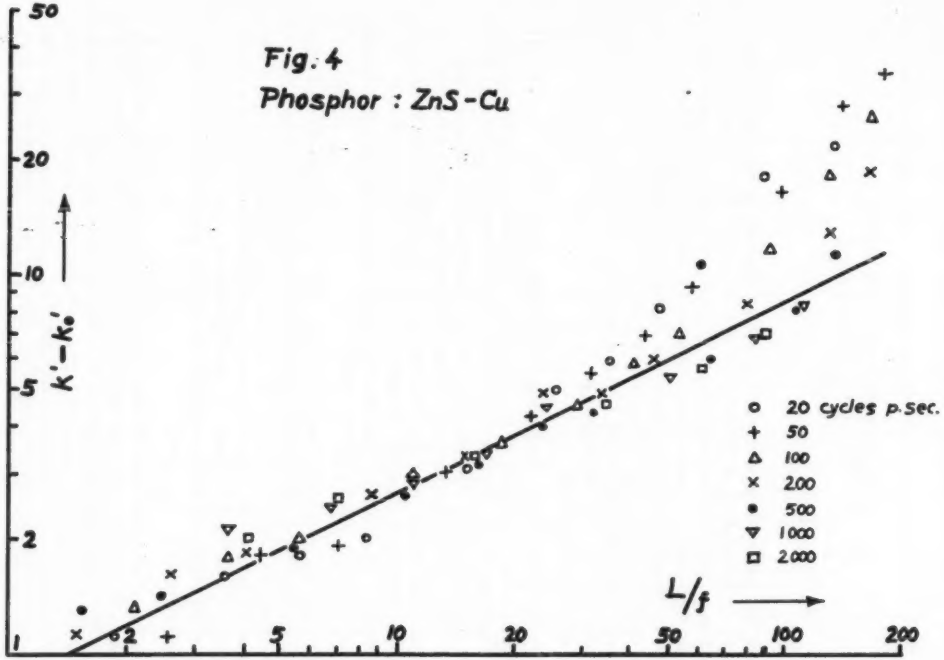
Fig. 4
Phosphor : ZnS-Cu
50
20
10
5
2
1
k'-k'₀
2
5
10
20
50
100
200
L/f
20 cycles p.sec.
50
100
200
500
1000
2000

Abstract Number 32

ELECTROLUMINESCENCE IN ZnS SINGLE CRYSTALS

D. R. Frankl

Sylvania Electric Products Inc.
Physics Laboratories
Bayside, L. I., N. Y.

At the 1954 Symposium, Watson et al[1] described the electroluminescent emission from single crystals of zinc sulfide subjected to half-wave rectified 60 cycle sinusoidal voltage. The emission intensity has peaks at the voltage maximum (denoted 90 degrees phase angle in the cycle) and near the point where the voltage falls to zero (usually about 150 degrees phase angle) and decays in the second half cycle while the voltage remains zero. The 150-degree peak is the larger at low voltage amplitudes, but the 90-degree peak grows the more rapidly with increasing voltage amplitude.

The present paper describes extensions of this work. Particular emphasis has been placed on making the measurements quantitative. For this purpose, the absolute spectral sensitivity of a photomultiplier was determined by comparison with a calibrated thermopile under monochromatic illumination. This photomultiplier was then used in conjunction with a series of narrow band interference filters to measure the emission intensity in each of a number of small "slices" of the spectrum. In this way, both the spectral distribution and the absolute intensity of the emission are obtained.

Among the crystals studied to date, only those which showed blue fluorescence are appreciably electroluminescent. The latter emission also appears blue to the eye, but actually contains appreciable amounts of green and yellow. Spectral results on a typical crystal are shown in Figure 1. It is particularly to be noted that the spectral distribution is about the same for both peaks and is roughly independent of voltage amplitude.

All crystals observed to date have suffered a progressive deterioration in brightness, usually rapid at first and sometimes much slower later on. Annealing in a bed of pure ZnS powder has restored some of the crystals, but has failed to restore others. The cause of deterioration is not known. The measurements reported here were made on crystals which had been "aged" beyond the initial rapid deterioration.

The current through the crystals was measured by displaying on an oscilloscope the voltage drop across a small resistor in series with the crystal. After subtracting out the displacement current in the crystal and its holder, the conduction current is found to be a nearly exponential function of voltage. Thus, in the half-wave cycle, the current wave

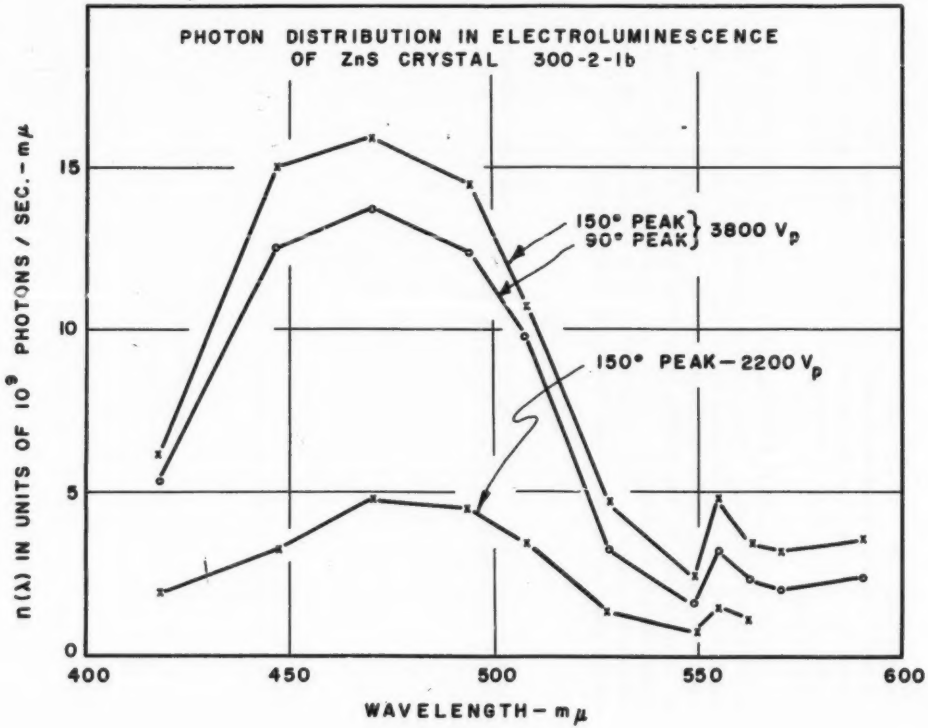
PHOTON DISTRIBUTION IN ELECTROLUMINESCENCE
OF ZnS CRYSTAL 300-2-1b
150° PEAK
90° PEAK
3800 Vp
150° PEAK—2200 Vp
n(λ) IN UNITS OF 10⁹ PHOTONS / SEC. - mμ
WAVELENGTH - mμ
0
5
10
15
400
450
500
550
600

consists of a fairly narrow peak at 90 degrees. In particular, there is no reverse current at any time in the cycle, showing that no space-charge polarization occurs.

Figure 2 shows typical quantitative results. We plot as function of the voltage amplitude the intensities of the two emission peaks and the average intensity over the whole cycle (solid curves, left scale) and the current amplitude (broken curve, right scale). The 90-degree peak intensity and the current increase at about the same rate with voltage amplitude. In other words, the ratio of photons emitted at the 90-degree phase to electrons traversing the crystal is roughly independent of the voltage.

Similar measurements have been carried out at temperatures down to 77°K (liquid nitrogen). From room temperature to about -80°C, the same two major emission peaks occur, but at lower temperatures the peak structure changes in a complex manner. In the higher temperature range, the photon:electron ratio in the 90-degree peak is nearly independent of temperature. That is, the 90-degree peak and the current decrease at the same rate with decreasing temperature. The 150-degree peak, on the other hand, decreases more rapidly.

References

1. W. R. Watson, J. J. Dropkin, and A. T. Halpin, Enlarged Abstracts of the Electrochemical Society Spring Meeting (May, 1954), p. 42.

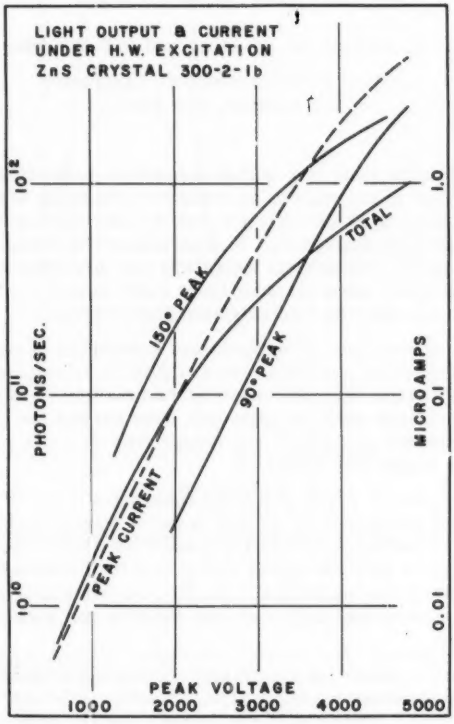
LIGHT OUTPUT & CURRENT
UNDER H.W. EXCITATION
ZnS CRYSTAL 300-2-1b
10^{12}
10^{11}
10^{10}
PHOTONS/SEC.
1.0
0.1
0.01
MICROAMPS
150° PEAK
90° PEAK
TOTAL
PEAK CURRENT
PEAK VOLTAGE
1000
2000
3000
4000
5000

Abstract Number 33

THE EFFECT OF ELECTRON TRAPS ON ELECTROLUMINESCENCE

P. D. Johnson, W. W. Piper, and F. E. Williams

General Electric Research Laboratory
Schenectady, New York

In electroluminescent zinc sulfide phosphors, filled electron traps or donors serve as the sources of conduction electrons which are accelerated in regions of high electric field to velocities sufficient for impact excitation of activators.[1] Comparison of the temperature dependence of electroluminescent brightness and thermoluminescence suggests that either these traps or those in the bulk of the crystal may have an adverse effect on electroluminescent brightness.

Thermoluminescence and temperature dependence of electroluminescent brightness of powder samples of ZnS:Cu,Al suspended in lucite and on ZnS:Cu single crystals grown by sublimation[2] were determined. Measurements were made on apparatus, used earlier for thermoluminescence of powder phosphors[3] and conductivity of single crystals,[4] modified for the present work.

The glow curve of a typical powder suspension in lucite using excitation by 3650 Å ultraviolet (G. E. BH4 lamp) is shown in Figure 1. With electroluminescent excitation at 400 v and 1000 cps the glow curves were the same as with ultraviolet except that the intensities were lower by factors ranging from 100 to 1000. Only a single glow peak at 150°K is detected in the single crystals and this only with 3650 Å excitation.

In Figure 2 is shown the electroluminescent and photoluminescent brightness of the same powder cell as a function of temperature at several different frequencies of excitation. Variations of electroluminescent brightness with temperature are peculiar to electroluminescent excitation rather than to the activator system itself. The fact that similar behavior is observed in single crystals, as shown in Figure 3, indicates that the variations in brightness are not due to characteristics of the dielectric. This view is further substantiated by measurements of dielectric constant and loss of phosphor suspensions and of pure lucite as a function of temperature.

It will be noted that the minimum in electroluminescent brightness occurs at a few degrees above the temperature of the principal glow peak and that the structure in the temperature dependence of brightness shifts to higher temperatures with higher frequency of excitation.

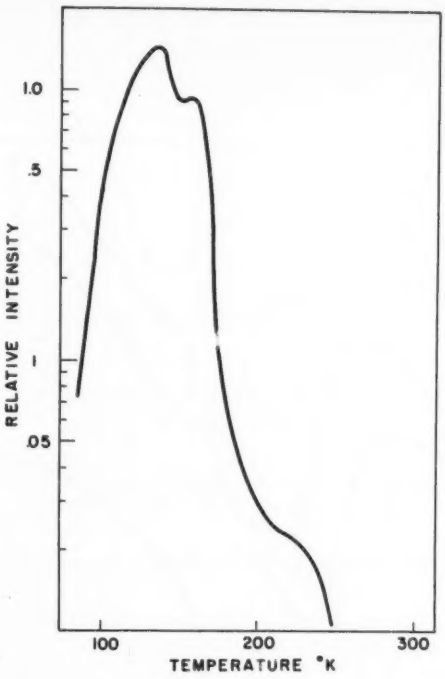

Fig. 1 Thermoluminescence of ZnS:Cu,Al powder phosphor.

Changing the voltage of excitation only shifts the characteristic temperature-brightness curve in brightness, not in temperature.

In this and in other investigations[5] powder suspensions have been found in which the brightness drops off as temperature is decreased and does not again rise at the lowest temperature measured, in contrast to the behavior of the samples reported here.

Both of these types of behavior in addition to the shift of the characteristic brightness-temperature curve to higher temperature with higher excitation frequency are in accord with the same mechanism. Excitation of activators occurs in the region of high field on the side of the crystal near that electrode which is becoming negative. At room temperature or above, because of thermal ionization or lack of significant trapping, electrons from excited activators become ionized and are free to move about the crystal. In the absence of trapping, these electrons may return to the ionized activators on the reverse half-cycle of excitation and recombine. At lower temperatures where trapping occurs, the electrons are not entirely free to move either a very

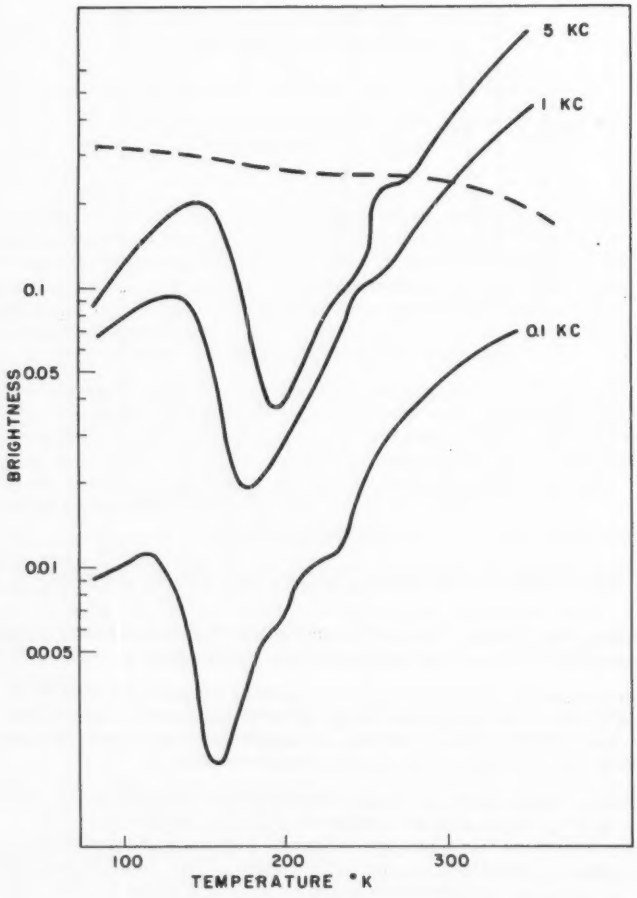

Fig. 2 Temperature dependence of electroluminescent brightness (solid line) and photoluminescent brightness (dashed line, different scale) of ZnS:Cu,Al powder phosphor in lucite

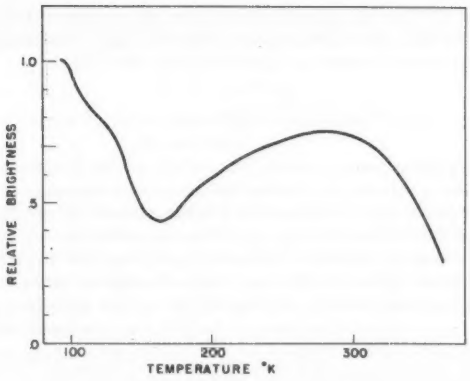

Fig. 3 Temperature dependence of electroluminescent brightness of a ZnS:Cu single crystal.

great distance from the activator or to return from whatever distance they have gone.

In general, the rates of removal from and return to the region of excited activators are determined by activated processes of rate $k_2 = s_2 e^{-\xi_2/kT}$ and $k_1 = s_1 e^{-\xi_1/kT}$ respectively. The quantities ξ_2 and ξ_1 are the activation energies of the processes involved and s_2 and s_1 the frequency factors for these processes. The rate constant k_1 may immediately be identified as the rate of untrapping from the principal traps filled at the temperature in question. For generality the process of rate k_2 will not be identified for the present.

If N_0 is the number of activators excited in one-half cycle of excitation, then N_i, the number of electrons transported to traps from the activators, is

$$N_i = N_0(1 - e^{-K_2 t}), \tag{1}$$

where t is one-half of the reciprocal of the frequency of excitation. The number of electrons thus trapped which remain trapped at the end of the following half-cycle of excitation N_T is

$$N_T = N_i e^{-k_1 t} \tag{2}$$

The brightness, B, is proportional to the number of excited activators which can recombine during the complete voltage cycle and is given by

(3) $$B \approx \frac{N_0 - N_T}{N_0} = 1 - (1 - e^{-k_2 t}) e^{-k_1 t}$$

If the rate of removal of electrons from the region of the activator is governed by the rate of untrapping, then $k_1 = k_2$. The temperature, T_m, of the minimum found by differentiation of (3) is

(4) $$T_m = \frac{\xi}{k \ln(st/\ln 2)}$$

When retrapping occurs during the return of the electrons to the activators, the minimum in electroluminescence becomes more pronounced. At low temperatures with a large amount of retrapping the electrons fail during the voltage cycle to return to the activators, resulting in the type of behavior reported by Alfrey and Taylor. The presence of more than a single trap depth results in increasing the half-width of the depression. The positions of the principal glow peak and the principal electroluminescent brightness minimum in both powder cells and single crystals are in accord with a trap depth of 0.25 ev and a frequency factor for untrapping of 10^{10} sec^{-1}. There is evidence in both thermoluminescence and temperature dependence of electroluminescent brightness for a considerable amount of retrapping and for the presence of more than a single trap depth.

References

1. W. W. Piper and F. E. Williams, Phys. Rev. 87, 151 (1952).
2. W. W. Piper, J. Chem. Phys. 20, 1343 (1952).
3. P. D. Johnson and F. E. Williams, J. Chem. Phys. 21, 126 (1953).
4. W. W. Piper, Phys. Rev. 92, 23 (1953).
5. G. Alfrey and J. B. Taylor, Supplement No. 4, Brit. J. Appl. Phys., Discussion on Paper No. 7 (Piper and Williams) 1954.

INFRA-RED QUENCHING OF CADMIUM SULPHIDE

S. H. Liebson

United States Naval Research Laboratory
Washington, D. C.

The luminescence and electrical properties of the hexagonal form of cadmium and zinc sulphide crystals are affected by exposure to infra-red radiation. Cadmium sulphide crystals through which a current due to photo-excitation passes, exhibits a decrease in this current when infra-red is added to the incident radiation.[1] This behavior is called infra-red quenching.

We have investigated the infra-red quenching of cadmium sulphide as a function of applied voltage, infra-red and photoconductive light intensities, and temperature. In general, the proportional quenching, defined as the change in photoconductive current due to infra-red divided by the current due to the photoconductive light alone, increases as the voltage across the crystal is increased. For some crystals with rectifying contacts, oscillations of the current were observed when infra-red and photoconductive light were simultaneously incident on the crystal. For crystals with ohmic contacts, the change in current due to infra-red at first increased then became constant as the photoconductive light was increased.

The infra-red quenching spectrum consists of two bands with peaks at about 0.9 and 1.5 ev. These peaks were found to shift with temperature to approximately the same extent as the corresponding shift of the absorption edge,[2] of the order of 1 Å per degree centigrade.

The proportional quenching was measured as a function of temperature and found to have a maximum near room temperature for most of the crystals examined. No peaks in the thermo-stimulated currents were found at this temperature. For two other crystals, both taken from the same growth, proportional infra-red quenching was found to increase from -40°C to +75°C. Measurements were not continued beyond 75°C due to the fact that irreversible changes in photoconductive behavior are likely to occur at higher temperatures. A measurement of the photocurrent versus temperature without infra-red showed no appreciable difference between those crystals exhibiting a maximum in proportional infra-red quenching at room temperature and those which increased with temperature. Since it has been postulated[3,4] that copper impurities were responsible for the infra-red quenching behavior in sulphides, a crystal with added copper was among those examined. Another of the crystals examined had silver added during the growth and one more had been heated in an atmosphere of sulphur for

30 hours at 550°C. Here too, no appreciable difference was observed between these crystals. Spectroscopic analysis indicated that all crystals contained from 0.001% to 0.01% of copper.

The increase of photovoltage and photocurrent by the addition of infra-red at a rectifying contact has been interpreted to indicate that infra-red frees holes within the barrier region, tending to increase both the barrier thickness and the barrier potential.[5] The oscillatory character of some of the observed crystals with rectifying contacts is probably related to the ability of infra-red to increase the barrier height.

The increase of proportional quenching with increase of applied field may be interpreted in several ways. Klasens has suggested[6] that at the higher voltages the greater field may increase the range of travel of holes to recombination regions, resulting in enhanced quenching action. Another possible explanation is that the increased fields increase the internal space charge or polarization. For either case the following explanation is offered for infra-red quenching. Infra-red excited holes which, perhaps with the aid of thermal ionization, are made mobile in the valence band. They may now be swept by the field to a potential barrier due to trapped electrons where recombination takes place. The empty electron trap is now available for capturing electrons from the conduction band, resulting in quenching. The thermal ionization of excited holes has previously been proposed by Taft and Hebb,[7] and Klasens.[3] The measurements of proportional quenching as a function of temperature does indeed indicate that at least for temperatures below about 35°C, the proportional quenching increases with increasing temperature as these theories predict. However, the decrease in proportional quenching for most of the crystals as the temperature is increased above room temperature is not in accord with this simple concept. Since we postulate the quenching process to consist of a recombination of mobile holes with trapped electrons, an explanation of the decrease of quenching at high temperatures is offered based on a thermal ionization of these trapped electrons. Some evidence for this is found in the measurements of Ramanna and Duggal,[8] who have found that the internal polarization of cadmium sulphide decreases at high temperatures.

The shift with temperature of the peaks of the infra-red quenching spectrum of cadmium sulphide, of the same amount as the change in forbidden band width, implies that either the bottom of the conduction band or the top of the valence band moves with respect to the infra-red absorption centers. If the nature of change in forbidden band with temperature were known it could help to decisively determine whether infra-red frees electrons or holes.

References

1. A. E. Hardy, Trans. Am. Electrochem. Soc. 87, 355 (1945)

2. F. A. Kröger, Physica 7, 1 (1940)

3. H. A. Klasens, J. Electrochem. Soc. 100, 72 (1953)
4. H. C. Froelich, J. Electrochem. Soc. 100, 280 (1953)
5. S. H. Liebson, J. Electrochem. Soc. 101, 362 (1954)
6. H. A. Klasens, Private Communication
7. E. A. Taft and M. H. Hebb, JOSA, 42, 249, (1952)
8. R. Ramanna and V. P. Duggal, Phys. Rev. 84, 1251 (1951)

Abstract Number 35

RECOMBINATION PROCESSES IN CADMIUM SULFIDE

John Lambe

Naval Research Laboratory
Washington, D. C.

An experimental study has been carried out on the photoconductivity and luminescence of cadmium sulfide crystals. This study was primarily concerned with the role which the various recombination processes play in determining the photoconductive properties. The two main problems investigated were the photoconductive spectral response and the relationship between luminescence and photoconductivity. The approach used in this study is based on observations of the transient response of photocurrent and luminescence to varying excitations.

The photoconductive spectral response of CdS is such that the peak in photoconductivity lies to the long wavelength side of the region of maximum optical absorption. This means that although the absorption decreases, the photoconductive spectral response increases. Most explanations for this behavior assume that either the mobility,[1] or the lifetime[2,3] of an electron in the conduction bands is dependent upon the wavelength of the exciting light. Measurements were carried out therefore, to examine the wavelength dependence of the lifetime of conduction electrons, and to what extent this factor determined the observed photoconductive spectral response. The lifetime of conduction electrons was measured by observing the initial rate of decay of photoconductivity when excitation was interrupted. These observations indicated a considerable dependence of the lifetime upon wavelength of exciting light. The lifetime of conduction electrons increased by a factor of about 10 in going from 4800 Å to 5200 Å. In addition, measurements were made of the photoconductive spectral response and optical absorption characteristics. Using these lifetime measurements and the optical absorption, a photoconductive spectral response was calculated which was in good agreement with the observed spectral response. Some crystals of CdS were encountered which showed no photoconductive peak in spectral response and also no wavelength dependence in the lifetime measurements. These observations indicate that the dependence of the lifetime of conduction electrons upon wavelength of exciting light plays the major role in determining the photoconductive spectral response.

A comparative study was made of the rise and decay rates of luminescence and photoconductivity for the orange luminescence of CdS (Ag) and for the green edge luminescence and red luminescence of "unactivated" CdS. In all cases, the crystals were excited by light at 3650 Å.

In the case of CdS (Ag) at 77°K, the decay time of luminescence (time required to drop to $\frac{1}{2}$ of initial value) was about .05 milliseconds while the decay time of photoconductivity was about 5 milliseconds. Such a result is difficult to explain on the basis of the usual model for photoconducting phosphors in which luminescence occurs after the capture of a conduction electron at a luminescent center. A somewhat simpler explanation of this difference in decay time can be made on the basis of a model which has been proposed for CdS (Ag).[4] In this model, luminescence is assumed to result from the recombination of a bound electron and a free hole. Thus, if free holes have a short lifetime, the decay time of luminescence will be short. The decay time of the photoconductivity on the other hand is to be associated with the lifetime of conduction electrons which can be quite different from the lifetime of free holes. Such a model was also found to be consistent with observations on infra-red stimulation of luminescence and photocurrent in CdS (Ag).[4] At 200°K it is found that although the decay time of luminescence is much more rapid than the decay of photoconductivity, the rise of luminescence parallels the rise of photoconductivity. At 77°K both rise and decay of luminescence are much more rapid than the rise and decay of photoconductivity. This effect in the rise time of luminescence at 200°K is explicable on the basis of the proposed model.

The green edge luminescence of CdS was observed at 77°K and at 4°K. The decay time of the green edge luminescence is roughly .07 milliseconds, while the decay time for photoconductivity is about 5 milliseconds. This result can be explained on the basis of a model similar to that proposed for CdS (Ag). That is, if one assumes that luminescence results from the recombination of a free hole and a bound electron, then the decay time of luminescence can be associated with the lifetime of free holes. If free holes have a short lifetime, the decay of luminescence will be rapid. At 77°K the rise of photoconductivity parallels the rise of the green luminescence. At 4°K, both rise and decay of the green luminescence are much more rapid than the rise and decay of photoconductivity.

The red luminescence of "unactivated" CdS was studied at 300°K. The decay time of luminescence was about .2 milliseconds while the decay time for photoconductivity was about 4 milliseconds. This result can also be explained on the basis of the above model, but since little is known of the center responsible for this luminescence, just as in the case of the green luminescence, such an explanation is largely phenomenological.

References

1. H. W. Leverenz, Introduction to Luminescence of Solids (John Wiley and Sons, Inc., New York, 1950)
2. J. Fassbender, Ann. Physik, Vol. 5, 33 (1949)
3. A. Rose, R. C. A. Review, 362 (Sept. 1951)
4. C. C. Klick and J. Lambe - to be published.

Abstract Number 36

SENSITIZED LUMINESCENCE OF NaCl:Ag+Cu

Esther W. Claffy and Clifford C. Klick

United States Naval Research Laboratory
Washington, D. C.

Partly because of their widespread use in lamps, doubly activated inorganic phosphors have been widely investigated. In most of these phosphors it has been shown that one center—called the sensitizer or absorber—absorbs the exciting light and transfers its energy to the other center—called the activator or emitter—which then luminesces. In all the cases investigated experimentally the luminescence emission in the activator was of a "forbidden" type and this center was most frequently manganese.

In organic solutions, on the other hand, a large amount of experimental data has been collected on transfer of energy between organic molecules which have "allowed" luminescence transitions. Considerable theoretical work has also been done in the organic field, especially by Förster,[1] treating the energy transfer process quantum mechanically. Recently Dexter[2] has extended these theoretical considerations to the case of inorganic phosphors and to cases where various types of forbidden transitions were involved. The agreement with experiment seems satisfactory.

From the theoretical arguments advanced, however, it should be possible to observe sensitized luminescence in inorganic phosphors using suitably chosen activators both of which have allowed transitions. The present investigation of such a system was undertaken as a further check of the theory.

The system chosen for study was NaCl:Ag+Cu. The silver ion has an absorption peak at 2170A as well as an absorption structure extending into the region on the shortwavelength side of 2000A. Irradiation into the 2170A band produces an emission peaking at 2500A. The copper ion has an absorption peak at 2550A and it, too, has absorption to the shortwavelength side of 2000A. Irradiation into the 2550A peak of copper leads to emission peaking at 3580A. Thus the emission spectrum of the silver ion and the absorption spectrum of the copper ion overlap allowing for efficient energy transfer, according to the theory. This phosphor should therefore show sensitized luminescence with the silver as sensitizer and the copper as activator. Both of these centers are generally considered to have allowed transitions as indicated by their relatively high absorption strength and fast decay times.

The reagents used to prepare the samples were: (1) NaCl, specially purified with dithizone to remove traces of the heavy metals Pb, Tl,

Cu, Ag; (2) AgCl, "CP" grade; and (3) CuCl, synthesized for the purpose and protected against oxidation to the cupric form.

Elaborate precautions were taken to avoid contamination of the samples during processing, and to prevent oxidation. The dry reagents were mixed mechanically in a mullite mortar and pestle in the presence of calcium hydride desiccant, and the charge was fired in a platinum crucible in an atmosphere of purified and dried helium. The polycrystalline melts were stored in a desiccator. Just before measurement, the samples were pulverized and sieved to a particle size of 179-149 micron diameter (# 80-100 mesh fraction). The final grinding and sieving were done in a low humidity room. In all the samples the concentration of silver was kept constant at 100 parts per million, thus keeping the absorption constant. The copper concentration was varied over the range of 0.1 to 1000 parts per million.

In addition to the transfer of energy from silver to copper ions by sensitized luminescence there is a transfer by direct emission from the silver and reabsorption by the copper ions. This "cascade" process involves the actual emission of a photon from the sensitizer, which is not the case for the sensitized luminescence mechanism being considered. The efficiency of the cascade process depends not only on the concentration of activators but also on the sample size and shape; for the sensitized luminescence process the efficiency is dependent only on the activator concentration.

The variation of the quantum efficiency with activator concentration due to transfer by the cascade process was computed using methods developed by Johnson[3] for evaluating the reflectivity of powders. In the present case there are two separate steps in the computations: first, the fraction of the exciting light absorbed by the silver ion is computed as a function of the depth below the powder surface; second, the probability that luminescence of the silver ion is absorbed by the copper centers is computed for luminescence beginning at various depths below the surface. From this data it is possible to compute the efficiency of transfer by the cascade process alone. The results of this calculation indicate that the efficiency is high and varies slowly with activator concentration in the range investigated. This may be understood in a qualitative way by a simple argument. The absorption strength for the copper ion is considerably larger than that for the silver ion. Therefore the exciting light penetrates fairly deeply into the powder before being absorbed by the silver centers. The silver luminescence originating at this relatively large distance below the surface is almost completely absorbed by the copper centers with their high absorption strength. Since this is true even for fairly low concentrations of copper, the variation of emission with copper concentration is slow. By contrast the transfer due to sensitized luminescence varies linearly with activator concentration at low concentrations.

Measurements were made of the quantum efficiency of the copper emission on irradiation into the silver absorption band using apparatus developed in this laboratory.[4] The experimental results show a linear

variation of efficiency of transfer with activator concentration up to 30 parts per million. At 100 parts per million, concentration quenching begins to occur. In the linear range of efficiency versus activator concentration, the measured values are larger by a factor of three than the sensitized luminescence theoretical values but are as much as a factor of ten less than the computed cascade values.

Since both the absolute value of the transfer efficiency and its variation with activator concentration agree reasonably well with the predictions of sensitized luminescence theory, it appears that this process does occur between activators with allowed transitions in inorganic phosphors. The absence of appreciable transfer by the cascade process is probably due to the presence of the sensitizer in its excited state for a longer time than expected for a simple center. It is possible that the presence of higher excited states leads to crossovers or metastable states as in KCl:Tl and that these increase the sensitized luminescence transfer probability.

References

1. Th. Förster, Fluoresezenz Organische Verbindungen (Vandenhoeck and Ruprecht, Göttingen, 1951)
2. D. L. Dexter, J. Chem. Phys., 21, 836 (1953)
3. P. D. Johnson, J. Opt. Soc. Am., 42, 978 (1952)
4. R. J. Ginther and C. C. Klick, unpublished.

Abstract Number 37

FLUORESCENCE OF THALLIUM ACTIVATED HALIDE PHOSPHORS

I SPECTRA OF NH_4 Br:Tl

Keith H. Butler

Sylvania Electric Products Inc.
Salem, Massachusetts

Ammonium bromide phosphors can be readily made by grinding crystals of the pure compound with thallous chloride in a mortar. The emission and excitation spectra of such phosphors with thallium contents between 10^{-5} and 10^{-2} mole fraction were determined with a radiometer which permitted automatic recording of either the emission spectrum, with excitation by a narrow band of U.V. of any wavelength above 220mμ, or else recording of the excitation spectrum with analysis at any selected wavelength above 280mμ.

The NH_4 Br:Tl phosphors have a strong emission band at 400mμ which is excited by U.V. radiation in either of two bands peaking at 227mμ and 258mμ. Transitions between $^1S_0$ ($6s^2$) and $^1P_1^o$ (6s6p) account for the 258 and 400mμ bands while the absorption band at 227mμ is due to excitation to the $^1P_1^o$ (6s7p) state.

A weaker emission band at 535mμ is excited by bands centered at 242 and 280mμ. These are due to transitions from $^1S_0$ ($6s^2$) to the $^3P_1^o$ states of the 6s6p and 6s7p configurations.

In the case of excitation to the 6s7p configuration the electron returns through 6s7s to 6s6p without radiation in the visible. The usual selection rules applying to free ions appear to be also applicable to ions in the lattice. There is no evidence for thermal equilibrium between the $^1P_1^o$ and $^3P_1^o$ states of the 6s6p configuration.

Similar spectra have been found for NH_4 Cl, KBr and KI activated by thallium.

Abstract Number 38

FLUORESCENCE OF THALLIUM ACTIVATED HALIDE PHOSPHORS
II SPECTRA OF KCl:Tl

Keith H. Butler

Sylvania Electric Products Inc.
Salem, Massachusetts

The excitation and emission spectra of potassium chloride phosphors activated by thallium concentrations between $1x10^{-3}$ and $3x10^{-2}$ mole fraction have been measured on an automatic recording radiometer. The broad excitation band found by other observers at 240 to 275mμ has been resolved into two components peaking at about 245 and 260mμ. The 245mμ band is attributed to excitation from the $^1S_0$ ($6s^2$) state to $^1P_1^o$ (6s6p) and it is responsible for the strong emission band at 302mμ.

The weaker emission band at 492mμ is excited by the 260mμ component of the excitation band and these can be attributed to transitions between $^1S_0$ and $^3P_1^o$ (6s6p).

It is believed that transitions in the excited ion can be made from $^1P_1^o$ to $^3P_1^o$ but that the reverse transition does not occur.

The shorter wavelength excitation band at 195mμ can then be ascribed to transitions to the 6s7p configuration.

Similar spectra with two close components in the main excitation band have been observed for NaCl, NaBr and NaI.

SOME GENERAL CONSIDERATIONS ON THE PREPARATION OF OXYGEN-DOMINATED PHOSPHORS

J. L. Ouweltjes and W. L. Wanmaker

North American Philips Company, Inc.
New York, New York

In the preparation of phosphors for practical applications the object is, of course, to attain as high an efficiency as is possible. It has been known for a long time that it is essential to use very pure ingredients for the purpose. In the case of the sulphides the purity is often the limiting factor in the efficiency. The oxygen-dominated phosphors are in most cases prepared by firing a mixture of different oxides, or materials which form oxides on decomposition. In the making of a phosphor of high efficiency various factors are of importance.

1) The formation of the crystal lattice desired generally presents no difficulties. If the lattice is difficult to produce, this can often be facilitated by firing in steam or by the addition of mineralisers. The influence of fluorides in this latter connection is well known. It is considered that the introduction of fluoride into the lattice produces open metal sites thereby increasing the diffusion rate.

2) The composition of the crystal lattice. In several cases it is known that an excess of one or more of the constituents can be incorporated. An excess of silica may be incorporated in zinc silicate-manganese without appreciably affecting the efficiency of the phosphor. An excess of phosphoric acid can be taken up in halophosphates, whilst an excess of calcium leads to the formation of calcium antimonate owing to which the fluorescence is lost. The question arises as to whether an excess of one of the components can occur locally in a stoichiometric firing mixture. If, in a halophosphate, many grains containing an excess of calcium were to occur, these grains would not luminesce, thus reducing the efficiency.

Firing tests in which a normal halophosphate is mixed with a non-activated halophosphate containing an excess of calcium show that even among already-formed phosphor grains a considerable exchange of ions still takes place, which equalizes possible variations in composition.

3) The presence of foreign materials. When the reaction among the starting materials is not complete, no homogeneous phase is obtained and part of the starting materials or compounds formed intermediately must remain in existence alongside the crystal lattice. The influence of this on the efficiency depends on the absorption of the exciting radiation. This is shown by the influence of 2537 Å - absorbing calcium antimonate and non-absorbing unactivated halophosphate on the luminous

output of a halophosphate. The course of the formation-reaction of many phosphors is such that U.V.-absorbing oxides diffuse into compounds which do not show U.V. absorption. If the reaction is not complete the chance is great that U.V. absorbing material remains on the surface, so that the efficiency is reduced. An excess of the non-diffusing constituent is often added to counteract this. Examples of this are the addition of an excess of silica in the preparation of zinc silicate, and the addition of an excess of magnesium oxide in the preparation of magnesium tungstate. It has proved to be possible, in several cases, to make practically stoichiometric phosphors, provided that sufficiently reactive primary materials are employed, and a second firing with a little of the non-diffusing constituent is carried out.

4) The properties of the materials used. Materials with a high reactivity are generally used. In the preparation of zinc beryllium silicate, however, too reactive a beryllium oxide will interfere with the incorporation of the manganese. In the preparation of halophosphates difficulties occur when a highly reactive calcium fluoride is used. It is interesting to consider the relation between the grain size of the materials used and the grain size of the fired phosphor. The latter is often determined by the grain size of the non-diffusing main constituent. If this has a strong tendency to sintering at the firing temperature, however, the grain size of the other components also plays an important part.

Abstract Number 40

THE ACTIVATOR SYSTEMS IN ZINC SULFIDE AND HALOPHOSPHATE PHOSPHORS

J. S. Prener and F. E. Williams

General Electric Research Laboratory
Schenectady, New York

The nature of the activator systems in copper- and silver-activated zinc sulfide has been a subject of much discussion.[1] In order to learn more about these phosphors, we prepared zinc sulfide containing copper located unambiguously at substitutional zinc sites.

High purity zinc oxide was irradiated in the Idaho Falls Reactor until the concentration of radioactive zinc-65 was 0.0034 per cent. The zinc oxide was then converted to zinc sulfide by heating at 900°C in a stream of dry H_2S containing a small quantity of HCl. Zinc-65 decays with a half-life of two hundred fifty days to stable copper-65 by K-electron capture and the emission of a 1.12 mev. gamma ray. The recoil energy associated with this gamma ray emission is 10.3 ev.

In the case of Ge, Lark-Horovitz[2] found that 30 ev were necessary to produce vacancies and interstitials. A calculation based on an ionic model of ZnS indicated that at least one-half of the Cu atoms remain at substitutional zinc sites. We concluded, therefore, that in the experimental material most of the Cu atoms formed by the decay of zinc-65 remain at the zinc sites.

The initial copper content, due to the decay of zinc-65 during irradiation and before the zinc sulfide was prepared, amounted to 0.00025 per cent. This initial Cu content together with the halogen used in the preparation of the zinc sulfide gave rise to an emission spectrum when excited by 3650 Å ultraviolet that consisted of the green Cu band peaking at 5160 Å and the blue "self-activated" band at about 4500 Å. We obtained additional emission spectra as the transmutation of zinc to copper occurred until the copper content rose to .00154 per cent. We could observe no change in the ratio of the green to blue peak, although based on the data of Urbach[3] and our own experiments, there should have been a detectable change had the coppers, formed by the decay of zinc-65, given rise to activator centers. These results and the known independence of the emission spectrum on the nature of the coactivator in zinc sulfide phosphors indicated two things consistent with the substitutional model described in this paper:

1. Isolated copper at zinc sites does not give rise to an activator system.

2. The chlorine and copper in zinc sulfide are spatially associated but are not nearest neighbors.

We propose the following substitutional model of the activator system in copper-activated zinc sulfide phosphors based on the covalent bonding existing in this material. The electronic configuration of zinc in zinc sulfide is $1s^2 2s^2 2p^6 3s^2 3p^6 3d^{10} 4s 4p^3$ and four tetrahedral bonds can be formed. Copper, having one less nuclear charge can make only three complete bonds to neighboring sulfurs with the remaining bond being incomplete. This gives rise to an empty state associated with the bonding electrons, and this state is located above the filled band of zinc sulfide. Thus, while copper introduces a localized level, the level is empty and cannot give rise to luminescence. The presence of halogen having one nuclear charge more than sulfur can form four complete bonds to neighboring zincs with an extra electron trapped in the coulombic field of the excess positive charge. This gives rise to a filled localized level below the conduction band of zinc sulfide. At equilibrium the electron in the field of the halogen will be transferred to the copper yielding a filled localized level above the conduction band and an empty trapping level below the filled band. Thus the presence of halide is necessary for the production of an activator system and its function is not primarily that of a flux or charge compensator.

A halogen and a copper in zinc sulfide will be attracted coulombically and at the firing temperatures of phosphors where diffusion is rapid, this attraction will give rise to a halogen near a copper rather than a random distribution of the two. The free energy of the system will be a minimum when the halogen is at a second or third nearest neighbor sulfur site rather than at nearest neighbor sites. This results from the condition that for the nearest neighbor configuration, the polarizability of the copper-halogen bond leads to a partial neutralization of the charges resulting in a very small coulomb attraction. The independence of the emission spectrum on the nature of the coactivator and the high efficiency of these phosphors with both ultraviolet and cathode-ray excitation are in accord with this interpretation.

The crystal structure of the calcium halophosphate phosphors activated by Mn^{++} and Sb^{+++} is that of the mineral apatite. The structure of the apatites has been studied.[4,5] There are ten Ca^{++} ions in the unit cell occupying two different crystallographic sites. Six of the ten Ca^{++} ions have as nearest neighbors five oxide ions and a fluoride ion, or two chloride ions, although the details of the halide positions in mixed chloro-fluoro apatites are not known. It has been recognized[6] that the Mn^{++} ions probably occupy these Ca^{++} sites since the position of the Mn^{++} emission band is sensitive to changes in the ratio of chloride to fluoride. We propose that the Sb^{+++} also occupy these sites and that concurrently an $0^{=}$ replaces a halide ion at the $00\frac{1}{4}$ and $00\frac{3}{4}$ sites. In this manner charge balance is achieved locally leading to a configuration of minimum free energy. The Sb band would be relatively insensitive to changes in the halide ratio since its nearest neighbors would be $0^{=}$ ions. Such a replacement by $0^{=}$ is reasonable in view of the similarity in the ion sizes of $0^{=}$ and F^{-} and the similarity in structure of the halo- and oxy-apatites.[5]

In the stoichiometric apatite structure the ratio of CaX_2 to P_2O_5 is 1:3. If x/2 moles of Sb_2O_3 are added per mole of apatite, this ratio would be reduced. Thus pure calcium halophosphate could be written as $9CaO:3P_2O_5:CaX_2$, whereas the phosphor containing x/2 moles of Sb_2O_3 and y moles of MnO would be $x/2\ Sb_2O_3:yMnO:9-x/2-yCaO:3P_2O_5$: $1-x/2\ CaX_2$. We therefore predict a lower CaX_2 to P_2O_5 ratio in the activated phosphor as compared to the pure halophosphate.

The authors would like to thank Dr. Louis Stang and his group at the Hot Laboratory of the Brookhaven National Laboratory for their help in the preparation of the zinc sulfide from the highly radioactive ZnO. We also wish to thank the Phillips Petroleum Company and the staff at the Idaho Falls Reactor for irradiation of the sample of zinc oxide.

References

1. H. A. Klasens, J. Elect. Soc. 100, 72 (1953).
2. Lark-Horovitz, Semi-Conducting Materials, Academic Press, p. 64 (1951).
3. D. Pearlman, N. R. Nail and F. Urbach, Preparation and Characteristics of Solid Luminescent Materials, John Wiley and Sons, p. 358 (1948).
4. St. Naray-Szabo, Zeit. Krist. 75, 387 (1930).
5. S. B. Hendricks, M. E. Jefferson and V. M. Mosley, Zeit. Krist. 81, 352 (1932).
6. K. H. Butler and C. W. Jerome, J. Elect. Soc. 97, 256 (1950).

Abstract Number 42

RETENTION OF CHLORIDE IN FIRED ZINC SULFIDE

P. Goldberg, D. J. Bracco, and A. Kremheller

Chemistry Laboratory
Sylvania Electric Products Inc.
Flushing, N. Y.

Many recent investigations[1] show that small traces of fluxes are of paramount importance in the preparation of commercial luminescent solids. Except for cases similar to manganese-activated zinc sulfide, efficient phosphors can only be prepared from zinc sulfide under high pressure at elevated temperatures when no flux is used. The presence of flux exerts a pronounced influence on the luminescence properties, the crystal structure and the particle size of zinc sulfide powders. Different fluxes, e.g. alkali and zinc halides, differ considerably with respect to the effect of the anions and cations of the fluxes on the above properties. These investigations of the quantitative influence of fluxes depend on the determination of small traces of halides. This paper presents a method for determining chloride in zinc sulfide by a concentration cell procedure according to Furman and Low (Jour. Am. Chem. Soc. 57, 1585 (1935)), and this technique can as well be used for the determination of other halides. This method may be employed to study the correlation of traces of chloride in ZnS with particle size, crystal structure and luminescence properties. Some of these correlations will be discussed in the next paper.

The determination of chloride is attained by measuring the e.m.f. between two silver-silver chloride electrodes which are suspended in solutions with different concentrations of chloride. In one part of the cell the concentration is $0.01 + x$ and in the other x, where x is the molarity to be determined. The theory leads to the following equation:

$$E = 0.0591 \log \left(2(x + 0.01)/\left(x + \sqrt{x^2 + 4\,P_0/f^2}\right)\right)$$

With E = e.m.f., x = moles of chloride per liter, P_0 = solubility of AgCl in pure H_2O and f = activity coefficient. The value of f is found experimentally by using a solution with $x = 0$ and measuring the e.m.f. A graph for the above equation facilitates the determination of x. The results obtained by this technique are accurate and reproducible, as many other investigators and our own determinations have proven. Amounts of 10^{-5} mols of chloride per liter of solution were determined quantitatively.

The experiments were conducted in order to study the concentration of Cl^- at various stages of preparation of luminescent zinc sulfide powders. Samples of zinc sulfide powders containing chloride between

less than 0.002 and 30% by weight were fired in open boats and sealed vials. The firing procedure was conducted in a boat or vial and combustion tube of transparent quartz. A slow flow of helium eliminated the contamination of samples by air during the open boat firings. The vials were evacuated for 1 hour at 150°C before they were sealed off. The samples of zinc sulfide powders were precipitated from zinc chloride or zinc sulfate with hydrogen sulfide. They contained very small amounts of heavy metals, generally below the limit of detectability by spectrographic procedures. The size of the precipitate was always below 0.1 micron. The fired samples were washed in water and sodium or zinc sulfate solution[2] in order to remove surface chloride. Samples of powder with added zinc chloride (28% of Cl^-, the powder contained no volume chloride) showed an increase in volume chloride up to about 600°C when fired for 2 hours in open boats. In the vicinity of this temperature a maximum of retained (volume) chloride occurs, and the amount of (volume) chloride decreases again at higher temperatures. Open boat firing of samples with added chloride or such acquired during precipitation led always to reduction of chloride, even down to the limit of detectibility, if the temperature and time of firing were high and long enough. The above retention of chloride may take place essentially in the lattice, as D. T. Palumbo and A. K. Levine have suggested recently.

The observed retention of chloride in zinc sulfide powder fired above 800°C in sealed vials is quite different. Here the amount of chloride in the powder increases with the time and temperature of firing. However, if growth occurs simultaneously there is also some dependence of retained chloride on the particle size obtained to be observed. Powders fired at 850°C for 4 hours contain more than twice as much chloride as those fired at 1000°C. for the same time. The mean diameter of particles fired at 1000°C is in this case about 20 times larger. A suggested explanation for this behavior may be the competition between a chloride-rejecting growth process and the chloride-introducing diffusion. The relatively large surface of small particles permits the diffusion of a high amount of chloride into the volume.

Another series of experiments shows the comparatively slow diffusion of chloride into the bulk of the powder. Samples with 0.5% of zinc chloride by weight added were fired in sealed vials for 3 hours at 850°C. The amount of volume chloride was found to be 0.014%. A portion of these samples was washed in order to remove surface chloride, while other batches were not washed (these contained 0.22% of chloride). Both categories of samples are presumed to contain, however, the same amount of volume chloride. The washed and unwashed samples were now fired in open boats for 3 hours at 900°C. If the diffusion rate of chloride is high we should now find a larger amount of chloride in the unwashed sample; however it contains only 0.009% of chloride, only 10% more than the washed sample. This result shows that the diffusion rate of chloride into the volume is much smaller than the evaporation of chloride from the surface of the particles.

References

1. P. Goldberg and A. K. Levine, An Examination of the Role of Fluxes in Zinc Sulfide Phosphors, Presented at the Chicago Meeting of the Electrochemical Society, May 2 to 6, 1954.

2. D. T. Palumbo and A. K. Levine, The Adsorption of ZnS Precipitates for Chloride and Sulfate Ions, Presented at the Chicago Meeting of the Electrochemical Society, May 2 to 6, 1954.

Abstract Number 43

PARTICLE SIZE AND STRUCTURE OF FIRED ZINC SULFIDE POWDERS

A. Kremheller, D. J. Bracco, and P. Goldberg

Chemistry Laboratory
Sylvania Electric Products Inc.
Flushing, N. Y.

Many investigators have emphasized the importance of flux on the properties of zinc sulfide as a phosphor. This paper will deal particularly with the influence of time and temperature of firing and the effect of various fluxes on particle size, crystal structure and luminescence of zinc sulfide powder. The experimental arrangement is the same as described in the paper by these authors on the retention of chloride, but in this investigation more emphasis has been laid on experiments in sealed evacuated vials in order to keep a constant proportion of flux during the firing procedure. The purest available ZnS powder was used containing metallic impurities below the limit of spectrographic detectability, amounts of chloride below 0.002% and of sulfate about 0.45% by weight.

The particle size of fired samples was determined by gas adsorption (BET method) and microscopic counting. The gas adsorption and counting procedures are in good agreement for particle sizes above 4 microns, and the deviation was then below 10%, especially, if the material was well crystallized. The reproducibility of the particle size with the firing conditions proved to be as good as the measurements of the mean diameter. Some samples were checked by a simplified, rapid BET method developed by D. T. Palumbo and F. Starkweather of our laboratory. The luminescence decay times and intensities were estimated visually by comparison with standards. A similar classification procedure was applied in the determination of the ratios of hexagonal to cubic structure of powders. The magnitude of the effects observed justifies, however, these comparatively fast qualitative procedures.

Samples without flux added were fired from 850° to 1200°C for 1 to 16 hours in sealed evacuated vials of transparent quartz. Even at 850°C and firing times of 3 hours as much as ten percent of the fired cubic powder is transformed to the hexagonal structure. At higher temperatures the structure turns gradually to the hexagonal form until above 1050°C the fired powders are completely hexagonal. The particle size increases exponentially with the temperature and with the square root of the firing time, and follows very closely the formula:

$x = A\, t^{\frac{1}{2}} \exp\left(-\frac{a}{T}\right)$ where x = mean diameter of particles, a and

A = constants (which were found to depend on the kind and amount of flux added), t = time and T = absolute temperature. The equation can be derived with the assumptions that dx/dt is proportional to 1/x, the initial x_0 is much smaller than x, and the supersaturation is proportional to the vapor pressure. The first assumption implies that the growth process may be understood as a diffusion problem, and a reasonable basis can be shown for the other assumptions. The growth energy is included in a, and A is a parameter containing the concentration of the vapor in the vicinity of the surface of the growing particle. The size of particles obeyed the same equation as in the case of sealed vials when powders were fired for 4 hours at the same temperatures in open boats without flux added. Luminescence intensities increase about proportional with the temperature to nearly 100 times the values at 850°C, a slight decrease seems to occur at the highest temperature of 1200°C.

Another series of experiments yielded quite unexpected results, when 0.1 to 0.5% by weight of zinc chloride was added to the zinc sulfide powder in sealed vials. The particle size vs. temperature plot shows a marked peak near 970°C for three different firing times. A final explanation for this observation is still being sought, but it seems likely there are 2 implications: a. The presence of lattice chloride has a pronounced influence on the crystal structure, and b. The rate of diffusion of chloride into the zinc sulfide lattice is different for the cubic and hexagonal form. Another, probably closely related explanation is the coincidence between maximum crystallographic disorder and the anomalous particle growth in the very same temperature region. The crystal structure was partially hexagonal for powders fired at 850 and 900°C and completely hexagonal for those fired above 1050°C; the large crystals belonging to the peak at 970°C were completely cubic. The latter crystals contained also 5 times less chloride than the small crystals obtained below 900°C and above 1050°C. This result may suggest the simultaneous presence of a chloride-rejecting growth process and diffusion.

The growth equation is also accurate within 10% for the particle size data published by Leverenz (Luminescence of Solids, Wiley and Sons, New York, 1950, p. 50) for zinc sulfide powder with 2% of sodium chloride added and fired for various times and temperatures. It is supposed that in Leverenz' experiments the effective flux concentration does not change during the firing in covered crucibles, because the vapor pressure of the flux, and accordingly the rate of evaporation, is low up to 1200°C. The value of a in the formula is 3 times smaller for Leverenz' data than for our own data with no flux added. This may indicate a lowering of the growth energy by the presence of the flux.

If time and temperature are held constant in the above equation, it might be possible to find the parameters on which 'a' and 'A' depend. Correlations between particle size, flux, and crystal structure, have been obtained by firing powders with 0.007 gm atoms of flux per mol of zinc sulfide added in sealed vials at 850°C for 3 hours as shown in the accompanying table.

	Kind of flux									
	NaF	NaCl	NaBr	NaI	ZnF_2	$ZnCl_2$	$ZnBr_2$	ZnI_2	ZnO	$ZnSO_4$
Part. size μ	1	10	14	8	<1	1	<1	3	1	1.5
Hex.: Cubic	1:9	0:10	0:10	0:10	2:8	2:8	3:7	0:10	1:9	1:9

One should observe that these experiments yielded hexagonal structure only with very small particle size. The crystal habit of powders fired with sodium halides is in the form of triangular plates compared to the spherical polyhedra observed without flux and with $ZnCl_2$ added. It is expected that the vapor pressure, the melting point, i.e., the state of aggregation of the flux, profoundly influence the properties under study.

References

1. P. Goldberg and A. K. Levine, An Examination of the Role of Fluxes in Zinc Sulfide Phosphors, Presented at the Chicago Meeting of the Electrochemical Society, May 2 to 6, 1954.

Abstract Number 44

THE OXIDATION OF ZINC SULFIDE PRECIPITATES TO ZINC SULFATE

Dominic T. Palumbo and Albert K. Levine*

Chemistry Laboratory
Sylvania Electric Products Inc.
Flushing, N. Y.

INTRODUCTION

The effect of moisture and oxygen on precipitated ZnS is an unresolved problem in the chemistry of this material. The sum of the literature is a report by Babkin[1] that on remaining in water for 75 days at room temperature about 3% of the sulfide is converted to the sulfate and a paper by Work and Odell[2] who report that 7.5% of ZnS was converted to ZnO by heating in the presence of water vapor at 600°C.

The extent to which the following reactions occur:

$$(1)\quad ZnS + H_2O \longrightarrow ZnO + H_2S$$
$$(2)\quad ZnS + 2O_2 \longrightarrow ZnSO_4$$

under normal processing of precipitated ZnS, i.e., filtering at room temperature and drying at 110°C are of interest. Quantitative data of this nature would be useful in attempting to prepare ZnS phosphor with the minimum possible oxide content.

EXPERIMENTAL

Samples of ZnS were prepared from $ZnCl_2$ and $ZnSO_4$ solutions by precipitation with H_2S. After precipitation, the samples were washed until the filtrate was free of sulfate and chloride, and then dried at 110°C for 24 hours.

Drying of ZnS

The effect of drying wet ZnS cakes was investigated by following the change in weight of precipitates and of fired ZnS samples during cyclic wetting and drying at 110°C. For the reaction of ZnS with H_2O to form the oxide we would expect a decrease in weight of the sample of 1.6 mg/gm ZnS for each 1% conversion. For the formation of sulfate an increase of 6.5 mg/gmZnS/1% conversion is expected. With precipitated samples the fluctuations in weight were too great to indicate a trend. For fired samples the weight changes were small indicating no

*Assistant Professor, Brooklyn College, New York; Consultant, Chemistry Laboratory, Sylvania Electric Products Inc.

appreciable conversion to the oxide or sulfate takes place.

Oxidation of ZnS to $ZnSO_4$

In investigating the removal of contaminating $SO_4^=$ from precipitated ZnS by digestion in H_2O it was found that the sulfate content of the system increased. No attempt was made to exclude air during the digestion. Samples of ZnS refluxed with water through which air was bubbled also showed increases in sulfate content.

To determine whether air (oxygen) is required for the reaction samples of ZnS free of $SO_4^=$ contamination were refluxed under a helium atmosphere. The helium was scrubbed with VSO_4 solution to remove oxygen[3] and then with H_2O to prevent entrainment of VSO_4 into the reaction vessel. Precautions were taken to insure that oxygen did not enter elsewhere in the experimental procedure. It was found that only 0.008% $SO_4^=$** was formed after 138 hours refluxing. Where air was introduced in the system 0.11% $SO_4^=$ was formed after 96 hours refluxing.

As a measure of the rate of sulfate formation as a function of temperature duplicate samples of ZnS were digested at 25°C and 70°C for 280 hours. In the case of samples digested at room temperature the increase in sulfate content was 0.02% compared to an increase of 0.10% at 70°C.

To measure the effect of surface area of the sample on the rate of sulfate formation a precipitated ZnS and a fired ZnS were digested for times up to 400 hours at 25°C and 70°C. After 400 hours at 70°C the precipitated samples showed an increase in sulfate of 0.08% while the fired samples increased by 0.012% .

DISCUSSION

The investigation of the formation of sulfate was designed to determine the effect of water, air (oxygen), temperature and sample surface area on the rate of reaction. The data show (1) that little if any sulfate is formed when dry zinc sulfide is heated in air, (2) sulfate formation increases with increased temperature and surface area in the presence of air and water, (3) when zinc sulfide is in contact with water, and air is excluded from the system, there is negligible or no formation of sulfate. The data support the hypothesis that the reaction to form the sulfate cannot proceed in the absence of O_2 and water. The requirement that water be present to effect conversion implies that the oxidation occurs in the aqueous phase via the sulfide ion.

**0.003% is the lower limit of quantitative determination in the gravimetric method employed.

References

1. M. P. Babkin, Zhur. Anal. Chem., 2, 118 (1947)
2. L. T. Work and I. H. Odell, Ind. Eng. Chem., 25, 411, 543 (1933)
3. L. Mietes and T. Mietes, Anal. Chem., 20, 984 (1948)

Abstract Number 45

LEAD AND MANGANESE ACTIVATED CADMIUM FLUOROPHOSPHATES

R. W. Wollentin

Westinghouse Electric Corporation
Bloomfield, N. J.

Previous work on cadmium phosphate phosphors containing fluorine by McKeag[1], McKeag and Ranby,[2,3] and Prener[4] describe the effects of lead and fluorine on the phosphorescence of cadmium phosphate activated by manganese. In these instances the concentrations of the lead and fluoride were of a low order of magnitude. Also the introduction of sodium fluoride to the manganese activated cadmium phosphate is mentioned as producing a red emitting material by McKeag.[1] Prener[4] describes a red emitting phosphor of manganese activated cadmium phosphate containing 5 to 20% zinc fluoride.

In the course of an investigation of the cadmium phosphate phosphors for consideration in fluorescent lamp applications, it was found that lead and manganese, in proper proportions, will activate cadmium phosphate containing a substantial amount of fluorine to give a double-band emission, with both peaks in the visible region, under 2537A ultra-violet excitation. The relative heights of the emission peaks are dependent upon the concentration of activators.

The introduction of lead alone into cadmium fluorophosphate produces a small but measurable blue fluorescence with an optimum at about 1% lead by weight of cadmium phosphate. The emission is peaked at about 4600A for small amounts of lead and about 4700A for larger amounts. Manganese alone gives a fairly strong emission peaked at 6000A and a slight secondary peak about 4000A. The 4000A peak is probably traceable to a small amount of lead present as an impurity in the raw materials. Combinations of lead and manganese produce spectral emission curves displaying two peaks in all instances and differing only in the relative heights of one peak to the other. The lower wavelength peak at about 4600A is suppressed by increasing proportions of both manganese and lead to give predominantly the characteristic manganese emission at about 5900A. The longer wavelength peak is affected by the presence of foreign ions added in appreciable quantities to the base material as fluorides. For example, magnesium, zinc, sodium, and potassium fluorides cause a shift of the longer wavelength peak towards the red. For potassium and sodium the maximum shift is about 300A, for zinc about 250A, and for magnesium about 100A. Calcium, barium, aluminum, and strontium do not influence the emission spectrum.

The effect of activator concentration on the spectral emission of the sodium fluoride modification differs from that of the pure cadmium

fluorophosphate in that the blue emission is less prominent except when the sodium fluoride is below two moles per three moles of cadmium phosphate. Also the longer wavelength peak becomes sensitive to the manganese concentration in that there is a shift towards the red on increasing manganese.

The emission spectra of the cadmium fluorophosphates are influenced by temperature. At -196°C the yellow or red manganese emission is greatly suppressed. At temperatures of 50°C or higher the emission becomes more yellow as the blue emission is suppressed. The phosphorescence is yellow in all instances and at all temperatures of observation.

The relative brightness of these phosphors is dependent upon the activator concentrations and presence of foreign ions. Representing the basic formula as $Cd_3(PO_4)_2 \cdot CdF_2$:Mn,Pb, the optimum concentrations are 0.695 percent manganese and about 6.0 percent lead based upon the weight of $Cd_3(PO_4)_2$. The lead concentration is not critical and may be varied from two to ten percent without influencing the brightness greatly. In the sodium modification, which may be represented as $3Cd_3(PO_4)_2 \cdot 4NaF$:Mn,Pb, the optimum concentrations are about 4.0 percent manganese and 4.0 percent lead. In this case the brightness is more sensitive to the lead concentration than before. The brightest phosphor is the yellow emitting cadmium fluorophosphate. The red emitting sodium modification has about the same brightness as a well prepared cadmium borate and just slightly less than calcium silicate, lead and manganese activated.

Structure studies of these materials by means of x-ray diffraction indicate a number of complex structures. The patterns contain more than forty lines, in some instances, that vary in order of intensities and line positions from sample to sample. In general the samples may be classified into four groups, one of which agrees with the apatite structure reported by Rooksby and McKeag.[5] Another of these groups is quite similar with respect to line positions but differs notably in line intensities. The third group differs in both line positions and intensities from an apatite pattern and the fourth group consists of a number of completely different patterns, that may better be termed miscellaneous. Positive identification of most of the patterns is complicated by the lack of published data and standard x-ray patterns on cadmium phosphate compounds. The materials showing a definite apatite structure consists of those in which each of the following were reacted with three moles of cadmium orthophosphate: 2.5 moles of cadmium fluoride, 2.0 moles of aluminum fluoride, and 1.5 moles of barium fluoride. Higher amounts of cadmium and aluminum fluorides gave similar line positions but different orders of intensities. Oddly enough, both higher and lower amounts of barium fluoride produced completely different patterns as did also sodium and potassium fluorides.

References

1. A. H. McKeag — U.S. Patent 2,214,643, — 1940
2. A. H. McKeag and P. W. Ranby — British Patent 581,778, — 1946
3. A. H. McKeag and P. W. Ranby — U.S. Patent 2,476,676, — 1949
4. J. S. Prener — U.S. Patent 2,636,010, — 1953
5. H. P. Rooksby and A. H. McKeag, "X-rays In The Development of Inorganic Phosphors," G.E.C. Journal, Volume XVII, 2, April 1950

Abstract Number 46

CALCIUM HALOPHOSPHATE PHOSPHORS
II OPTICAL PROPERTIES OF THE PARTICLE SURFACE

M. J. Bergin, K. H. Butler, and H. H. Homer

Sylvania Electric Products, Inc.
Salem, Mass.

In most discussions of phosphor behaviour an implicit assumption is made, namely, that the phosphor particles are homogeneous and uniformly fluorescent throughout. In the case of halophosphate phosphors particularly it is quite probable that the surface of the phosphor crystal may be quite different from the body of the particle. Two characteristics contribute to this; first is the ready loss of chloride and antimony during firing which would tend to give a surface layer different in composition from that within the crystal; the second is the ready oxidation of manganese present in solid solution in the lattice near the surface.

When the halophosphate phosphors contain manganese, oxidation tends to give a pink discoloration due to Mn ion in the lattice with a valence above 2, while deviation from the normal chloride content tends to give a grey discoloration due to separation of a free manganese oxide. Complete loss of antimony will of course give non-fluorescent material.

The ready solubility of the halophosphates in dilute mineral acids makes it possible to investigate readily the properties of the surface of the phosphor crystals by observing the changes in the optical properties of the powder resulting from treatment with acids.

The brightness of fluorescence with excitation by 2537 radiation, and the reflectance spectrum between 2500 and 4000A have been found to be rather sensitive indicators of the condition of the phosphor surface. Removal by acid treatment of the surface layer formed in firing gives some increase in brightness of fluorescence when small amounts of manganese are present and this increase in brightness is more marked as the manganese content increases. The reflectance is also improved by the acid treatment indicating the presence of some absorbing material in the surface layer.

A very mild acid treatment is sufficient to remove this absorbing layer of phosphors with low manganese content while a more severe treatment is needed for complete removal of the layer when the manganese content is high.

In addition to these effects both the emission and the excitation spectra are somewhat affected by the removal of the surface layer indicating that the composition of the surface is different from that of the body of the crystal. Other evidence, such as reflectance in the visible,

suggests that partial oxidation of the manganese may also take place.

While changes in phosphor behaviour can be observed directly on the powder there are also changes in the performance of lamps made with acid treated phosphors. As would be expected, the initial LPW is increased by the use of acid treated phosphor, but it is rather unexpected to find also that the lumen maintenance during burning of the lamps is appreciably improved.

Abstract Number 47

A NEW BLUE-EMITTING PHOSPHOR WITH MANGANESE ACTIVATOR

Edward L. Lind

Radio Corporation of America
RCA Laboratories
Princeton, N. J.

Manganese is unique in functioning as an almost universal activator providing efficient phosphors. In addition manganese has a long-lived excited state and gives some of the longest exponential decays known. The emission of phosphors with manganese activator is known to vary from the green-blue to the infrared. Kröger[1] has called attention to the lack of a blue-emitting phosphor with manganese activator. The shortest peak wavelengths previously described for efficient manganese activated materials are 5060Å[2] for $ZnGa_2O_4$:Mn, an oxygen dominated system, and 4950Å[3] for CaF_2:Mn, a fluorine dominated material. A recent paper[4] reporting research on fluorides with manganese activator describes the properties of a number of materials in which a blue emission was sought but not found.

Smith[5] and Klasens, et al[4] have extended the Linwood-Weyl[6] correlation between the color of manganese emission and the structure of the host crystal to include the size of the host crystal cation and cation-anion distances. From these correlations, a blue-emitting phosphor with manganese activator might be expected from a fluoride having a coordination number of eight and a cation size larger than that found in CaF_2. However, incorporation of SrF_2 in CaF_2:Mn to expand the CaF_2 lattice results in a shift of the emission band toward longer wavelengths.*

Since an expansion of the lattice of CaF_2:Mn causes a shift to longer wavelengths, a means of contraction was sought in the hope of obtaining a shift to shorter wavelengths. Because beryllium is a smaller cation than calcium, the system CaF_2-BeF_2 was investigated with manganese activator, and $CaBeF_4$:Mn synthesized. The cathodo-luminescence of $CaBeF_4$:Mn was found to be a blue emission band with a peak wavelength of 4750Å.

An investigation of the properties of $CaBeF_4$:Mn shows definitely that the blue emission of this material is to be attributed to the manganese activator. The decay of luminescence is exponential with the long decay time (60 to 70 milliseconds) expected for a manganese activated fluoride. The host crystal emission of pure $CaBeF_4$ is sufficiently different from that of the same material with manganese activator to demonstrate

*This result is independent confirmation of that found by Klasens, et. al., (4).

that manganese acts here as an originative activator. The optimum manganese proportion was found to be 0.006 mole of manganese per mole of $CaBeF_4$, which is typical of the optimum proportion required for other manganese activated phosphors. For this proportion, the peak efficiency of cathodoluminescence is 25% that of Zn_2SiO_4:Mn (RCA 33-W-2A).

X-ray analysis of $CaBeF_4$ by J. A. Amick[7] has shown that four of the eight nearest fluorine atoms surrounding the calcium (and manganese in $CaBeF_4$:Mn) are closer than in CaF_2. Thus, in CaF_2, $(Ca\text{-}Sr)F_2$ and $CaBeF_4$ phosphors with manganese activator the emission band shifts to shorter wavelengths as the cation-fluorine distance in these materials decreases.

References

1. F. A. Kröger, "Some Aspects of the Luminescence of Solids," p. 55, Elsevier Publishing Company, Inc., New York (1948).
2. H. W. Leverenz, "An Introduction to Luminescence of Solids," p. 72, John Wiley and Sons, Inc., New York (1950).
3. R. J. Ginther, J. Electrochem. Soc., 101, 248 (1954).
4. H. A. Klasens, P. Zalm and F. O. Huysman, Philips Research Reports 8, 441 (1953).
5. A. L. Smith, J. Electrochem. Soc., 101, 189 (1954).
6. S. H. Linwood and W. A. Weyl, J. Opt. Soc. Amer., 32, 443 (1942).
7. J. A. Amick, private communication.

Abstract Number 48

MAGNESIUM FLUOSILICATE PHOSPHORS

P. W. Ranby and S. T. Henderson

Thorn Electrical Industries, Limited
London, England

It is generally characteristic of titanium-activated phosphors which are excited by short wave ultra-violet radiation, that the optimum concentration of titanium must be high, usually of the order of several molar percent of the matrix, and similarly the efficiency of the luminescence is reduced, but without appreciable change in colour, when manganese is incorporated in the phosphor. This is in contrast to the behaviour of the magnesium fluosilicate phosphors described in this paper, in which the optimum concentration of titanium activator is low, and the incorporation of increasing proportions of manganese shifts the colour of the luminescence from greenish yellow through intermediate colours to orange pink. These phosphors are strongly excited by ultra-violet of wavelength 2537A and the intensity of luminescence decreases only slowly with rise in temperature above room temperature.

Magnesium fluosilicates are prepared from mixtures containing magnesium, silicon and titanium oxides with fluoride additions, using normal techniques of phosphor chemistry; they require no elaborate atmosphere control during the preparation. Some aspects of the preparation and the effects of impurities are described. These phosphors are stable to the various processes involved in the manufacture of fluorescent lamps and to the conditions within such a discharge tube. Initial efficiencies in a 48T12 40 watt lamp of nearly 60 lumens per watt, with good maintenance throughout life, have been obtained from fluosilicates activated by titanium alone. The chromaticity locus of a series of lamps made from phosphors with increasing concentrations of manganese crosses the black body locus at about 4000°K. The high proportion of red in the emission spectrum of these phosphors makes them of interest in the manufacture of lamps with improved colour rendering properties. As an example, lamps of 4500°K colour with good red emission can be obtained from mixtures of fluosilicates with barium titanium phosphate and calcium silicate (Pb,Mn); the properties of this lamp are compared with those of a conventional Cool White de luxe.

X-ray examination of the magnesium fluosilicate phosphors shows the existence of a new phase different from previously reported magnesium silicate structures. Some magnesium silicate phosphors which are prepared in the presence of magnesium fluoride and contain high concentrations of titanium have been described by Anderson and Wells (British Patent 74057, 25th August, 1954). These latter materials fluoresce greenish yellow when excited by ultra-violet and the colour

of the luminescence excited by cathode rays is moved towards the red if manganese is present in addition to titanium. However, X-ray examination of samples prepared according to the examples given by Anderson and Wells shows that these have a crystal structure very similar to magnesium orthosilicate and, therefore, are different from the magnesium fluosilicates.

Spectral energy distribution measurements on magnesium fluosilicates excited by 2537A radiation show a number of unusual features. For example, the emission from a material activated by titanium alone consists of a wide symmetrical band with a peak at about 17700 cm^{-1}, but this peak shows signs of two closely spaced maxima. Two distinct peaks appear with increasing amounts of manganese activator in the phosphor. Analysis of the emission attributed to manganese shows that it consists of a number of bands in which the frequency separation of the two main ones is close to that found for manganese bands in other doubly activated phosphors. On the other hand, the peak of the main manganese band (at 16400 cm^{-1}) appears to be much closer to the peak of the titanium band than would be expected by analogy with other sensitized phosphor systems. Otherwise the general behaviour of these materials is in keeping with a sensitization process.

It is suggested that in general the separation of the primary and secondary activator peaks has a direct bearing on the luminous efficiency of sensitized phosphor systems, according to whether there is overlapping of the two emission bands or not. That is, there may be an optimum spacing of the two bands in terms of luminous output, and calculations indicate that it may possibly have been reached in certain phosphor systems.

Abstract Number 49

PRELIMINARY STUDIES OF THE PEROWSKITE-TYPE TERNARY OXIDES AS LUMINPHORS

Salvador Terol* and Roland Ward

Chemical Laboratories
University of Connecticut

The properties of lanthanum aluminum oxide as a phosphor base material have been studied. The purest available lanthanum oxide samples gave products which were weakly cathodoluminescent due to the pressure of praeseodymium or samarium as impurities. The rare earth ions Pr^{+3}, Sm^{+3} or Eu^{+3} were the only activators which were found to be effective. Emission spectra of these phosphors are given. Other usual activators were found to be ineffective. The presence of rare earth impurities causes a pronounced body color to develop in the lanthanum aluminum oxide when the samples are ignited in air. This proves to be a more sensitive means of detection of impurities than spectrographic analyses.

*Present address: Optical Institute and Naval Research Laboratory, Madrid, Spain.

Abstract Number 50

TWO ARSENATE PHOSPHORS AND THE SIGNIFICANCE OF THEIR EMISSION

Gorton R. Fonda*

Arsenates and haloarsenates have been investigated as possible sources of luminescence because of their similarity in structure to the corresponding phosphate phosphors.[1] Two active compounds were found, zinc arsenate activated with manganese and calcium fluorarsenate activated with antimony and manganese. Their spectral emission was at longer wavelengths than exhibited by the corresponding phosphates. No fluorescence to speak of could be obtained with the arsenates of calcium, magnesium, and cadmium.

Zinc arsenate responded to activation by both manganese and lead to emit fluorescence of moderate intensity, lying in the orange and whitish blue respectively. It was prepared by firing an activated mixture of zinc oxide and arsenic pentoxide at 700-1000°C, preferably in an atmosphere of nitrogen. The concentration of manganese was 0.5% by weight. Its fluorescence was reduced when lead was present as well. Its peak emission at 25°C is at 6550Å, compared with 6380Å for the phosphate;[1] at 80°K it is displaced to 6720Å. Under excitation by 2537Å, its quantum output at 25°C is about 10% of that of magnesium tungstate. When it was prepared with 2% PbO, it emitted a broad band at 25°C with a peak at 4500Å but extending so strongly into higher wavelengths that its fluorescence was a blueish white. Reduction in temperature to 80°K served likewise to shift its peak emission to longer wavelength, 4700Å. At 25°C its quantum output was somewhat higher than that of the manganese activated phosphor.

Among the haloarsenates, calcium fluorarsenate was the only compound found to show a notable response to excitation. It was prepared from a mixture of 9 moles calcium oxide, 3 moles arsenic pentoxide, and 1 mole calcium fluoride. Weak fluorescence was obtained by activation with bismuth, cerium, lead, tin, and thallium. The brightest phosphors were those activated with antimony or manganese or both, fired at 1150°C. With antimony alone the fluorescence was a greenish yellow with a peak at 5000Å, compared with 4800Å for the fluorphosphate.[2] Its brightness was a maximum within the range of 0.5-4.0% Sb, added to the mixture before firing. Its quantum output under excitation by 2537Å was 15% of that of magnesium tungstate. With an 81% absorption of 2537Å, its quantum efficiency was 19% of magnesium tungstate. With manganese alone, there was a weak red emission. Its intensity was greatly increased on addition of antimony, denoting that the latter has a sensitizing action. The peak of the manganese emission was at

*Consultant to the General Electric Co.

6200Å, compared with 5680Å for the fluorphosphate.[2] With 1% Mn its brightness remained at a maximum over the range of 0.5-2.0% Sb. Despite the content of appreciable antimony, the antimony band was almost completely suppressed by the manganese. Under excitation by 2537Å, its quantum output was 27% of that of magnesium tungstate. With an 84% absorption of 2537Å, its quantum efficiency became about 30% of magnesium tungstate. X-ray diffraction patterns showed the fluorarsenates to be of apatite structure with a somewhat larger unit cell than characterizes the fluorphosphate.

The explanation for the shifts in emission seems to lie in the changes in field strength to which activator ions are subjected by their environment. Such a relation has been found by Klasens, Zalm and Huysman for manganese activated double fluorides.[3] An increase in spacing between manganese and fluorine ions was accompanied by a shift of the peak emission to longer wavelengths. As the authors phrase it, "the greater the space available for the manganese ion, the more the state of the free ion will be approached, hence the shift to shorter wavelength."

When an activator ion is in the field of the crystal lattice, the distances between its energy levels are smaller than for a free ion. The outer excitation orbits are under the repulsive force exerted by the field of the adjacent anions and their energy levels are correspondingly depressed. The extent depends upon the field exercised by the anions and this, in turn, upon their proximity. The shorter the spacing, the greater is the resulting crowding; hence, the shift in emission to longer wavelength. This view is of general application to phosphors of related composition. Although quantitative data are lacking for most phosphors, yet the direction in which the change in spacing occurs can frequently be perceived from related characteristics, such as the relative ionic sizes of the cations in a series of related compounds, or from the relative spacings of cations and anions in their oxides.

Greater crowding between an activator ion and the anions with which it is coordinated can be produced in the following three ways:-

1) Increasing the size of the cation of the compound. The manganese activated silicate phosphors furnish an illustration. The oxides of zinc, calcium, cadmium, and magnesium have a decreasing spacing between cation and oxygen in the order named and it is presumable that the same relation should persist in the silicates. Inasmuch as manganese substitutes for the cation, the spacing of manganese and oxygen should change in the same order and consequently the emission should be shifted to longer wavelengths, as is in fact observed. Even partial substitution in zinc silicate of a foreign cation of smaller ionic size, such as beryllium, lithium, or barium, has the same effect on the emission by producing a secondary band of longer wavelength; the greater crowding which produces it occurs wherever a Mn ion is adjacent to the small foreign cation.

2) Increasing the size of the anion. The alkaline metal halides activated with thallium furnish one example. Another is given by the

calcium halophosphates; a change in halogen from fluorine to chlorine shifts the manganese emission from 5680Å to 6000Å.

3) Increasing the size of the cation serving as kernel of an oxygen tetrahedral group. This case includes the arsenate and phosphate phosphors. It is illustrated also by the silicate and germinate of zinc, manganese activated. In the latter pair, the shift in emission, from 5250Å to 5370Å is produced by the substitution of the larger acid-forming cation, germanium. This is the same relation found for zinc arsenate and calcium fluorarsenate whose emission is shifted to longer wavelengths than in the corresponding phosphates, again by substitution of a larger acid-forming cation, arsenic. Because of this enlarging of the tetrahedral group, there is a closer crowding of oxygen ions about the activator ions, with the resulting shift in emission.

References

1. A. L. Smith, J. Electrochem. Soc., 98, 363 (1951); H. G. Jenkins, A. H. McKeag and P. W. Ranby, J. (and Trans.) Electrochem. Soc., 96, 1 (1949)
2. G. R. Fonda, J. Opt. Soc. Amer., 40, 347 (1950)
3. H. A. Klasens, P. Zalm and F. O. Huysman, Philips Research Reports, 8, 441 (1953)

Abstract Number 51

THE SYSTEM CADMIUM OXIDE-BORIC OXIDE

E. C. Subbarao and F. A. Hummel

Department of Ceramics
College of Mineral Industries
Pennsylvania State University
State College, Pa.

INTRODUCTION

Many investigators[1, 2, 3, 4] have reported on the luminescence of manganese-activated cadmium borate compositions, but very little documented information has accumulated on the number of compounds which exist in the system $CdO-B_2O_3$. Likewise, the phase diagram (Figure 1) of Mazetti and deCarli[5] appears to be incomplete in view

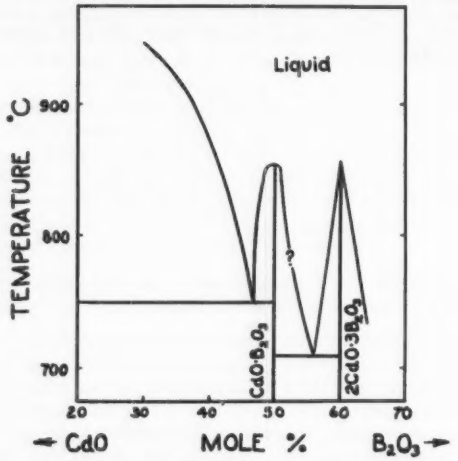

Fig. 1—System $CdO-B_2O_3$ (after C. Mazetti and F. deCarli, see footnote 1).

of more recent work on binary borate systems such as $CaO-B_2O_3$, $ZnO-B_2O_3$, $BaO-B_2O_3$, etc. The present work was undertaken to clarify the phase relationships in the system and to provide a substantial background for further work on the luminescent behavior of the cadmium borates.

EXPERIMENTAL

The chemically pure materials boric acid, cadmium carbonate and manganous carbonate were used for all preparations. Ten gram batches were mixed with ethyl alcohol, dried at 110°C and melted to glasses for use in quench work when possible. Only those compositions containing 50-60 mole per cent B_2O_3 would melt to a homogeneous glass. Compositions richer in B_2O_3 than 60 mole per cent developed immiscible liquids. Mixtures richer in CdO than the 1:1 ratio would crystallize very rapidly from the fused condition and in this portion of the system differential thermal analysis, thermal expansion, and high temperature X-ray data were used to determine the phase relationships.

Table I shows the analyzed compositions which were investigated and the refractive indices of those compositions which could be obtained as glasses. Several supplemental compositions were prepared during the course of the work, but they were not analyzed. The molecular compositions 2:3, 3:2, 2:1 and 3:1 are included in the table as reference points.

Table I

Analyzed Compositions and Refractive Indices of Glasses

No.	$\%B_2O_3$	Refractive Index of Glass (±.003)
1	46.09	1.670
$2CdO.3B_2O_3$	44.86	---
2	44.13	1.676
3	43.73	1.677
4	37.82	1.715
5	34.93	1.726
6	33.34	1.736
7	29.15	1.765
8	27.32	---
$3CdO.2B_2O_3$	26.55	---
9	26.38	---
10	22.49	---
11	21.44	---
$2CdO.B_2O_3$	21.33	---
12	20.16	---
13	19.00	---
$3CdO.B_2O_3$	15.31	---

RESULTS

A. The Immiscible Liquid Region

A very extensive region of immiscible liquids was established ranging from practically $100\%B_2O_3$ to $46.4\%B_2O_3$, in agreement with that found in other $RO\text{-}B_2O_3$ systems such as MgO-, CaO-, ZnO- and $BaO\text{-}B_2O_3$. No compounds exist under the immiscibility gap. The only crystalline phase which appears in this region below 980°C is the 2:3

compound whose composition lies just outside the two liquid area.

Only the 2:3 phase is observed in compositions which contain more than 46.4%B_2O_3 since any free B_2O_3 which is present will probably remain as a glassy film, undectectable by X-rays and difficult to detect under the microscope.

B. The Region Between the Compounds 3:2 and 2:3

The two compounds melt congruently, the 3:2 a little above 1000°C and the 2:3 (44.86%B_2O_3) a little below 1000°C. They form a simple eutectic system, with the eutectic located at 900°C and 36 weight per cent B_2O_3. The 2:3 compound has a high birefringence, with the minimum index of refraction 1.617, and the maximum 1.630. A few of the crystals develop sharp hexagonal outlines. The 3:2 crystals are elongated, with high birefringence, n_{max}>1.790 and n_{min} = 1.745. X-ray diffraction data for these compounds are given in Table II.

C. The Cadmium-Rich Region

The part of the system ranging from the 3:2 compound (26.55%B_2O_3) toward the CdO composition comprised the most difficult portion of the phase equilibrium work, since no compositions could be quenched to a glass, even in 100 milligram quantities. It was necessary to rely mainly on D.T.A. data, supported by some high temperature X-ray and dilatometric data, the latter being used only as a very indirect means of examination. Volatility problems become very severe in compositions containing more CdO than the 2:1 molecular ratio.

The 2:1 compound apparently melts incongruently at 892°C to the 3:2 compound and a cadmium-rich liquid. A eutectic between the 2:1 and 3:1 compound forms at 834°C and 17.6 weight per cent B_2O_3. The 3:1 compound melts congruently slightly above 1020°C.

The 3:1 compound exists in at least two polymorphic forms, a reversible inversion occurring at 870°C. The high temperature form on cooling from fusion reverts to the low temperature form with a very large change in volume, causing the sample to fall to dust, reminiscent of the well-known β to γ "dusting" of dicalcium silicate, one of the constituents of cement clinker. The X-ray patterns of the 2:1 compound and both forms of the 3:1 compound are given in Table II. The phase diagram for the entire system is shown in Figure 2, including the large region of immiscible liquids. In Figure 3, the two-liquid area is omitted and the diagram is enlarged to show the region of greatest interest with respect to phosphors, that lying between the 2:3 and 3:1 molecular ratios.

D. The Solubility of MnO in the 2:1, 3:2 and 2:3 Compounds

Since MnO is the most commonly used activator in cadmium borate compositions, a study of the solid solubility of the oxide was made using the three compounds of interest in the luminescent field. Petrographic and X-ray studies were made on compositions which were fused and others which were reacted below the temperature of liquid formation. It is estimated that about 0.5% MnO may be soluble in the 2:1 compound, 1% MnO in the 3:2 compound and 10% MnO in the 2:3 compound.

Table II

X-ray Data on Cadmium Borates

2:3		3:2		2:1		β 3:1		α 3:1	
d	R.I.	d	R.I.	d	R.I.	d	R.I.	d	R.I.
5.53	65	6.15	7	4.64	50	4.32	7	4.64	20
5.38	75	5.98	7	4.41	10	4.22	40	4.48	5
4.57	12	4.64	50	4.32	27	3.73	18	3.54	27
4.16	85	4.41	6	4.05	30	3.53	6	3.20	15
4.12	30	3.50	5	3.61	15	3.41	10	3.06	6
3.73	85	3.37	5	3.42	30	3.36	7	3.01	10
3.66	65	3.21	20	3.22	60	3.24	6	2.83	20
3.55	55	3.06	30	3.21	60	2.99	43	2.77) b.	20
3.21	100	2.96	44	3.06	25	2.87	100	2.76)	
2.99	30	2.83	100	2.99	90	2.80	8	2.54	8
2.93	70	2.76	25	2.96	50	2.68	50	2.49	7
2.75	30	2.72	25	2.91	60	2.55	8	2.34	10
2.69	20	2.58	10	2.82	100	2.43	40	2.29	9
2.56	85	2.40	10	2.79	15	2.39	15	2.25	10
2.45	18	2.24	6	2.76	60	2.24	4	2.08	17
2.37	25	2.22	6	2.71	30	2.11	4	2.06	3
2.34	8	2.09	35	2.58	35	1.93	7	2.01	6
2.28	80	1.96	10	2.46	5	1.86	30	2.95	5
2.19	7	1.88	7	2.40	30	1.84	5	2.92	30
2.17	40	1.84	8	2.32	30	1.78	35	1.89	16
2.06	13	1.78	7	2.22	20	1.703	20	1.79	4
2.01	50	1.776	9	2.16	15	1.688	10	1.743	9
1.97	75	1.732	20	2.09	50	1.641	5	1.726	10
1.92	18	1.723	20	2.02	5	1.493	7	1.660	31
1.85	18	1.703	5	2.00	8	1.468	11	1.646	12
1.84	5	1.694	5	1.88	5	1.458	11	1.569	5
1.79	25	1.682	5	1.85	17	1.416	36	1.562	10
1.792	35	1.641	20	1.80	3	1.363	9	1.541	3
1.781	45	1.617	4	1.776	10	1.267	6	1.527	8
1.757	6	1.592	12	1.729	16	1.199	6	1.502	4
1.732	40	1.534	4	1.705	10	1.195	4	1.460	30
1.691	8	1.509	6	1.657	5	1.123	4	1.407	8
1.676	8	1.474	5	1.641	10	1.110	8	1.390	10
1.660	18	1.430	6	1.611	5			1.360	10
1.604	14	1.416	4	1.594	17			1.341	5
1.571	12	1.407	5	1.431	7			1.271	3
1.524	16	1.358	50	1.394	10			1.205	3
1.520	15	1.348	5	1.352	5			1.169	10
1.461	19	1.241	10	1.344	8			1.118	4
1.422	10	1.185	5	1.232	6			1.092	8
1.403	12								
1.370	10								
1.353	12								
1.303	10								
1.277	8								
1.265	9								
1.168	6								
1.161	6								
1.157	6								
1.148	6								
1.131	8								
1.128	8								

R.I. = Relative Intensity
b. = broad line

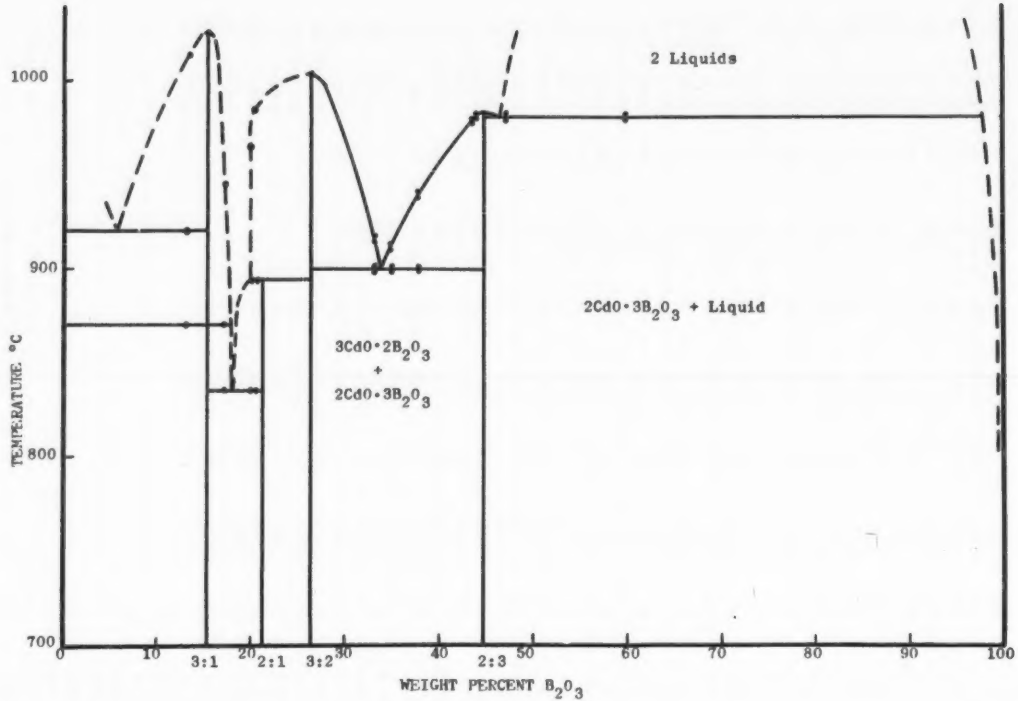

Fig. 2. System $CdO-B_2O_3$

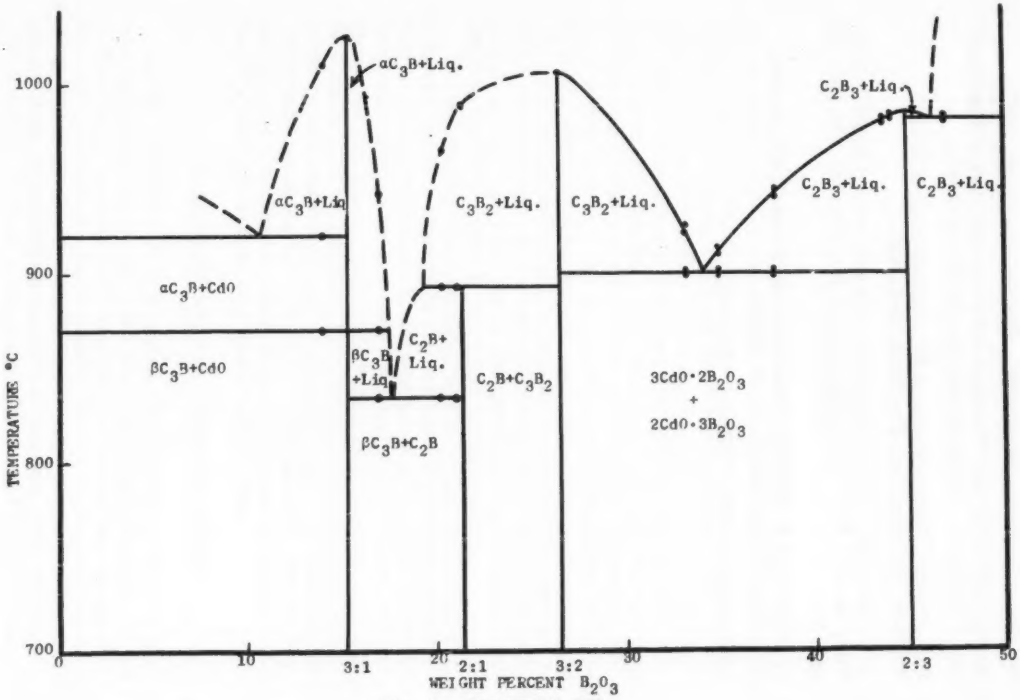

Fig. 3. System CdO-B_2O_3

References

1. Th. P. J. Botden and F. A. Kroger, "Fluorescence of Cadmium Borates Activated by Manganese", Physica, 13, 216-24 (1947).

2. R. Nagy and C. K. Lui, "Thermal and X-ray Analyses of Some Common Phosphors", J. Optical Soc. Am. 37, 37-41, (1947).

3. F. A. Kroger, "Some Aspects of the Luminescence of Solids", Elsevier Publishing Co., New York, 1948, p. 60.

4. H. W. Leverenz, "An Introduction to Luminescence of Solids", John Wiley and Son, New York, 1950, pp. 147, 168, 175, 233, 234, 256, 359 and 417.

5. C. Mazetti and F. deCarli, "Borate Anhydrides of Si, Cd, Pb, and Mn", Gazz. Chim. Ital. 56, 19-28 (1926).

   International Critical Tables, 4, 55 (1928).

Abstract Number 52

LUMINESCENT SCREENS MADE BY VAPOR REACTION

D. A. Cusano and F. J. Studer

General Electric Research Laboratory
Schenectady, New York

INTRODUCTION

A luminescent screen consisting of a continuous coating of transparent material has the advantage over a conventional screen of settled powder phosphor, that it is free from scattered light. In a powder screen it is not possible to avoid the diffuse scattering either of any light that is incident on it from outside, or of that which originates in the phosphor layer itself. Consequently, in a cathode-ray tube such as is used in an oscilloscope or a television picture tube, there is always a background illumination due either to the ambient light or to light from the luminescing area of the screen itself, which is diffused from grain to grain. This scattered light obviously puts a limitation on the contrast and resolution that can be attained in a cathode-ray tube presentation. The behavior of a powder screen is illustrated in a general way in Fig. 1. Fig. 2 gives an actual photograph of a linear cathode-ray trace on a powder screen in room light and in the dark.

The desirability of a non-scattering CRT screen has attracted considerable effort in attempts to produce one. The obvious approach - that of vacuum evaporation of luminescent materials with condensation of a clear layer on the face-plate - has not proved fruitful. In general, though the process may result in a very good transparent screen of the base material of the phosphor, the activator is almost invariably lost. In the results reported to date, in all cases where the evaporated film showed any luminescence, it has been of low intensity, with the lone exception of zinc fluoride. This phosphor is ruled out in practice because of its rapid deterioration under cathode rays.

ARRANGEMENT FOR VAPOR REACTION

Another method, that of producing the luminescent layer directly by vapor reaction, has yielded much more encouraging results. In this method the components which react to give the luminescent layer are brought together in the vapor phase at the heated glass surface on which the phosphor is to be deposited. Under proper conditions a continuous glassy layer of luminescent material is produced. Fig. 3 shows schematically the basic arrangement which has been used in this laboratory, particularly for zinc sulfide screens. The surface to be coated is supported in a quartz tube inside a furnace so that the temperature can be held at any appropriate point in the temperature range 400°C to

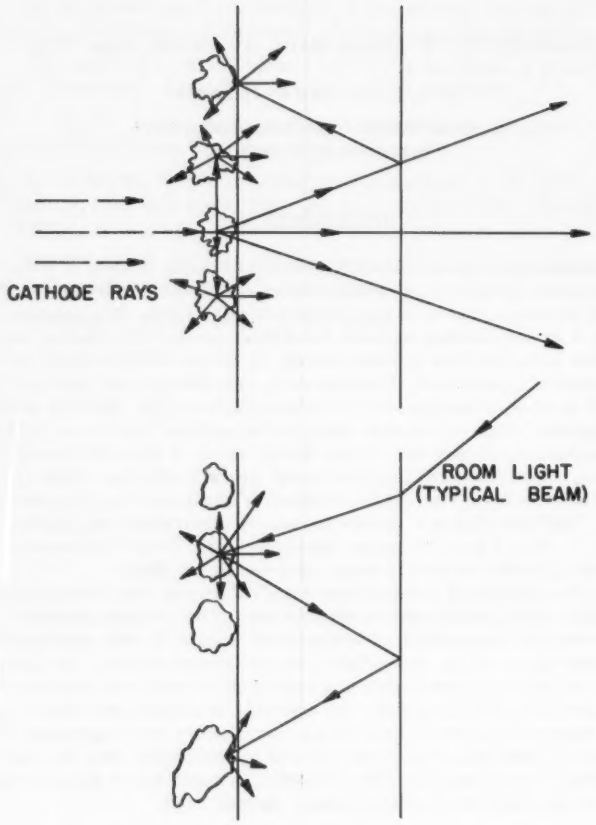

Fig. 1—Light scattering by powder phosphor screen.

700°C. The quartz tube extends far enough above the furnace so that it can be closed with a rubber stopper which has inlet tubes through it - one for connection to a vacuum pump, one for admission of H_2S, and one for introducing the reaction materials. It has been found advantageous to drop these materials onto the vaporizing appendix in powder form at a gradual rate, rather than as a single charge. In this way, the several vapor components will, on the average, be continuously present in the same proportion. If all the material were placed at one time in the evaporator, the high vapor pressure components would evaporate

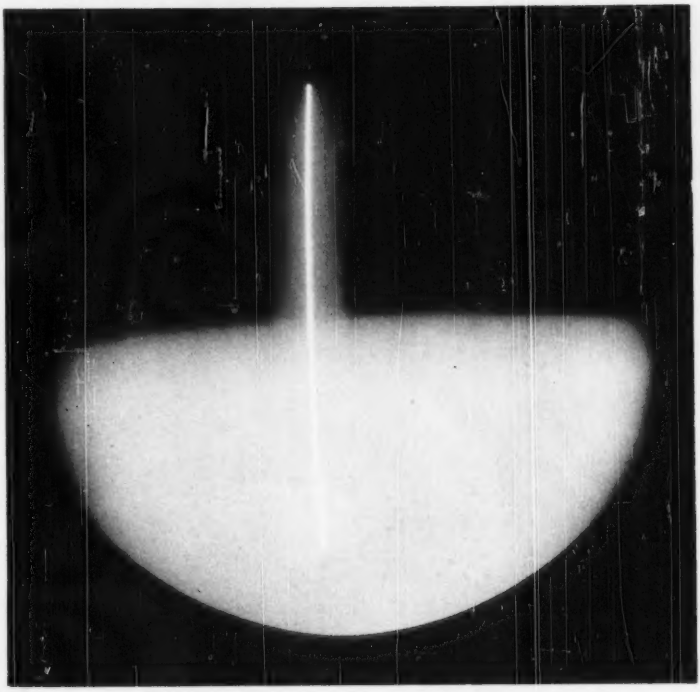

Fig. 2—Linear trace on powder phosphor screen with and without room light.

and be gone much sooner than the others. In addition, a shell tends to form over the material, which greatly retards evaporation. Fig. 4 is a photograph of one of the coating chambers actually used. In this case there was no separately heated appendix, the powder being simply dropped to the bottom of the chamber. A typical powder mixture for making a screen of ZnS:Mn is as follows:

25 g Zn
12.5 g $ZnCl_2$
0.38g $MnCl_2$

Chemical analysis of typical films indicates that their response to cathode rays is optimum when approximately 1 per cent of Mn by weight is incorporated.

The layer of zinc sulfide produced in this way is very durable, and so firmly bonded to the glass that it can be put through the same

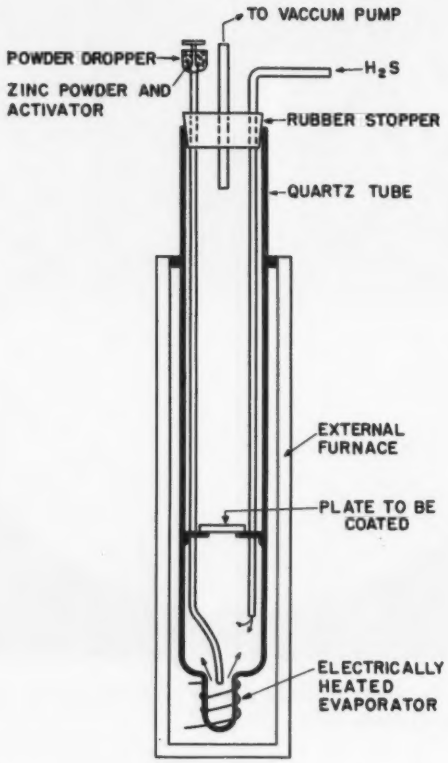

Fig. 3—Arrangement for vapor reaction deposition of phosphor screen.

polishing operations as the glass itself. In fact, in removing the deposited layer, it is usually necessary to resort to using HCl or a mixture of HCl and HNO_3 to dissolve it. These screens will stand high temperatures and severe heat shock, in a dry inert atmosphere, with essentially no damage. A coated face-plate of pyrex can be sealed to a cathode ray tube shell with little effect on the coating, except for a narrow line along the fused edge. In doing this, dry nitrogen is used for blowing, and high frequency heating for fusing the edges. The arrangement for sealing on a coated faceplate is shown in Fig. 5.

The thickness of the layer increases with the amount of powder that is introduced, provided a given rate of dropping is maintained. As the

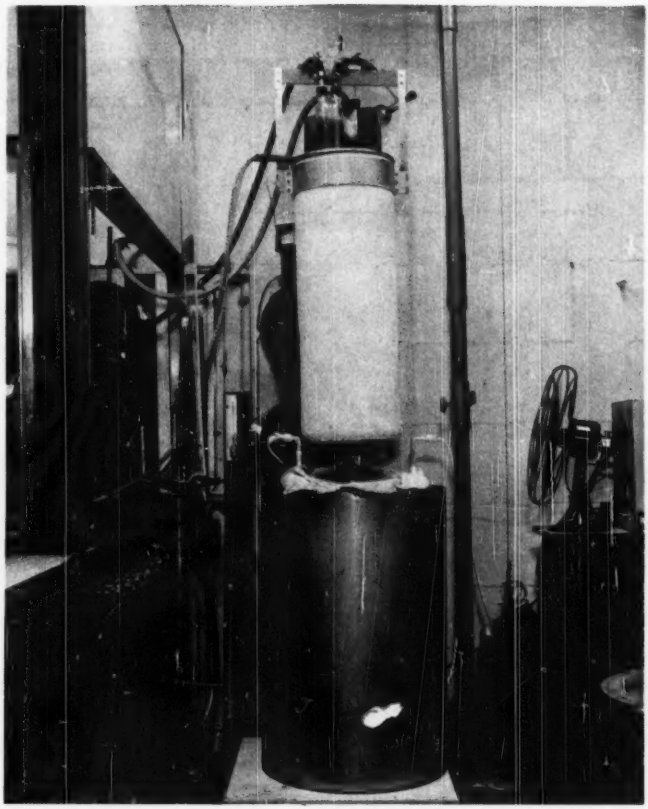

Fig. 4—Apparatus used for making 8 cathode ray tube screen.

thickness increases beyond approximately half a micron, it tends to develop a roughness on the surface as is illustrated in the electron micrograph of Fig. 6. This roughness gives rise to some light scattering, and this increases with thickness of deposit. However, when the surface is polished with a fine abrasive, transparency is restored in coatings 10 to 20 microns thick or more. For a continuous clear deposit to form, it is, of course, necessary to carefully clean the glass surface before carrying out the coating operation. We have found that the most satisfactory procedure is to clean the glass carefully with one of the commercial metallographic polishing powders, wash in distilled water, and allow the surface to drain dry.

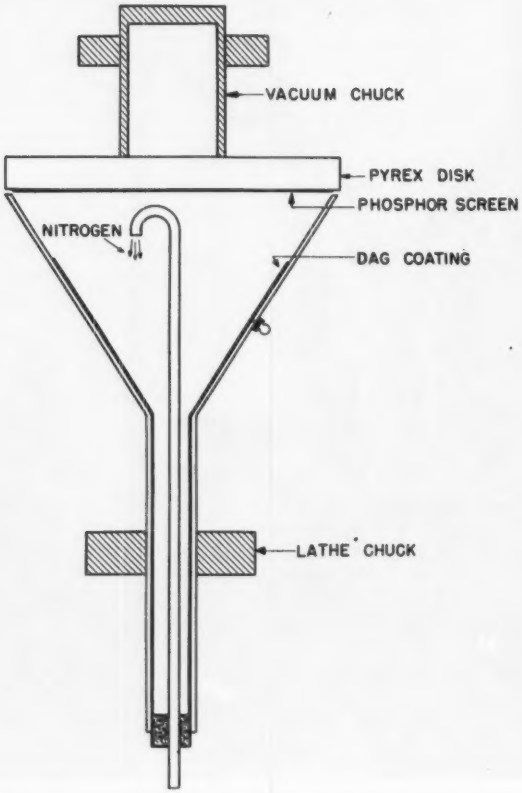

Fig. 5—Method for sealing transparent screen to cathode ray tube.

ACTIVATORS

Activators in ZnS deposits made by vapor phase reaction that have been found to give relatively high response under cathode ray excitation are arsenic, copper, manganese and phosphorus. The self activated ZnS can also be made in this way. The emission spectra of these coatings are shown in Figs. 6, 7, 8 and 9. In most cases the response of these deposits to ultraviolet excitation is weak, although it may be varied by changing the conditions in the coating chamber.

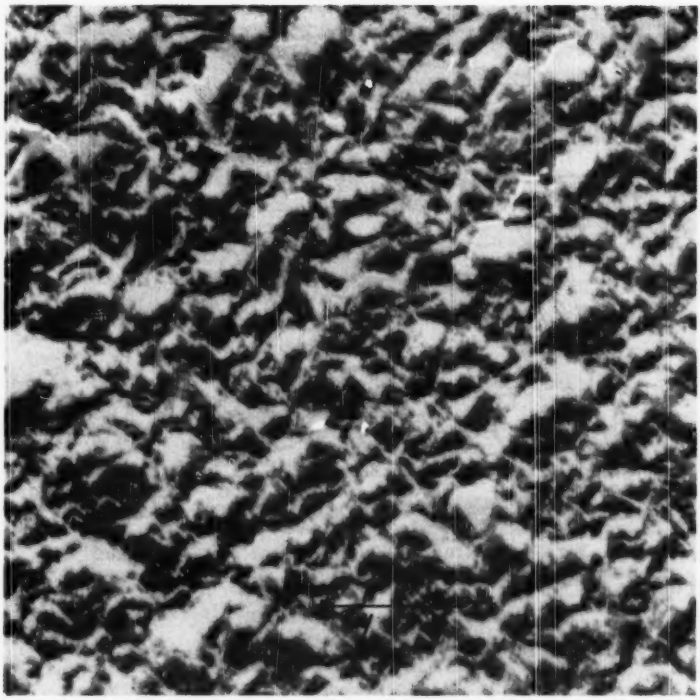

Fig. 6—Electron microscope picture of unpolished vapor reaction coating.

BRIGHTNESS

The brightness response of typical transparent screens under cathode-ray excitation is given in Fig. 10. These values were obtained with a current of 1 microampere per sq. cm. and accelerating voltages up to 25 KV a layer of aluminum about 0.1 micron thick was evaporated directly onto the phosphor to eliminate charging of the surface. There is no evidence of deterioration of these screens under cathode ray bombardment of normal intensity. The brightness which has been attained up to the present with transparent coatings is several fold less than can be realized with the best white phosphor.

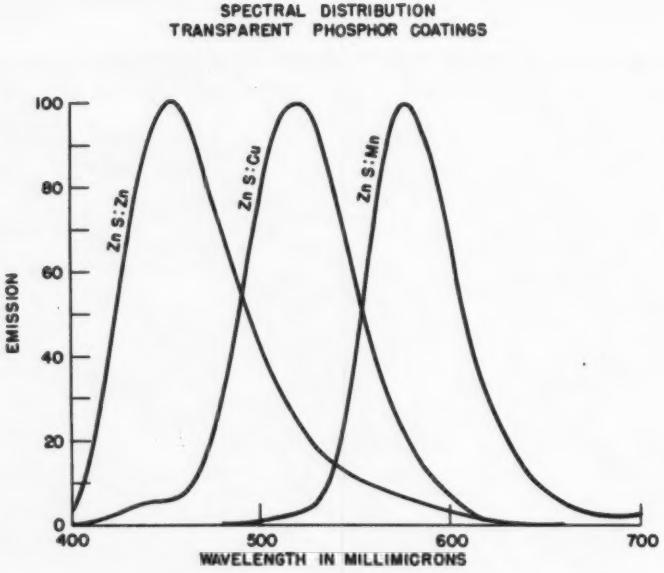

Fig. 7—Spectral distribution of ZnS:Zn, ZnS:Cu and ZnSMMn made by vapor reaction.

ELECTROLUMINESCENCE

Layers of ZnS:Mn produced by vapor reaction may be made to exhibit electroluminescence. If the glass upon which the deposition is to be made has an initial transparent coating of TiO_2, the TiO_2 layer becomes electrically conducting as the ZnS forms on it. An electroluminescent cell can thus be made by evaporating or painting an electrode on the front surface of the ZnS. The details are indicated in Fig. 11. The properties of such cells have been reported by Halsted and Koller.[1]

ENHANCEMENT OF ULTRAVIOLET EXCITED LUMINESCENCE BY D.C. FIELD

Under d.c. excitation cells made in this way show only a transient flash of light when the field is applied or turned off. However, if ultraviolet (3650Å) is incident on the cell, giving rise to photoluminescence, the brightness of the emitted light may be greatly increased when the

1. R. E. Halsted and L. R. Koller, Phys. Rev. 93, 2, 349, Jan. 1954.

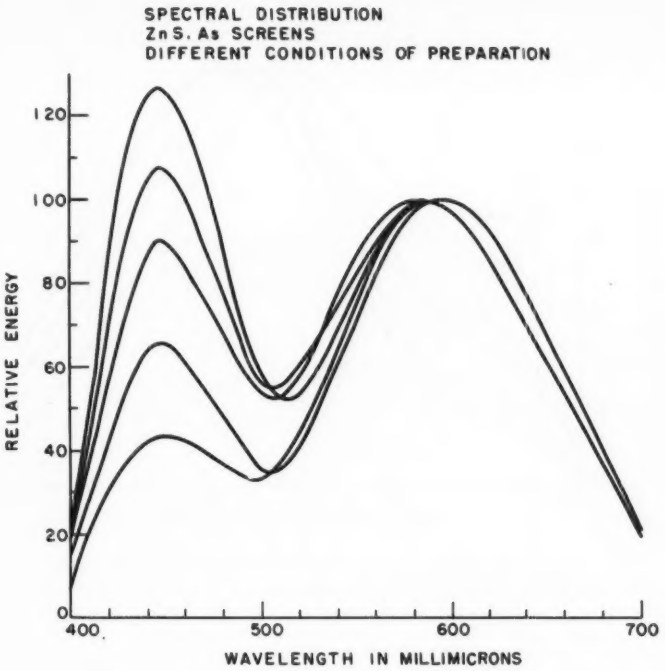

Fig. 8—Spectral distribution of ZnS:As screens for different conditions of preparation.

d.c. voltage is turned on. The study of this phenomenon[2] is still in the preliminary stage but in the samples studied thus far, an increase in brightness as great as fifty fold has been observed when a difference of potential of 100 volts is applied across a layer 10 microns thick. At low ultraviolet intensity true light amplification has been observed; that is, the energy given out in the visible with the field applied is greater than that incident in the ultraviolet exciting beam. The intensity under a given field increases with the intensity of the incident ultraviolet and consequently a cell of this type may be used to intensify a low brightness picture projected with ultraviolet.

2. D. A. Cusano, Bulletin Am. Phys. Soc. 30, 1, Jan. 1955.

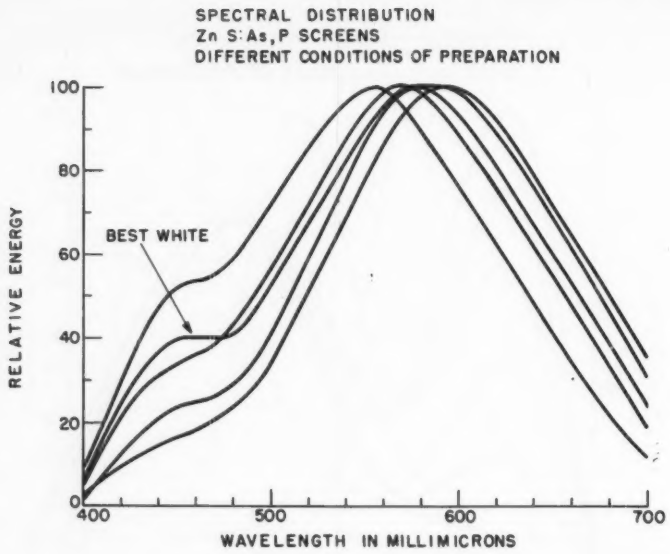

Fig. 9—Spectral distribution of ZnS:As,P, screens for different conditions of preparation.

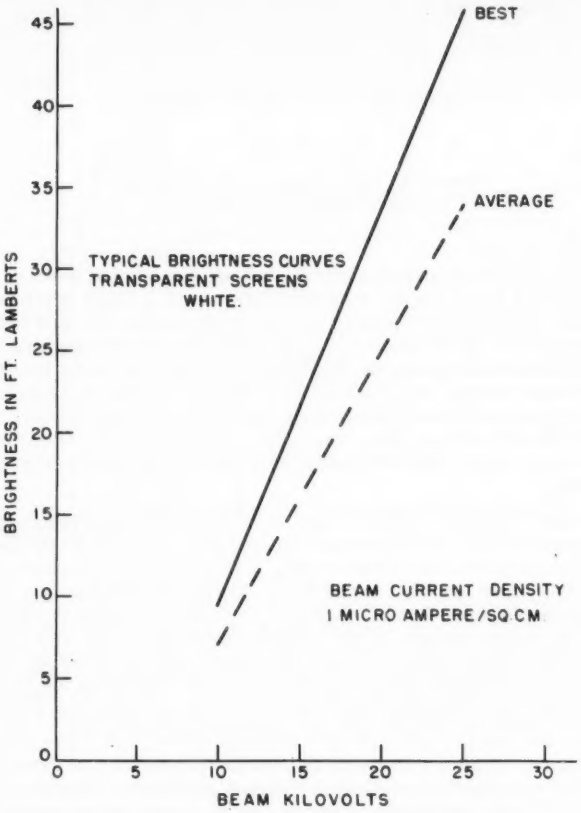

Fig. 10—Typical brightness curves for white transparent screens.

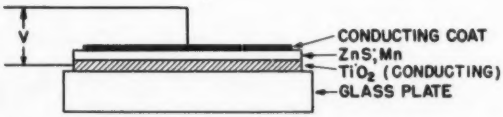

Fig. 11—Cell of vapor reaction ZnS:Mn for studying electroluminescence and enhancement of luminescence.

Abstract Number 53

CATHODOLUMINESCENT LAMPS

L. R. Koller

General Electric Research Laboratory
Schenectady, New York

The excitation of luminescence by cathode ray bombardment of a phosphor at a beam energy of several kilovolts is a fairly efficient process. Luminous efficiencies as high as 98 lumens per watt have been reported.[1] Such values are high enough to warrant considering cathodoluminescent lamps as illuminants. In contrast to the performance at high voltage, it has not been possible in the past to operate cathodoluminescent lamps made with most phosphors at ordinary line voltages of 120 volts or less. Zinc oxide is an exception. Shrader and Kaisel[2] have shown that zinc oxide can be excited by very low energy electrons.

The first obstacle to low voltage operation is that the secondary emission ratio for many phosphors is less than one (i.e., below the first crossover) in this voltage range. It is also subject to fluctuations during the life of the tube. Accordingly, these phosphors on an insulating surface cannot be excited by electron bombardment in a pure electron discharge at low voltage. This obstacle may be overcome by placing the phosphor on a conducting electrode which also serves as anode. The phosphor is then prevented from charging up by leakage to the anode. Under these conditions the voltage drop through the phosphor screen is an important factor in determining the operating conditions.

Measurements were made of the voltage drop through screens of different thickness of a number of different phosphors. The observations were made by a comparison of the electrical characteristics of a number of simple cathode ray tubes which differed only in the nature of their phosphor screens.

The current voltage relation was found to be of the general form shown in Figure 1. The knee of the curve was in the region of 100-200 volts, depending upon the nature of the phosphor. It appeared at higher voltages the thicker the screen. For low voltages and small currents the volt ampere relation is nearly linear. At higher voltages the current increases exponentially with the voltage. Accordingly, below the knee of the curve, the screen impedance is high while above the knee the screen impedance becomes lower.

1. A. Bril and H. A. Klassens, Philips Tech. Rev. 15, 67 (1953).
2. R. E. Shrader and S. F. Kaisel, J. O. S. A. 44, 135 (1954).

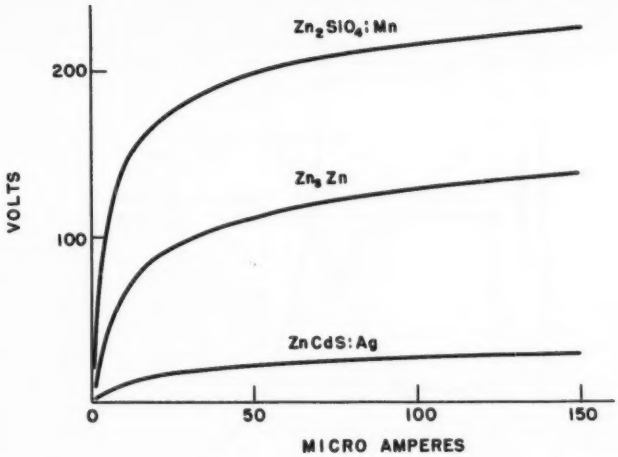

Fig. 1—Voltage drop through monolayer powder phosphor screens.

A lamp such as a bulb with the inside walls of conducting glass upon which a layer of phosphor is deposited and a central hot cathode may be considered as two impedances in series. One is the anode cathode space, where the current voltage relations are determined by the 3/2 power space charge law. The other is the phosphor screen where the relations shown in Figure 1 apply. The lamp current at any given applied voltage must satisfy both the 3/2 power law for the geometry of the lamp and the screen volt ampere relation shown in Figure 1. This is indicated schematically in Figure 2. The lamp will operate at a current corresponding to the intersection of the two curves, and the applied voltage will be divided between the two impedances as shown by V_S and V_P. For most phosphors, at low voltages the operating point falls on the linear portion of the phosphor charactersitic. Thus the lamp current is relatively small and most of the voltage drop takes place across the phosphor. As the applied voltage is increased, the operating point moves toward larger currents. In addition, due to the exponential nature of the phosphor characteristic, most of the increased voltage is impressed across the space and results in increased energy for the electrons which bombard the phosphor.

These considerations lead to the conclusion that a necessary condition for the operation of low voltage cathode ray lamps is the use of phosphors having high conductivity. Measurements of conductivity on samples of pressed powders showed that the conductivity of ZnO phosphor is lower by several orders of magnitude than phosphors such as

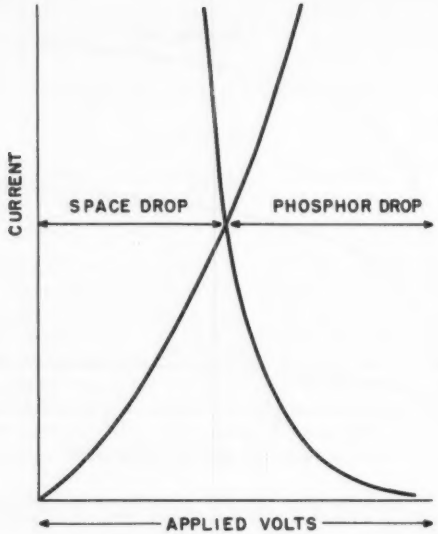

Fig. 2—Current voltage relations in cathode ray lamp.

Zn_2SiO_4:Mn, ZnS:Zn, ZnS:Ag, ZnCdS:Ag and a number of other commercial phosphors. These measurements checked the results obtained in the cathode ray tubes.

Lamps were then made by depositing phosphors on the inner surface of 3-inch Pyrex glass bulbs which had first been given a conducting by tin oxide coating. This served as anode. Indirectly heated oxide-coated cathodes were mounted centrally. The bulbs were given a conventional bake out and exhaust. The electrical and luminescent properties of these lamps were measured and found to confirm the predictions of Figure 2. At 120 volts the current through the Zn_2SiO_4 lamps was only a few microamperes. The luminescence was negligible and occurred only at a few discrete spots. The current through the ZnS lamp was 1-2 milliamperes and the luminescence feeble. It was observed only over some rather large patches. The ZnO lamps passed a current of $10\text{-}20 \times 10^{-3}$ amperes at 120 volts and showed strong uniform luminescence over the entire bulb.

The relative space and phosphor voltage drops in these lamps derived from the measurements made in the cathode ray tubes are shown in Figure 3. The value of the product of lamp current and space voltage drop is a measure of the energy available for excitation of the phosphor. The relative values of this product for Zn_2SiO_4, ZnS and ZnO were 1, 92 and 160 respectively. The measurements in the CR tubes and lamps

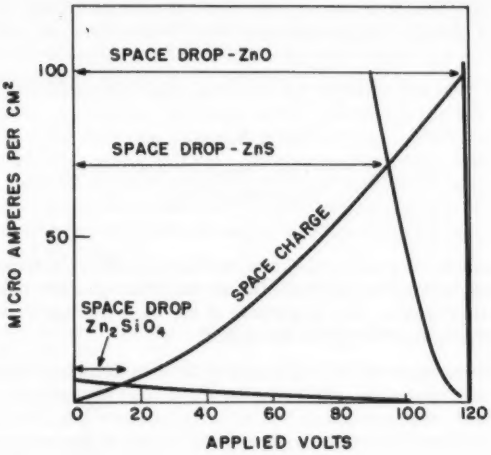

Fig. 3—Voltage current relations for cathode ray lamps with various phosphors.

are not strictly comparable since the phosphor coatings were applied by different methods, but the general nature of the effects is the same.

A rough estimate of the efficiency of the ZnO lamps was about 1L/W. Measurements on about thirty lamps were in fairly good quantitative agreement for the ZnO. The measurements on the other phosphors were in agreement qualitatively but were not reproducible. The conduction through the phosphor is in the nature of a breakdown phenomenon and depends upon the detailed structure of the coating and its history.

The conclusion to be drawn from these observations is that the voltage drop through phosphor screens is considerable and is a limiting factor in the operation of cathodoluminescent lamps at low voltages.

Abstract Number 54

COLOR SHIFTS IN Zn-Cd-S (Ag) PHOSPHORS

Vanja Svepel

Cathode Ray Tube, General Electric Co.
Syracuse, N. Y.

The emission of a zinc-cadmium-sulfide phosphor, activated with Silver, shifts to shorter wavelengths as the density of the exciting electron beam increases. The magnitude of the shift increases with increasing content of Cd in the phosphor.

This phenomenon can be explained by Schoen-Klasens Theory[1, 2, 3, 4] of double-band emission applied to Zn-Cd-S (Ag) phosphors. One, main emission band, appears due to the lattice structure (also called the Zinc-, or selfactivation-band). The other is due to the activator (silver) centers.

The energy level changes in the system are presented schematically in Fig. 1, showing the effect of increasing Cd content. Numerous

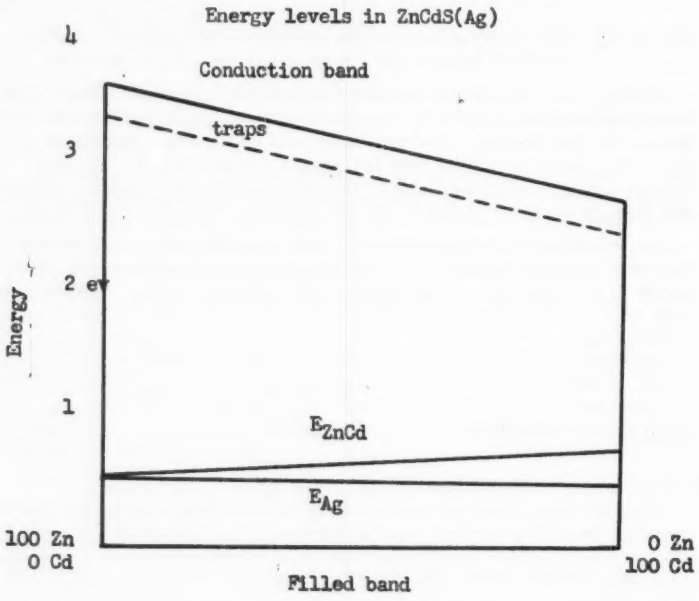

Fig. 1

examples[5, 6] support the indicated pattern. As the cadmium content increases the two peaks shift more and more apart causing the color shift with increasing current density to become more and more prominent as the amount of silver in the phosphor increases.

At standard cathode-ray rube operating conditions the two peaks are not noticeable, but they can be resolved at low (eg. - 196°C) temperatures under ultraviolet excitation.[7] In phosphors of high cadmium and high silver content the position of the second peak can be determined in spectral emission curves obtained at high current density excitation. Other peaks may be resolved belonging to other centers (eg. edge emission band[8] and Na-band[7]).

The system was investigated by using the following set of phosphors:

I. -	100	ZnS -	Cubic	a)No Ag,	b)0.0001% Ag,	c)0.001% Ag,	d)0.01% Ag,	e)0.1% Ag
II. -	75	ZnS -	25	CdS	"	"	"	"	"
III. -	45	ZnS -	55	CdS	"	"	"	"	"
IV. -	15	ZnS -	85	CdS	"	"	"	"	"
V. -			100	CdS	"	"	"	"	"

The deepening of body color with increasing activator concentration is increasing with higher Cd and is very strong in pure CdS.

The emission spectra show that the edge-emission band is suppressed at high activator concentrations. Then the silver band gains in importance causing the shift of emission color toward the shorter wavelength. As an example, the spectroradiometer readings for IV set of phosphors is given.

Color Coordinates (CIE) x, y

Ea = constant) Current density:	Samples a		b		c		d		e	
	x	y	x	y	x	y	x	y	x	y
0.2 ua/cm²	.656	.344	.670	.330	.667	.333	.655	.345	.629	.371
2.0	.619	.364	.638	.352	.646	.354	.598	.401	.606	.392
4.0	.617	.367	.633	.353	.629	.363	.590	.408	.595	.403
20.0	.530	.404	.599	.371	(.610	.380)	.567	.429	.576	.422

Excluding the short-wavelength tail (edge-emission and Na-bands) the following set of color readings is obtained:

0.2 ua/cm²	.656	.344	.670	.330	.667	.333	As above
2.0	.634	.366	.648	.352	.646	.354	"
4.0	.631	.369	.647	.353	.637	.363	"
20.0	.603	.397	.633	.367	(.630	.360)	"

It follows that the color shift is a logarithmic function of current density.

The effect of increasing silver content is illustrated in Fig. 2. At low activator concentrations the edge (-resonance-) emission band is present. It disappears at high activator content; at that point the Ag-band, and also Na-band, have grown in importance relative to the main emission band.

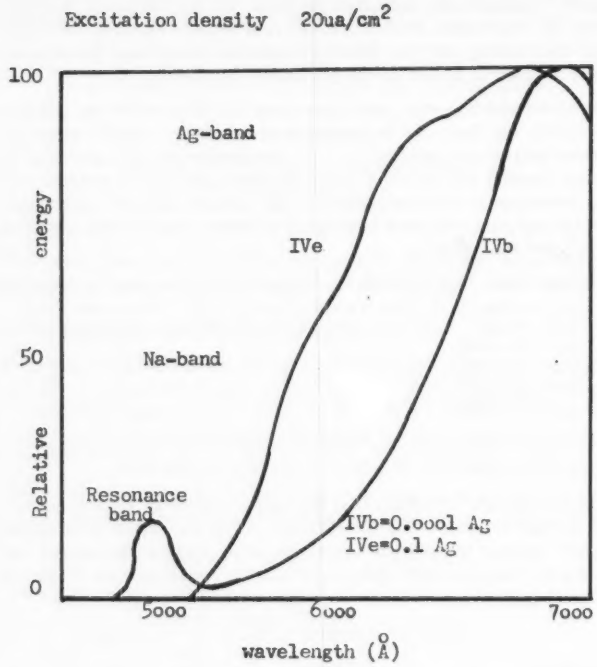

Fig. 2—Effect of increasing Ag content on spectral energy distribution of .15 Zn .85 Ca S (Ag).

There is usually a slight shift of the peak toward the shorter wavelengths with increasing activator content and, relatively less so, with increasing excitation density.

Numerous applications of the effect could be cited. In monochrome application the observable shift toward the blue with increased density may be attributed to the emission shift of the yellow component. Another possible explanation is the probable saturation effect taking place in the "yellow" component at lower current density than it does in the "blue"component. The sensitivity to copper contamination is easy to explain by considering the higher energy level of Cu activator-centers in relation to Ag-and Zn- levels. Screen burning mechanisms can also be explained by taking into account the relative abundance and sensitivities of different type centers. Flying spot scanner tubes, in color television application, if using ZnS type phosphors for screens, show the described shift effects. For the same reason the ZnCdS (Ag)

green, and even more the red, phosphors are unsuitable for the screen application in color television picture tube.

References

1. H. Schoen: Z. Physik 119(1942), p. 463
2. H. A. Klasens: Nature 158 (1946), p. 483
3. Klasens, Ramsden, Quantio: J. Opt. Soc. 38 (1948), p. 60
4. H. A. Klasens: J. Elchem Soc., Vol. 100 (1953) No. 2, p. 72-80
5. H. W. Leverenz: Luminescence of solids (Wiley 1950)
6. Solid Luminescence Materials (Cornell Symposium, A. Phys. Soc. 1946)
7. Fehr, Friedman, Studer, Fonda: J. Opt. Soc., Vol. 42 (1952) No. 12 p. 917-922
8. Bril-Krōger: Philips Technical Review, Vol. 12 ( ) No. 4, p. 120

Abstract Number 56

A NEW SINTERED TUNGSTEN MATRIX CATHODE

E. A. Thurber

Bell Laboratories

The history of magnetron cathodes will be briefly reviewed providing some background information essential to a fuller appreciation of recent design problems and their solution. In particular, the development of a new oxide-coated coexpansive system comprising a sintered tungsten matrix on a molybdenum base will be described. The new cathode will be compared with older types from the standpoints of electrical performance, mechanical strength, refractory properties, thermal and thermionic stability, and general reliability.

Abstract Number 57

SOME STUDIES ON PROBLEMS ASSOCIATED WITH THE MOLDED NICKEL CATHODE

Irving J. Bell and George R. Brewer

Electron Tube Laboratory, Hughes Research and Development Laboratories

Some problems encountered in the fabrication and processing of the molded nickel cathode will be discussed, together with methods which have been successful in their solution. Particular emphasis will be placed on the effect of composition and sintering schedule on the emission and life obtainable for cathodes containing carbon as a reducing agent. Data on pulsed and DC emission and life tests will be presented.

Abstract Number 58

SOME APPLICATIONS OF L CATHODES

J. Babakian* A. Matthewson J. Bloom

Air Force Cambride Research Center

Some years ago a general evaluation was made of the then new L cathode. Its pulse emission characteristics in high vacuum diodes received by far the greatest attention. Peak emissions of 40 - 45 Amperes per sq. cm were obtained at varying pulse lengths over periods of hundreds of hours. In this early work little if any effort was placed on high voltage applications in high vacuum and gas tubes.

This internal program in the tube section at Air Force Cambridge Research Center was expanded. In the course of an electron beam study early data was obtained on the effect of high voltages on L cathodes. This early tube was designed around a cavity type 3 mm disc cathode. An impregnated type cathode was later used in the same tube structure.

As larger cylindrical cathodes (impregnated type), became available, external anode tubes were designed and built. Several tubes were successfully processed using a 3 cm^2 cylindrical cathode. The most recent tubes have been designed around a 9 cm^2 cathode and a number of these tubes have been processed.

In this study of high voltage triodes a number of trends became apparent. The early pulse diode results could not be obtained in pulse triodes of about the same size. The triodes proved harder to activate than the diodes and further difficulty was experienced when high pulse voltages were applied. The impregnated cathodes were easier to handle than the original cavity types but the emission levels obtainable proved to be somewhat lower.

When working with the larger cylindrical cathodes in external anode tubes these trends were carried further. Activation proved more difficult and processing techniques were more rigorous and much more time consuming. It proved impossible to attain in larger cathodes the emission densities originally obtained with the small ones. In the largest tubes, emission densities of about 10-12 Amps per sq. cm. were obtained at 1100^{0} C br. In these tubes peak voltages of as high as 26 KV were applied. In all of these triodes average power was severely limited by grid emission.

A major effort was expended in exploring the properties of L cathodes in gas tubes. In small gas diodes the original 3 mm dia. cathodes operated very well. However, as the gas pressures were reduced to sustain high voltage drops (up to 100 volts) the ion bombardment

rapidly destroyed the emissive qualities of the cathode. A number of tests indicated that this emission recovered very rapidly with the removal of plate voltage. It occurred to the authors that this recovery might be quick enough to allow pulse operation under high velocity ion bombardment conditions. It was decided to explore the characteristics of these cathodes in typical pulse thyratron structures. A small hydrogen thyratron similar to the 3C45 tube was chosen. Since these cathodes are inoperable in hydrogen helium was used as a gas fill.

A great deal of difficulty arose in activating L cathodes in this structure. It proved impossible to get more than sporadic activation with a nickel tube structure. Gradually a purified mobybdenum structure was developed. These tubes were activated under high vacuum conditions and then the gas was introduced. Time after time a well activated cathode would be poisoned during gas filling. This operation proved to be a very critical one throughout the entire investigation. After many failures it was demonstrated that these tubes could be operated as pulse thyratrons with cathode falls in the order of hundreds of volts.

The same tube structure was used with a 3 mm dia impregnated cathode. A number of these tubes were made and several operated for hundreds of hours. A structure was designed around the 3 cm^2 cylindrical cathode and a number of these tubes were built and processed. Several of these tubes have operated for hundreds of hours and one has lasted two thousand hours. In a newly activated tube the degree of cathode activity can be readily determined by the magnitude of the trigger voltage.

The significant aspect of these gas tube tests is the resistance to high ion velocities shown by the cathode. Even more remarkable is the rapid recovery of these cathodes from the inevitable damage such ion bombardment inflicts. These tubes were pulsed at repetition rates ranging up to 600 per second. Pulse lengths up to 12 usec were used at duty cycles up to .003. The tube structure used was originally designed for peak voltages up to 8 KV. Operation at this level was achieved using these impregnated cathodes.

These results are essentially preliminary as all of the tubes described are at best early developmental tubes. However, the properties of these cathodes are still of great interest. This is true despite the lower than expected peak emission densities available to date from the larger cathodes in high vacuum tubes. In summing up one can say that in high vacuum tubes these cathodes can be used under very high pulse voltage conditions with a minimum of difficulty from sparking. The fullest advantages are only apparent when the tube structure can be designed to minimize grid emission.

In gas tubes these cathodes can be operated continuously under low cathode fall conditions. When the cathode fall appreciably exceeds 30 volts, pulse operation becomes necessary. This is only possible because of the remarkably rapid recovery characteristics of these cathodes. To date the high peak currents obtained in these tubes have

been limited by the test circuits and not the cathode. Moreover, it becomes possible to obtain long pulse length operation (up to 12 usec), at greater than usual duty cycles (up to .003).

*Present Affiliation
Director of Research and Development
Central Sales & Mfg. Corp.
Denville, N. J.

MANUFACTURING ADVANTAGES OF PHILIPS IMPREGNATED CATHODE USED IN MAGNETRON APPLICATIONS

Markus Nowogrodzki

Amperex Electronic Corporation

ABSTRACT

The impregnated cathode is one of the porous-tungsten dispenser-type emitters recently developed. Its forerunner, the "L" cathode developed in Holland, used a reservoir of barium carbonate contained by a layer of porous tungsten. The new cathode uses an emissive layer of porous tungsten impregnated with barium aluminate. The cathode has an essentially metallic emitting surface, which may greatly contribute toward its excellence in magnetron applications.

Early designs of the "L" cathode necessitated higher heater powers than those used in an equivalent tube employing oxide-coated emitters. The impregnated cathode, particularly of the threaded design, obviates the higher heater-power requirement, so that a magnetron using an impregnated cathode, but completely interchangeable with the prototype tube, can be constructed.

The manufacturing advantages of the impregnated emitter fall into two main classes, viz., ease of processing (both of the cathode itself and the tube), and resistance to cathode poisoning. The cathode itself, because it is a metallic emitter, can be manufactured with greater ease and without resorting to coating, sintering, or compression devices. The finished cathode is rugged, smooth, and can be handled easily without danger of chipping or flaking. On the exhaust station further advantages appear: the "breakdown" of the oxide-coated cathode, leading to the conversion to oxides of the alkaline-earth carbonates, is not present in the case of the impregnated emitter. As a result, the exhaust procedure of either the cathode itself or the finished magnetron is greatly simplified.

The impregnated cathode is also superior from the viewpoint of aging the finished magnetron. Aging schedules in the 6507 - the tube incorporating and impregnated cathode - have been reduced by as much as 80% as compared with the prototype magnetron employing an oxide-coated cathode, the 4J52 type. In addition to a saving in aging time, the aging is also less violent, with a complete absence of large bursts of arcs which may prove detrimental to the tube being aged.

The resistance to poisoning of the impregnated cathode not only facilitates its handling, but also enables its re-use in new mounts after removal from a defective tube. From a production point of view this is

obviously an advantage. But in the process of tube development, the possibility of re-using cathodes is of even greater importance, since it enables the trial of variants of anode design for optimization of anode geometry without the complication of cathode variables in the successive experimental designs.

EMISSION FROM MOLYBDENUM ACTIVATED WITH BARIUM*

R. H. Ahlert and E. S. Rittner

Philips Laboratories,
Irvington-on-Hudson, New York

Since molybdenum parts are frequently incorporated into Philips dispenser cathode structures in close proximity to the tungsten emitting member, it is desirable to obtain information on the emission capabilities of molybdenum surfaces activated by barium, which is supplied either by evaporation or by surface migration from the active region of the cathode. It is also of interest to determine the average migration length of barium over molybdenum.

Data on the emission capabilities of barium-activated molybdenum have been obtained by exposing a molybdenum wire to a molecular beam of barium of known intensity and measuring the emission current from the wire as a function of the arrival rate of the barium, of the temperature of the molybdenum, and of the state of oxidation of the wire. These experiments have revealed that the emission vs. barium arrival rate characteristics of superficially oxidized molybdenum are identical initially with those of tungsten in a similar state of oxidation. However, the molybdenum loses its adsorbed oxygen content much more rapidly than tungsten, thus resulting in a large decrease in emission with time. This decrease in emission can be avoided for the most part by exposing the molybdenum to a stream containing in addition to barium some barium oxide to replace losses of adsorbed oxygen.

The migration length of barium over molybdenum has been determined by measuring the space charge limited emission from the top side of a slotted molybdenum ribbon, the bottom of which is maintained at a constant coverage of adsorbed barium. Since the emission current density for a given voltage and cathode-anode separation may be readily computed from Child's law, the magnitude of the emission current collected by an anode of known area positioned above the slotted region of the ribbon provides a measure of the effective emitting area of the ribbon and thus also of the migration length of the barium. The value of the migration length determined in this manner proves to be of the order of a small fraction of a millimeter and decreases with increasing temperature. If losses of adsorbed oxygen as the result of thermal treatment are not replenished, then the migration length decreases progressively with aging time.

*Work supported by the Bureau of Ships under Contract No. NObsr-64043.

Abstract Number 61

AN INVESTIGATION OF THE IMPREGNATED CATHODE*

W. C. Rutledge, E. S. Rittner and R. H. Ahlert

Philips Laboratories,
Irvington-on-Hudson, New York

In view of the interest stimulated by the first commercial version of the impregnated cathode,[1] a detailed investigation of the basic performance characteristics of a standard 3 mm planar type cathode**(thickness 1 mm) was undertaken. The information so obtained serves as a partial basis for elucidating several aspects of the mechanism of operation of the cathode. Of particular interest are the differences in the electron emission and product evaporation between this version of the impregnated cathode and the earlier-developed L-cathode.[2]

Measurements of emission density from a planar diode as a function of voltage, temperature and cathode life are described. Schottky plots of the data show that the zero-field emission from the impregnated cathode is about one-fifth that from an L-cathode. Richardson plots yield nearly identical work functions for the two cathodes ($\phi_{T=0^oK}$ = 1.6 ev). Therefore, the impregnated cathode must be operated about 150°K higher than the L-cathode in order to deliver the same emission density. Both cathodes exhibit relatively constant emission throughout accelerated life-tests, but the life of the impregnated cathode at a given temperature is roughly twice as long.

Evidence is presented to show that the electron emission originates from the entire top surface of the cathode, which includes a supporting rim of molybdenum. At temperatures below 1250°K the migration length of barium on molybdenum increases sufficiently so that the sides of the molybdenum sleeve contribute significantly to the total emission, if a guard electrode is not employed.

The evaporation products from both cathodes were found by polarographic and by chemical means to consist solely of barium and of barium oxide. Since these methods of analysis yield only average evaporation rates, a physical method was developed in order to determine the "instantaneous" evaporation rates of both barium and barium oxide as a function of time throughout the life of the cathode. This method is based in part on the well-known[3] electron emission—time

*Work supported by the Bureau of Ships under Contract No. NObsr-64043.

**This cathode represents the first version of the impregnated cathode, and not the improved version which is described by Dr. R. Levi in an accompanying paper.

characteristics of a tungsten wire exposed to a stream of barium. The reciprocal of the time required for the emission to reach a maximum value is a direct measure of the relative barium evaporation rate. Further experiments* show that a tungsten wire may be calibrated as an absolute detector of total barium content and that the calibration is valid for a mixture of barium and barium oxide. It is also possible to determine the percentage of barium oxide in the evaporation products by exposing the tungsten wire to the stream of evaporant until optimum emission is attained, aging the wire at a temperature at which free barium is selectively removed, and re-exposing the wire to the products evaporated from the cathode until optimum emission is again obtained.

Measurements of the total barium evaporation rate as a function of cathode life show that initially the rate from the impregnated cathode exceeds that from an L-cathode of comparable porosity by about an order of magnitude. However, the rate from the impregnated cathode decreases continuously throughout life, becoming less than that from the L-cathode after 200 hours of aging at 1465°K. The barium oxide content of the evaporant is roughly 25 per cent for the L-cathode and also for the impregnated cathode early in life. During subsequent aging of the latter, the barium oxide content decreases by a factor of about three. Measurements of the temperature dependence of the total barium evaporation rates show nearly identical results for both cathodes.

That barium is transported to the emitting surface of the L-cathode principally by Knudsen flow has been previously shown.[4] The dominant barium transport mechanism in the impregnated cathode is also Knudsen flow, in this case however through partially clogged pores. This conclusion is based on the observed temperature dependence of the total barium evaporation rate, on the constancy of the emission throughout life, and on the observed time dependence of the instantaneous evaporation rate.

One may conclude that the impregnated cathode operates in a manner highly similar to that of the L-cathode. There is one question, however, as to why the first commercial version of the impregnated cathode furnishes much smaller emission than the L-cathode. The best hypothesis which we can propose at present is that a poisoning gas may be gradually released from the interior of the cathode during life, thus neutralizing the activating effect of much of the barium.

References

1. R. Levi, J. Appl. Phys. 24, 233 (1953).

2. H. J. Lemmens, M. J. Jansen and R. Loosjes, Philips Tech. Rev. 11, 341 (1950).

*To be published.

3. J. A. Becker, Phys. Rev. 34, 1323 (1929).

4. E. S. Rittner, W. C. Rutledge, R. H. Ahlert, Technical Report No. 69, Philips Laboratories, January 1, 1953.

Abstract Number 62

IMPROVED PHILIPS "IMPREGNATED CATHODE"

Roberto Levi

Philips Laboratories
Irvington-on-Hudson, N.Y.

In recent years a dispenser type thermionic cathode, known as the L-cathode, has been developed in Holland.[1] In this cathode the barium source consists of barium carbonate contained in a large cavity reservoir; as a result the time required on the pumping system is rather long since the breakdown of the carbonate must be carried out very slowly. Furthermore, the large cavity reservoir causes a number of thermal problems and greatly limits the range of sizes and shapes in which the cathode can be made.

More recently an improved version of the L-cathode, called the Philips impregnated cathode, has been developed.[2] In the new emitter, the barium source, consisting of a mixture of normal and basic barium aluminates, is dispersed within the pores of the tungsten body, thus eliminating the need for the large cavity reservoir. As a result, cathode construction is greatly simplified, most thermal problems eliminated, and the range of sizes and shapes in which the cathode can be fabricated is vastly increased. Furthermore, the elimination of the carbonate as the barium source allows very rapid processing on the pumping system.

The impregnated cathode has created a great deal of interest in the electron tube industry in the United States and abroad; and it is now beginning to be introduced in a number of commercial tubes, in particular, magnetrons, klystrons and travelling wave tubes. Although the original version of the impregnated cathode is gaining wide acceptance, this cathode delivers an emission density significantly lower than the L-cathode at equal operating temperature. Since the rate of barium evaporation from the impregnated cathode is sufficiently high so as to maintain complete coverage of the emitting surface with a monolayer of barium, the relatively lower emission represents a paradox which has not yet been fully explained.

As a result of further work, a greatly improved version of the original impregnated cathode has now been developed. It has been found that by changing somewhat the impregnation technique and by adding calcium oxide to the mixture of aluminum oxide and barium oxide previously used, the resulting cathode has the following advantages over its predecessor.

First, the emission current density obtainable at any given temperature has been increased by a factor of about four.

Second, the aging process (after removal from the pumping system) required to yield full and stable emission has been cut to a few hours as compared to the previously required time of three days.

Third, the rate of barium evaporation has been lowered at equal operating temperature; since, however, lower operating temperatures are now required to obtain the same emission current densities, the barium evaporation rate for comparable emission density is further reduced by a factor of about eight. Furthermore, the lower cathode temperature required to obtain a given current density results in improved life for both cathode and heater.

The true (temperature dependent) work function of the improved emitter, as determined from a typical diode, is 2.12 ev at 1410°K, its temperature coefficient being 3.2×10^{-4} ev/degree. The corresponding values for the old impregnated cathode are 2.34 ev and 5.45×10^{-4} ev/degree.* The physical structure of the improved emitter remains identical to that of the original impregnated cathode; therefore, all of the latter's advantages over the L-cathode are retained.

References

1. Lemmens, Jansen, and Loosjes, Philips Tech. Rev. 11, 341 (1950).
2. R. Levi, J. Appl. Phys., 24, 233 (1953). This is the cathode the performance characteristics of which are discussed in the accompanying paper by Rutledge, Rittner and Ahlert.

*It follows from these data that the extrapolated values of the work function at T = O°K are 1.67 and 1.57 ev, respectively. These are the values that would be obtained from a conventional Richardson plot of the data.

CHEMICAL PROCESSES IN THIN-FILM DISPENSER CATHODES

R. C. Hughes and P. P. Coppola

Philips Laboratories
Irvington-on-Hudson, New York

Announcement of the "L" cathode and demonstration of its unusual capabilities as a source of high-density continuous emission has stimulated renewed interest in thin-film dispenser cathodes.* Much of this new interest has been directed toward the development of solid cathodes in which a reserve supply of barium materials is dispersed within a matrix of porous metal.

A consideration of the chemistry of various systems involving refractory metals and barium compounds has led to the development of improved cathodes of the solid type and indicates the reasons for poor performance of many priorly suggested compositions selected at random without knowledge of their chemical properties.

It has been proposed that elementary barium generated by reduction of BaO by tungsten is responsible for activation of the "L" cathode. It has been shown that this reaction is of the type:

$$6BaO + W \rightarrow Ba_3WO_6 + 3Ba$$

It has also been shown that, in solid cathodes having the barium compound dispersed in the refractory metal matrix, the barium source must not contain excess oxygen over that present in barium oxide. Oxidizing compounds react with production of no free barium, as typified by the reaction of barium carbonate:

$$3BaCO_3 + W \rightarrow Ba_3WO_6 + 3CO$$

Since BaO, upon air-exposure, is rapidly converted to carbonate, its use is also generally undesirable. The barium compound chosen for solid dispenser cathodes must therefore provide an air-stable, non-oxidizing source of barium oxide (or barium).

The reduction of BaO by various refractory metals to produce elementary barium involves an increase in free energy of the system. Thus, based on the thermodynamic principle that reaction tends to proceed in the direction of minimum free energy of the system, these reactions are thermodynamically improbable. The reaction will not

*A thin-film dispenser cathode is defined as that type of thermionic emitter in which activating materials contained within a reservoir are continuously fed to an emitting surface to form an adsorbed monolayer constituting a dipole which lowers the work function of the surface.

produce barium in its standard state; rather equilibrium in the reversible reaction:

$$6BaO + W \rightleftharpoons Ba_3WO_6 + 3Ba$$

is established at a very low barium pressure determined by the free energy change, and expressed by:

$$\Delta F = -RT \ln P_{Ba}$$

Reaction can therefore proceed only to the extent that barium evaporates from the system, or is otherwise removed. The energetic adsorption of barium by the refractory metal constitutes an effective means of removal, while evaporation can occur at a maximum rate determined by the equilibrium barium pressure.

The barium pressures produced by some of the refractory metals in contact with barium oxide are sufficiently large to cause excessive barium evaporation. Thus tungsten-barium oxide dispersions evaporate barium rapidly, and have a short life, while molybdenum reacts relatively slowly, producing a more durable emitter. The maximum rate at which barium may evaporate from the cathode can thus be fixed at one of several inflexible values predetermined by selection of the refractory matrix*. Further control, first demonstrated experimentally, can be obtained by alloying an active reducing agent with a metal producing no significant barium pressure. The equilibrium barium pressure over the alloy may be shown to be equal to the calculated pressure over a pure phase of the active metal multiplied by the activity of the reducing constituent in the alloy. Thus, by varying the composition of the alloy, the equilibrium pressure may be varied in a smooth manner between the limits imposed by the two constituents of the alloy. In general, this permits the attainment of any desired barium pressure.

A variety of barium compositions have been considered as air-stable sources of barium oxide. In general, these materials produce barium pressures lower than those given by barium oxide; their use requires adjustment in the reducing power of the matrix. Thus, a second principle of dispenser cathode formulation may be stated: The combination of matrix metal and barium source must be chosen to generate barium at an appropriate rate.

Still other chemical processes are of interest. For considering these, it is convenient to view the barium source as initially not in contact with the metal forming the matrix (i.e., the structure of the "L" cathode).

If the matrix is assumed to be initially perfectly clean (no adsorbed oxygen), and barium is brought onto it, the barium is chemisorbed. This condition, unattainable in practice, is of no interest. Barium brought onto tungsten having an adsorbed monolayer of oxygen will be chemisorbed to form a barium-on-oxygen-on-tungsten dipole, thus

*Density of the matrix is also effective in impeding escape of barium.

activating the emitter. If the tungsten (or other refractory metal) matrix contains a free phase of oxide, the sequence of reactions

$$3Ba + WO_3 \rightarrow 3BaO + W$$

and

$$BaO + WO_3 \rightarrow BaWO_4$$

occurs, consuming barium and converting it to an inert form. Any conditions leading to initial oxidation of the matrix are therefore to be avoided.

It has already been indicated that BaO and the refractory metal, in bulk, react to produce free barium. However, other chemical processes are to be considered. If BaO, in less than monolayer amount, is brought onto an oxygen-free refractory metal surface, chemisorption can occur. Such chemisorption occurs with a large decrease in free energy. This process occurs in preference to the chemical reaction involving an increase in free energy. The chemisorption must therefore proceed to the formation of a complete monolayer before any BaO can react chemically. At operating temperature of the cathode, the chemisorbed layer is mobile and diffuses through the matrix to the emitting surface. This process produces a barium-on-oxygen-on tungsten dipole, thus supplementing the dipole produced by adsorption of barium. This process of adsorption and transport of oxygen (in the form of BaO) ensures that the emitting surface will assume the Ba-O-W, rather than Ba-W composition. The depletion of surface oxygen is therefore prevented by the availability of BaO to the matrix. Barium sources providing only elementary barium and no barium oxide are therefore to be avoided.

In summary, the formulation of good thin-film dispenser cathodes of the solid type requires the provision of an air-stable, non-oxidizing source of barium and barium oxide, and the selection of a chemical system (combination of barium compound and metallic matrix) capable of evolving barium and barium oxide at minimum rate essential for full activation of the emitting surface. In the following paper the emitter characteristics realized by application of these principles are indicated.

Abstract Number 64

A NEW PRESSED DISPENSER CATHODE

P. P. Coppola and R. C. Hughes

Philips Laboratories
Irvington on Hudson, New York

In a preceding paper, the inherent chemical principles involved in dispenser cathodes have been discussed in detail. Here, only the experimental and practical phases concerned with the preparation and properties of a cathode of this type will be described.

The original goal was to produce a dispenser cathode through the application of standard powder metallurgy techniques wherein a barium compound could be dispersed throughout a porous matrix of refractory metal. In this manner, it was believed that the requirements of such a cathode, namely, a sufficient but controlled slow rate of barium dispensed to the emitting surface, could be met easily and with a minimum cost in fabrication.

In the early stages of the development program, a large variety of alkaline earth compounds were combined with a number of refractory metals such as tungsten and molybdenum. After considerable experimentation, it was found that a composition consisting of tungsten powder mixed with a basic barium aluminate provided a cathode of high emission density and moderate life. The basic barium aluminate was prepared by fusing in air, a mixture containing 5 moles of barium carbonate, and 2 moles of aluminum oxide. Improvement in the evaporation rate sought by substituting molybdenum for tungsten was unsuccessful. Insufficient barium was generated and consequently very low emission was obtained. An alloy of molybdenum and tungsten, however, produced sufficient barium to provide a cathode with an emission current similar to that obtained with pure tungsten, but with a diminution in total barium evaporation.

In addition to the recognition of a proper chemical composition for satisfactory cathode performance, the method of cathode preparation was improved. The new technique represents a considerable effort toward the reduction of cost.

The cathodes are prepared from a powder mixture of basic barium aluminate and molybdenum alloy containing 25% tungsten. The powder is introduced into an inexpensive tubular molybdenum sleeve positioned in a suitable die. By means of a hydraulic press, 70 tons per square inch pressure is applied. The compact is ejected from the die and sintered in vacuum at a temperature of 1750°C brightness. No further operations such as machining and polishing are necessary. The high sintering temperature produces a number of important advantages.

The basic barium aluminate melts, evolves residual gases, and homogeneously disperses throughout the metal matrix. The metal particles sinter to themselves without appreciable shrinking and simultaneously produce excellent bonding with the molybdenum sleeve. An essentially metallic, mechanically strong, gas-free, air-stable cathode capable of rapid activation is the result. The structure of a planar cathode presently being made is shown in Fig. 1.

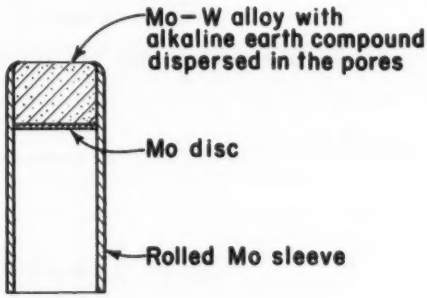

Fig. 1—Planar cathode

For evaluation, cathodes were mounted as simple diodes and processed on a vacuum system capable of providing a residual pressure less than 10^{-6} mm. Cathodes were also processed on a vacuum system providing a residual pressure not less than 10^{-5} mm. Each tube contained a "batalum" getter. Life tests were carried out at a cathode temperature of 1130°C. Periodically, emission measurements were made using pulse techniques (1000 volts, 100μ second pulse length, 20/second).

Figure 2, shows curves for emission density measured at 1020°C versus life in hours at 1130°C under space charge conditions (drawing $1\frac{1}{2}$ amps./cm^2 continuously). All cathodes represented were prepared with the basic barium aluminate but varying in respect to the type of metal matrix used. A range of $1\frac{1}{2}$ - 2 amps/cm^2 at 1020°C and about 5 amps/cm^2 at 1130°C is realized. Tubes life tested with no current drain show similar results. With molybdenum alloys, a pronounced increase in life is indicated with a similar emission level as obtained in the use of pure tungsten. The effective increase in life is due to a decreased evaporation rate of barium. Chemical tests showed that the total barium evolved with a molybdenum alloy containing only 10% by weight of tungsten is 1/3 that obtained with pure tungsten.

It has been found that the pulsed and D.C. emission current obtained from these cathodes are similar. Whenever severe heating of the anode occurs due to the application of high voltages (500 volts or more)

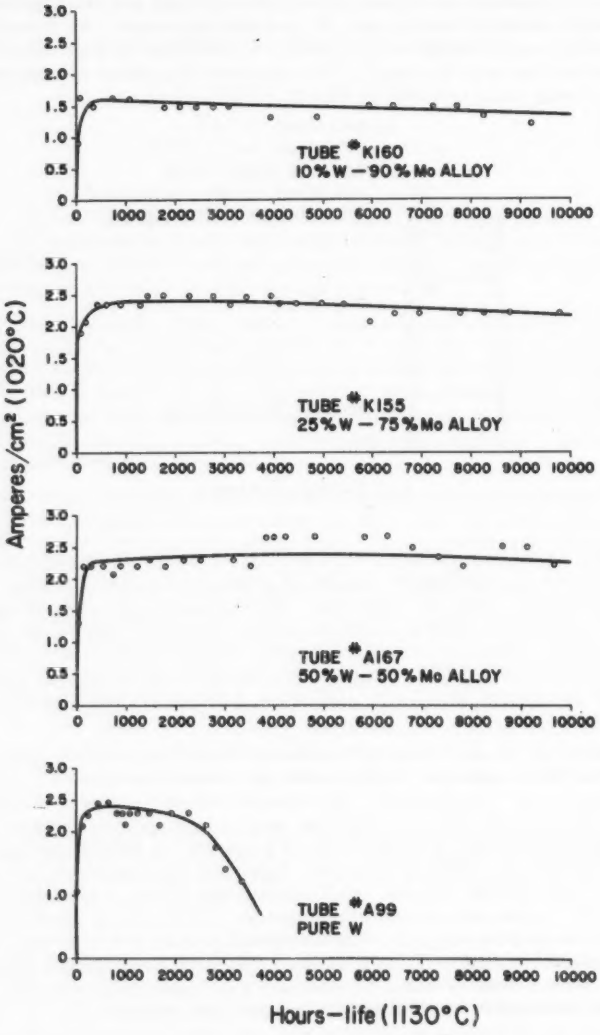

Fig. 2—Emission density (pulsed 1000 v, 100 μ sec. pulse length, 20/sec.) measured at 1020°C vs. life in hours at 1130°C.

gas release from the anode temporarily decreases the emission current, however, recovery is rapid. Upon application of similar voltages to a well degassed anode, no emission decay effects have been observed, nor has there been any noticeable mechanical deterioration of the cathode surface.

Cathodes processed under poor vacuum conditions (10^{-2} - 10^{-3} mm) were subjected to severe ion bombardment under applied anode voltage. This momentarily decreased the emission; however, after tip-off, activation time and emission level were similar to cathodes processed under excellent vacuum conditions.

Cathodes that were exposed to one atmosphere of air for several months showed no weight gain. Although the activation time increased approximately 100%, the equilibrium emission level was not decreased.

Tests on cathodes that were processed in the usual manner, opened to air at room temperature, and reprocessed showed little change in activation time or emission level for at least five exposures.

Cathode data obtained for Schottky and Richardson plots showed a work function of 1.7 e.v. at $0^{o}K$ and an A of 1.8 amps./cm^2/$deg.^2$. Figure 3, shows the relationship between the saturated emission (Schottky corrected) and cathode temperature.

In the foregoing discussion, the rugged nature of the pressed cathode has been demonstrated. It also possesses other desirable properties. Furthermore, the use of relatively inexpensive powder metallurgy techniques for its preparation provides a cathode of low cost.

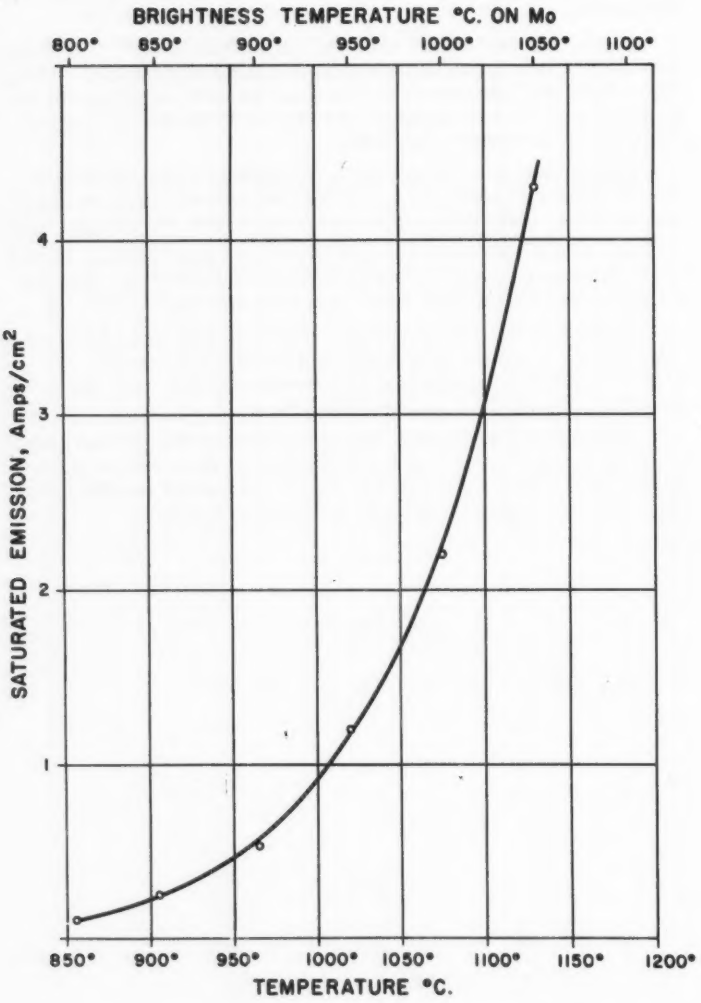

Fig. 3—Saturated emission (Schottky corrected) as a function of temperature.

Abstract Number 65

THERMIONIC EMISSION EVALUATION OF SINGLE CONSTITUENT ADDITIVES IN PURE NICKEL CATHODES

Frederick T. Hill and Edmund S. Mockus

Raytheon Manufacturing Company
Newton, Mass.

The evaluation of an oxide coated nickel sleeve has generally been carried out in a vacuum tube structure in which the cathode sleeve has always contained more than one major impurity. Also the other metallic components which are contributing to the build up of migratory impurities[1] in the cathode sleeve have never been made of pure nickel.

This work[2] undertook the problem of evaluating thermionic emission in a diode structure in which all the metallic parts were made from intrinsically pure nickel and the cathode alloys were made by adding pure metallic constituents to the same intrinsically pure nickel used in the fabrication of the parts.

The program for preparation of the pure nickel was carried out by National Research Corporation, Cambridge, Mass.[3] The process involved dissolving Mond nickel pellets in hydrochloric acid, removing the metallic impurities by chemical separation and then plating out the nickel from the nickel chloride solution. The nickel was further purified by vacuum melting to reduce the volatile metallic content and gas content.

The reducing impurities generally found in cathode alloys are silicon, magnesium and titanium. The three elements were selected for evaluation. Tungsten, aluminum and molybdenum were added to this.

The single constituent alloys were prepared by vacuum melting the pure nickel ingots, adding the appropriate charge of the alloying element and then vacuum casting the alloy.

The impurity content of the pure nickel and the nickel alloys was controlled by spectrographic analysis at each stage of preparation and fabrication.

The six elements to be studied were added to the pure nickel in the following concentrations (determined by analysis).

1. Silicon	0.123%	0.50%	---
2. Magnesium	0.013%	0.064%	0.092%
3. Titanium	0.13%	0.37%	0.53%
4. Tungsten	2.94%	4.36%	6.67%
5. Aluminum	0.098%	0.255%	0.500%
6. Molybdenum	0.99%	2.09%	2.90%

The structure used for emission studies is a plane parallel diode, ASTM construction,[4] to which has been added a tungsten wire welded to the inside of the cathode sleeve forming a tungsten-nickel thermocouple. Each single constituent alloy - tungsten thermocouple was calibrated against a platinum-platinum 10% rhodium thermocouple. The temperature calibrations were used to assure uniform processing at exhaust and activation and for emission testing.

Two lots of eight tubes each were fabricated for each cathode alloy sleeve. The tubes were exhausted in the conventional manner with cathode temperature control. One lot was exhausted at a peak cathode temperature of 1175°C and the other lot at 1250°C. Activation was carried out by heating the cathode for ten minutes at 1125°C if exhausted at 1175°C and at 1175°C if exhausted at 1250°C.

Each lot of diodes was lifed for 1000 hrs. at 6.3 volts on the heater (approx. 800°C) and 100 volts, thru a 1000 ohm resistor, to the anode. The current drain under these conditions was approximately 60 mAmperes or 120 mAmperes/sq. cm.

The tubes were tested at life intervals of 16, 50, 100, 250, 500 and 1000 hrs.

At testing the work factor[5] was determined by use of the following empirical form of Richardson's equation.

$$i = a\, e^{-\frac{\mathcal{E}\phi}{kT}}$$

where i = emission density

a = 1.2×10^6 amps/cm^2 empirical thermionic constant

$\mathcal{E}$ = electronic charge

ϕ = empirical work factor

k = Boltzmann's constant

T = temperature in degrees K

In the temperature range used, the work factor was 0.164 electron volts higher than the Richardson work function and the "a" value was 6×10^6 times the Richardson A value.

The work factor was determined by measuring the saturated emission current at 450°C and 360°C. Since previous experience showed what the "a" value should be, the work factor was determined from an emission versus temperature curve, the slope of the curve being the work factor. The difference between work factors at the two temperatures was not large for any alloy studied with the exception of the 4% and 6% tungsten nickel alloy. This showed that 1.2×10^6 amp/cm^2 was a good choice for an "a" value. The tungsten alloy had an "a" value below that of the other alloys.

Work factors were first evaluated for the pure nickel alloy which was to be used as a control lot for each alloy tested. But the pure

nickel cathode failed completely after 500 hours of life. A 699 alloy cathode was substituted and used as the control lot for each single constituent alloy. The results showed that the control lot, 699 alloy (average of 144 tubes), did not vary more than ± 0.015 electron volts. The best results for each metallic impurity are shown.

Alloy	Exhaust T°C	16	50	100	250	500	1000
Pure Ni	1250		1.29	1.16	1.14	failed	
0.5% Si	1250	1.09	1.08	1.09	1.12	1.16	1.20
0.092% Mg	1250	1.09	1.10	1.11	1.13	1.17	1.25
6.0% W	1175	1.10	1.09	1.12	1.19	1.19	1.21
0.3% Ti	1250	1.06	1.06	1.06	1.08	1.12	1.14
0.5% Al	1250	1.10	1.10	1.11	1.17	1.20	1.23
699 Alloy	1250	1.12	1.11	1.11	1.14	1.16	1.22

The titanium alloy cathode (0.3% Ti) showed the best work factor. The silicon-nickel alloy (0.5% Si) showed up second best. Tungsten, aluminum and magnesium were slightly better than 699 alloy for the first 500 hours of life. In later life, the 699 alloy would be preferred. The molybdenum nickel alloys were very poor for emission from 16 to 1000 hrs. of life and could not be evaluated by this method.

Four extra diodes from each lot were burned at 6.3 volts on the heater (800°C) at cut-off conditions. These tubes were read for interface resistance using the Frost bridge method. The only alloy showing interface was the 0.5% Si-Nickel.

Each lot of tubes was measured thruout life for heater-cathode leakage. The conditions of the test were 6.3 volts on the heater and 100 volts D.C. with the cathode positive and negative in respect to the heater. The readings were all in the range of one (1) μ ampere and below for all alloys tested.

A special diode, using a bare cathode sleeve opposite a target mica, was used for measuring changes in resistance due to the sublimed material deposited when the cathode sleeve was heat treated at 900°C. The Mg-Ni alloys were the only cathode sleeves showing any sublimation.

In summary, it can be said that the pure nickel and molybdenum nickel showed very poor emission potential. The silicon, magnesium, aluminum and tungsten nickel alloys were moderately good emitters. The titanium-nickel alloys were the best emitters and deserve further study in other vacuum tube structures.

References

1. Fundamental Research on Raw Materials used for Electron Emissivity, Raytheon Manufacturing Company, Contract NObsr-49138

2,3. Thermionic Emission Evaluation of Single Constituent Additives in Pure Nickel Cathode, Raytheon Manufacturing Company, Contract NObsr-63058

4. ASTM Bulletin B270-52T

5. The Theoretical Background for the Simplified Diode-Testing of Oxide Coated Cathodes, Dr. W. B. Nottingham, Fourteenth Annual Conference of Physical Electronics, March 25, 1954

Abstract Number 66

APPLICATION OF AUTOMATIC RECORDING INSTRUMENTS TO THE MEASUREMENT OF EMISSION

C. D. Richard, Jr., and R. D. Yeaton

Superior Tube Company
Norristown, Pa.

Automatic recording instruments applied to the measurement of thermionic emission from oxide coated cathodes provide new and improved data for interpreting performance characteristics of vacuum tube cathodes. The use of these instruments permits relatively unskilled personnel to obtain accurate electrical measurements. These facts have been proven during an investigation of the applicability of these instruments to emission testing conducted in the Electronic Laboratory at Superior Tube Company. The measurements were made on the ASTM Standard Diode described in the Tentative Method of Test, B270-52T. The diodes were processed on exhaust according to a standard schedule to facilitate the evaluation of cathode nickel alloys as a base for the oxide coated cathodes. In some separate investigations this schedule has been varied to determine the effect of processing upon the performance of the cathode. The tubes have then been life tested under standardized conditions. The aging schedule is deliberately omitted in order to show the variation in emission current during stabilization of the tubes.

Cathode base materials are evaluated with respect to a number of performance characteristics. One of the more important of these characteristics is the "rate of activation" of the cathode. This determines the ease with which vacuum tubes can be processed to an optimum emission characteristic. In the past, an estimation of the rate was made by determining the test period on life at which the tubes reached their optimum emission stability. This, at best, is a very crude measurement. Now, with the emission data plotted continuously, by a recording potentiometer, especially during the early life hours, the rate of activation is accurately depicted. The differences in activity between the various cathode nickel alloys are emphasized when the aging process is omitted. This activation characteristic is shown for several active and passive cathode nickel alloys indicating that a differentiation can be made.

This type of measurement is not only interesting from the standpoint of evaluating cathode base metals, but has also been used to determine the effects of variations in processing. The emission level and early hour slump are somewhat dependent upon both the exhaust processing and the subsequent aging. A continuous measurement of emission current under standard operating conditions for a few hours shows whether or not the best combination of exhaust and aging schedules has been used for the particular cathode nickel alloy and tube type under test.

The instrument commonly referred to as an X-Y plotter was also investigated. This instrument automatically plots the effect of two variables as a curve on rectangular coordinate paper. Any two variables may be compared providing they can be represented as potential differences. Use of this instrument has made possible the automatic plotting of tube characteristics, especially the static emission characteristic of the Standard . Diode.

A number of different measurements have been performed. These include the variation of emission current, with respect to cathode temperature; the variation of emission current, with respect to heater voltage; and the variation of emission current, with respect to plate voltage at constant heater voltage settings. The graph of emission current with respect to cathode temperature is very similar to the graph of emission current with respect to heater voltage. This relationship between emission current and heater voltage has been used for years to calculate the dc emission figure of merit for the evaluation of cathode materials. It is now possible to obtain this emission characteristic very conveniently and accurately by using the automatic plotting techniques.

The plotting of emission current with respect to plate voltage provides a measure of the stability of the tube and therefore, the completeness of the activation. This is accomplished by measuring the variation of emission current as the plate voltage is increased and then decreased. For a completely stable tube both of these curves are identical. For an incompletely activated tube the decreasing plate voltage traces a higher curve. If the curve produced by increasing the plate voltage is higher the tube is subject to a slumping characteristic caused either by overactivation or some poisoning effect. Therefore, this measurement provides another method for evaluating tube processing schedules.

The investigation of automatic instrumentation has made possible the accurate measurement of cathode performance characteristics such as "rate of activation" and "dc emission figure of merit". Other investigators have measured "triode characteristics" and metallic "sublimation". Further development

will permit reduction in the amount of testing by providing more accurate measurements and better control of processing. All of this testing can now be performed by relatively unskilled personnel as compared to that required by other methods.

Abstract Number 67

A SIMPLIFIED GAS ADSORPTION METHOD FOR THE DETERMINATION OF THE SURFACE AREA OF FINE POWDERS

Dominic T. Palumbo, Forest M. Starkweather, D. J. Bracco

Chemistry Laboratory
Sylvania Electric Products Inc.
Flushing, N. Y.

INTRODUCTION

In the investigation of the preparation of triple carbonates for use in oxide cathode studies a reliable measure of the surface area of the prepared carbonates is required. It was proposed to measure the area by the Brunnauer-Emmett-Teller (B.E.T.) gas adsorption method. Comparison of the B.E.T. measures of area with optical and electron microscope examinations of triple carbonates shows it to be a reliable method for the materials and size range investigated (0.07μ to 1.0μ). The major drawback of the B.E.T. procedure is the time required for a determination. At least two working days elapsed time per sample are required for the measurement.* The result is that any experimental program which depends on the B.E.T. measurements is correspondingly slowed down.

In preliminary experiments, such as those where various procedures for the preparation of carbonates are surveyed, a surface area value within 25% of the true area is usually sufficient for meaningful results. A simplification of the method to reduce the time per determination to about one hour with a negative error no greater than 10% of the standard E.E.T. value is presented below.

EXPERIMENTAL

1. Standard B.E.T. Adsorption Method

The apparatus used for the determination of surface area is of standard design. The apparatus and procedure have been described by Emmett[1] and need little comment here. Emmett[2] does point out, however, that the slope of an adsorption curve using zero intercept and one datum point is usually within 5% of the slope determined from three to four points. With a shorter outgassing schedule and a one point adsorption together with other modifications described below, it is possible to reduce the time for a determination to one hour.

*Actual operator time approximately six hours.

2. Simplified B.E.T. Procedure

The apparatus used for the determination was the same as in the standard method excepting that the sample tube position is fitted with a ground glass joint. This eliminates a glass sealing operation and recalibration of the sample tube volume for each run. The simplified procedure contains the following features:

1. Sample tube calibrated for volume with ground glass connection to the system.
2. Outgassing of the sample at room temperature for 10-20 minutes to a pressure of 1μ or less.
3. One point nitrogen adsorption run near 15 cm. pressure.
4. Assumed zero intercept for the curve.

The accuracy of the proposed method was checked by determining the surface area of samples of interest (phosphors and triple carbonates) by both procedures.

COMPARISON OF THE METHODS

In evaluating the methods the following comparisons were of interest:

1. Reproducibility of Each Method

Table I gives a comparison of the reproducibility of the methods. With the standard method the average deviation was 0 to 1.8%; for the simplified procedure the average deviation was 0.26 to 1.4%.

2. Agreement of Surface Area Values Between the Two Methods

In most cases it was found that the simplified B.E.T. method gave values that varied less than 10% from the standard value (Table II). Only in the case of a precipitated ZnS was the simplified method appreciably in error (about 27% low). Also, the reported values are, in all but one case, on the low side of the standard B.E.T. value. Table III indicates that with more complete outgassing, the values by the simplified method approach those by the standard method.

CONCLUSIONS

1. For the group of materials investigated (triple carbonates, zinc sulfide, cadmium sulfide, zinc silicate) a rapid and simplified B.E.T. method gives surface area values usually within 10% of those obtained by the standard method.

2. Surface areas determined by the simplified method are usually lower than those obtained by the standard method. By increasing the time and temperature of outgassing the rapid method gives results more closely in agreement with the standard value.

Bibliography

1. P. H. Emmett, Advances in Colloid Science, p.3, Interscience Publishers, Inc., New York (1942).

2. Ibid, p.13.

TABLE I

Reproducibility of Standard and Simplified B.E.T. Procedures

Standard Method				Simplified Method			
Sample	Run No. 1 M^2/gm	Run No. 2 M^2/gm	Avg. Dev. %	Sample	Run No. 1 M^2/gm	Run No. 2 M^2/gm	Avg. Dev. %
Triple Carbonate	5.76	5.74	0.17				
Triple Carbonate	2.45	2.45	0.00	Zn S	20.5	20.3	0.78
Triple Carbonate	9.31	9.00	1.67	Triple Carbonate	2.20	2.23	0.68
				Cd S	19.0	19.1	0.26

TABLE II

Comparison of Standard and Simplified B.E.T. Surface Area Determinations

Material	Standard BET M^2/gm	Simplified B.E.T. M^2/gm	Error - % of Standard Value
ZnS*	0.30	0.28	- 6.7
ZnS**	27.9	20.4	-26.9
Zn_2SiO_4	1.26	1.29	+ 2.4
Zn_2SiO_4	0.90	0.84	- 6.7
CdS	20.9	19.1	- 3.9
Triple Carbonate	2.45	2.21	- 9.8
Triple Carbonate	5.74	5.20	- 9.4

*Fired Sample
**Precipitated Sample

TABLE III

Effect of Time and Temperature of Outgassing on Surface Area

Time Minutes	Temperature ^{o}C	Simplified B.E.T. M^2/gm	Error - % of Standard Value
10	25	20.3	-26.9
30	110	24.2	-13.4
90	140	25.6	- 9.4
360	140	27.9*	0

*Standard value: outgas two hours at room temperature, four hours at 140^{o}C, three adsorption points for curve.

Abstract Number 68

THE ELECTRICAL PROPERTIES OF THE OXIDE CATHODE COATING

Ralph Forman

National Bureau of Standards

Over the years many theories have been proposed to explain oxide cathode emission. In recent years only two physical models have been seriously considered as offering a suitable explanation for this phenomenon. They are (1) the semiconductor model and (2) the porous semiconductor model suggested by Loosjes and Vink.[1] Below about 700° K both theories agree that the oxide cathode has semiconductor properties. It is at higher temperatures that they differ. Using the usual methods of preparing oxide cathodes, one obtains a coating which is quite porous. According to Loosjes and Vink, these pores become filled with an electron gas at high temperatures. If an electric field is then applied across the coating, the current is predominantly due to the electron gas in the pores.

There has been considerable controversy in recent years over the relative merit of the two models. Hall and conductivity measurements, which are commonly used in analyzing the properties of semiconductors, offer a means of differentiating between the two. Hall measurements on oxide cathodes have been previously reported by D. A. Wright[2] and Y. Ishihawa and collaborators.[3] They interpreted their results using a semiconductor model, but a number of anomalous details were reported which seem inconsistent with this model such as (1) high electron mobility values and (2) large magnetoresistive effects. As an example they found electron mobility values for the oxide cathode in the order of 2,000 cm^2/volt sec at a temperature of 1000° K. Pell[4] reported mobility values less than 10 cm^2/volt sec at 800° K for BaO single crystals. Since BaO is considered the most important constituent of the oxide cathode, this discrepancy between approximately 2000 and 10 should be explained.

The experiments which were undertaken at the National Bureau of Standards Tube Laboratory had the following objectives. First to see if data similar to that of Wright and Ishikawa could be obtained, and secondly to extend the measurements down to a much lower temperature (about 500° K). Previous measurements had been made above 700° K, and it was felt that a valid check on the Loosjes and Vink model could only be made if the measurements were made over the whole temperature range in which they claimed the transition from porous semiconductor to semiconductor took place. These measurements have been made, and the results are presented below.

The oxide cathode coatings studied were double carbonates (barium, strontium) for which the deposition was controlled so as to produce a marked variation in porosity from sample to sample. The coatings were deposited on slip cast bases[5] of very pure MgO which were provided with platinum current leads and voltage probes. A Pt-Pt(13% Rh) thermocouple was used for temperature determinations. The finished units were mounted in tubes and were processed on a vacuum system which included an oil diffusion pump, two Westinghouse metal valves, thermocouple and ionization gauges and an ethane gas bottle. Activation of the oxide coatings was accomplished by treating them in ethane, a procedure similar to that described by Wright.[2] The use of an electrometer in these measurements made it possible to extend the measurements from 1000° K to 500° K even though the resistivity at the latter temperature is very large.

The conductivity and Hall data obtained could be interpreted by using the porous semiconductor model.[6] Curves of logarithm of the conductivity versus the reciprocal of the temperature showed the characteristic break in slope noted by Loosjes and Vink.[1] Each of the curves of the logarithm of the Hall coefficient vs the reciprocal of the absolute temperature had maximum at a temperature the same as that at which the break in the conductivity curves occurred. An explanation of the results will show that the Hall voltage at high temperatures is controlled largely by conduction through the pores; while on the other hand the Hall data at low temperatures is dependent on two parallel mechanisms of electrical conduction; namely, semiconduction and conduction through pores.

Magnetoresistive measurements on the samples were also made. These measurements consist of measuring the change in resistance of the cathode coatings when a magnetic field is applied perpendicular to the direction of current flow. Very large magnetoresistive effects were observed. In some samples the resistance increased by a factor of 10 when a magnetic field of 500-1000 gauss was applied. The possible explanation[6] of the large magnetoresistive effect at a comparatively low magnetic field strength, which is offered by the pore conduction theory, will be discussed.

The magnitude of the mobility of the charged carriers in the porous cathode coatings was high at temperatures about 700°K. These values were computed from the relation $\mu = \sigma R_H$ where μ is the mobility, σ the conductivity and R_H the Hall coefficient. These large values are consistent with the theoretical interpretation of mobility based on the pore conduction model. At lower temperatures the values for mobility drop by orders of magnitude and approach values which are consistent with measurements on single crystals of BaO[4].

In conclusion, it is felt that the experimental results obtained in this investigation indicate the following physical model for the oxide cathode coating. At high temperatures the mechanism for electrical conduction is predominantly pore conduction. At about 700° K there is a transition range where two equivalent mechanisms exist, namely that

of pore conduction and semiconduction. At a temperature of 500° K semiconduction predominates.

References

1. R. Loosjes and H. J. Vink, Philips Research Repts. 4,449 (1949).
2. D. A. Wright, Brit. J. Appl. Phys. 1, 150 (1950).
3. Ishikawa, Sato, Okumura and Sasaki, Phys. Rev. 84, 371 (1951).
4. E. M. Pell, Phys. Rev. 87, 457 (1952).
5. W. B. Haliday and J. R. Nall, Rev. Sci. Instr. 25, 1225 (1954).
6. R. Forman, Phys. Rev. 96, 1479 (1954).

ACTIVATION OF AN OXIDE CATHODE BY Ba, Sr, Ca, AND Mg DEPOSITED VIA A MASS SPECTROMETER

R. M. Matheson and R. H. Plumlee

Nergaard[1] has recently advanced the hypothesis that the activity of an oxide cathode is due to oxygen vacancies present in the oxide lattice. The salient features of this hypothesis are:

1. An oxide cathode is an impurity semiconductor
2. The electron donors are oxygen vacancies containing two electrons, i.e., F-centers.
3. The donors are mobile, i.e., they can electrolyze and diffuse.
4. When no current is drawn from the cathode, the donors are uniformly distributed throughout the cathode.
5. When current is drawn, the donors electrolyze away from the positive surface of the cathode, leaving a donor-depleted layer where the electronic properties approach those of the intrinsic material.
6. Under equilibrium conditions, i.e., when the cathode current is stable, the electrolysis of donors is balanced by back diffusion.

Earlier experiments[1, 2, 3] have indicated that depositing Ba on the front surface of a cathode results in a marked increase in the activity of the cathode. The results of these experiments are explained by the oxygen vacancy hypothesis. Furthermore, it may be inferred from the hypothesis that the increase of cathode activity should be independent of the means employed to create oxygen vacancies at the surface of the cathode. The present experiments were performed to test this inference. If oxygen vacancies can be created by depositing Ba on the cathode surface, then it seems likely that deposition of other alkaline earth metals should also produce vacancies, and equal changes in activity should be observed whichever metal is deposited, provided the rate of reaction between the incident ions and the oxide lattice is not the controlling factor.

The experimental arrangement used in the present measurements has been described previously.[1] Mass separated beams of Ba^+, Sr^+, Ca^+, and Mg^+ were deposited on the surface of the cathode, which was coated with 10 mg. of pure BaO per cm^2. The activity of the cathode was measured by observing the change in plate current with a fixed 60-cycle anode voltage applied. As in earlier experiments[1] the cathode was deactivated prior to each deposit by heating to 1150°K for ten minutes without drawing plate current. This treatment results in a

major fraction of the diode voltage drop appearing across the cathode coating. To insure that the measurements were not influenced by the presence of background gases in the spectrometer, the plate current of a second diode located directly behind the test cathode was monitored. During the course of measurements the pressure was always less than 2×10^{-8} mm Hg. and the activity of the reference cathode remained constant.

At temperatures of 900°K or greater, the cathode activity rises sharply when Ba is deposited on the surface; amounts as small as one one-hundredth of a monolayer causing the plate current in the diode to rise by a factor of two. Continued deposition causes a slower rise in plate current, and the plate current finally approaches an asymptote. When deposition ceases, the plate current decays slowly to a final value greater than that before deposition. The shape and magnitude of the rise and decay curves were the same within experimental error for all four ions. In particular, the shift in the final asymptote was approximately proportional to the number of monolayers deposited regardless of which ion was used.

At lower temperatures the effects of deposition are much more complicated. The results for temperatures in the range 750° to 900°K will be described briefly.

MASS SPECTROMETRIC STUDY OF THE FIELD DEPENDENT EVOLUTION OF CONSTITUENTS OF A BaO CATHODE

R. H. Plumlee

RCA Laboratories
Princeton, N. J.

The purpose of this experiment was to measure the dependence of the evolution of oxygen and/or Ba, from a BaO cathode, upon temperature, time, state of activation, duty cycle, and upon electric field produced across the BaO coating during the drawing of electron emission.

The following volatile constituents were found to be loosed from the BaO cathode by application of positive anode voltages to the electron collector: H_2, H_2O, O_2, CO and/or N_2, and CO_2. For H_2O the increment in H_2O^+ peak height produced by an applied anode voltage increment was negative; for all the others listed above, the increment was positive. No Ba evaporation was found for temperatures up to 1085°K, the highest at which a search was made for Ba. The Ba evaporation, if it occurred, was concluded to be fully an order of magnitude less than the field-produced O_2 evolution. Field-produced increments in partial pressures of the common gas species listed were in the range of 10^{-9} to 5×10^{-8} mm Hg. Characteristic build-up curves for these increments with anode voltage on and decay curves for the increments after anode voltage was turned off can be represented as sums of two or three exponential terms with time constants ranging from less than a second to many minutes.

The asymptotic values of the field-produced increment in the CO_2^+ spectrum peak appear to be proportional to the background CO_2 partial pressure. The asymptotic values of the decrement in the H_2O^+ peak appear to be proportional to the square of the background H_2O partial pressure. The field-produced increments increased with cathode temperature. The "activation energy" derived for the CO_2 increment is the same as the literature value for the heat of dissociation of $BaCO_3$.

The increments showed hysteresis and saturation effects when the anode voltage was varied. Evidence of similar behavior was simultaneously detected in the electron emission; however, there was no consistent correlation between the electron emission and the field-produced increments.

Cathode activity was found to respond reversibly and within a few seconds to changes in H_2O partial pressure of the order of 10^{-8} mm. Cathode activity showed no striking response to similar changes in O_2 partial pressure. The conditions of these measurements suggest that

the H_2O was involved indirectly in the activation of the cathode by participation in an "equilibrium" reaction with other unidentified species.

Analysis of the data and of the pumping line characteristics suggests that the field-produced increments in the evolution rates of the various common gas species from BaO were actually field-produced shifts in steady state (near equilibrium) partial pressure values. The time constants of these shifts suggest that a labile equilibrium exists between the vapor phase species and some anionic forms or fragments of them which readily occupy the vacant oxygen sites of the BaO crystal and which compete with the oxygen for these sites.

Abstract Number 71

FACTORS INFLUENCING THE PARTICLE SIZE IN THE PREPARATION OF ALKALINE EARTH CARBONATES

D. T. Palumbo, D. J. Bracco and A. K. Levine

Chemistry Laboratory
Sylvania Electric Products Inc.
Flushing, N. Y.

The effect of pH, temperature, and concentration on the particle size of precipitated alkaline earth carbonates is shown. Particle size is measured by gas adsorption and checked by optical and electron microscopy. Preparation conditions studied are such as to give a range of mean particle diameters extending over three orders of magnitude.

Abstract Number 72

PARTICLE SIZE MEASUREMENTS OF TELEVISION PHOSPHORS

J. G. Rabatin, E. S. Palik and R. H. Gale

Chemical Products Works
General Electric Company
Cleveland, Ohio

Particle size measurements of television phosphors are of great value in the control of application processes. The importance of controlling the quality and uniformity of phosphors has necessitated the search for accurate, fast and relatively automatic methods for particle size analyses. Several methods were examined extensively to determine limitations of each method and its practicability for use in the particle size analyses of television phosphors. All methods considered require assumptions to be made in regard to Stokes Law and to complete dispersion of the phosphor in the medium. Thus the methods must be considered as relative only. In general, the sub-sieve size range of 1 to 50 microns can be covered.

The following instruments were examined:

(1) The Sharples Micromerograph is an automatic recording instrument using an air settling medium.

(2) The Roller Particle Analyzer is an instrument which can be used to isolate size fractions by means of a stream of air whose velocity is regulated in accordance with Stokes Law.

(3) The Andreasen pipette utilizes a liquid medium for dispersion of the powders. Samples are drawn off at various times from a given height then dried and weighed to determine size distributions.

(4) The automatic recording turbidimeter requires a liquid dispersing medium and as based on the postulate that the absorption of light is proportional to the projected areas of the particles.

(5) The automatic recording sedimentation pan utilizes a liquid medium in which is immersed a pan attached to a spring which extends slightly as particles fall on the pan. A shutter attached to the spring moves past a parallel light path. The resulting change in photocell current is recorded automatically. The recorded data is proportional to the weight on the pan and is easily converted to weight distribution curves.

(6) The Fisher Sub-Sieve Sizer is an air permeation instrument which requires a dry sample bed packed in a tube. A single value is obtained which is related to the total surface area of the phosphor powder.

A comparison of the results obtained by the methods described above is listed in Table I. The results clearly indicate that wide variations in

the cumulative percent weight curves were obtained using these methods, although the precision of each method is good. Invariably the Micromerograph results indicate much lower particle size distributions than those obtained by the other methods. The Roller Particle Analyzer curves lie between the Micromerograph curves and the sedimentation pan curves. The results obtained with the Andreasen pipette are in very good agreement with those obtained using the sedimentation pan technique. Comparison of the results of the turbidimeter method with the results of the other methods has limited value since the turbidimeter data must be converted to weight distributions. Since different means of dispersion are used in each method, the differences in the distribution curves are due partially to the degree to which each dispersing technique breaks down aggregates and agglomerates. The compressed nitrogen procedure used in the Micromerograph method is probably the most forceful. . A comparison of results from air medium with those from liquid medium is difficult.

The Fisher Sub-Sieve Sizer is used extensively giving particle diameter values which are related to the total surface of the powder. A comparison of these values with surface average diameters obtained from sedimentation pan and Micromerograph data is shown in Table II. The Fisher APD's are generally larger than the sedimentation pan APD's. This fact may indicate the presences of voids in the sample beds used for the sub-sieve sizer determinations. The Micromerograph values are lower than the sedimentation pan values. This may indicate that the Micromerograph dispersing technique breaks down aggregates. The Fisher APD's correlate poorly with the weight distribution curves and tend to give an incomplete description of the fineness of the phosphor powders.

Abstract Number 73

POLYVINYL ALCOHOL FOR PREPARATION OF COLOR TELEVISION SCREENS

C. W. Saltonstall

Research Division, Photo Products Department
E. I. du Pont de Nemours and Co., Inc.
Parlin, New Jersey

The properties and general chemistry of polyvinyl alcohol as used in the formation of phosphor patterns are reviewed. The basic application method depends on light sensitivity of bichromate containing films formed from dispersions of phosphors in polyvinyl alcohol. Exposure through a photographic negative forms a latent positive image which may be developed in water, and baking then removes organic material to leave a phosphor image.

Polyvinyl alcohol is a synthetic water soluble polyhydric alcohol prepared by hydrolysis of polyvinyl acetate. The degree of polymerization and hydrolysis affect such physical properties as solubility, tensile strength and adhesion. A number of grades differing in respect to these properties are commercially available, and the characteristics of typical examples are summarized.

Abstract Number 74

SCREEN POTENTIAL MEASUREMENTS IN CATHODE-RAY TUBES

J. R. Young

General Electric Research Laboratory
Schenectady, N. Y.

It has been known for many years that during normal operation the screen of a cathode-ray tube sometimes assumes a potential other than that of the anode. Various methods have been used to measure the potential taken up by an insulating material under electron bombardment. However, many of these methods cannot be employed for the measurement of screen potential in standard cathode-ray tubes. Of those which can be used, some serious disadvantages are present. The method employed in this investigation, the Kelvin vibrating condenser method, has been found to eliminate many of the disadvantages encountered previously. This method has been found to be accurate and quite easy to use. Extremely sensitive instruments are unnecessary—a standard vacuum tube voltmeter was used for a detector. Measurements can be made under normal operating conditions and without heating the face plate.

Screen potential measurements have been made on cathode-ray tubes having screens of ZnS powder phosphor, ZnS vapor deposited phosphor and bare glass. Results are similar in many respects to those obtained by previous observers. In every case, the screen remains very close to the anode in potential for low anode voltages, but at higher anode voltages the screen may be several kilovolts negative with respect to the anode. It has been found that "sticking" in the usual sense does not occur except in the case of bare glass. It is believed that the smoothness of the surface is an important factor in determining whether or not a material will stick. In the cases where sticking did not occur, a linear relationship was found to exist between the screen-anode potential difference and the anode voltage.

Abstract Number 75

POSITIVE ION PRODUCTION, ION-FOCUSSING FIELDS AND X-BURN IN COMMERCIAL CATHODE-RAY TUBES

W. A. Thornton

General Electric Research Laboratory
Schenectady, N. Y.

Under the conditions leading to internal electrostatic fields in cathode-ray tubes, ion acceleration and focussing will occur. The production, acceleration, and focussing of positive ions under these conditions, and phosphor deterioration by the ions, are considered here.

POSITIVE ION PRODUCTION

Bombardment of residual gas by high-energy primary electrons and by lower-energy secondary electrons appears to be the major positive ion producing process; bombardment of tube walls by secondaries is probably less important. By comparison to the yield of positive ions in a typical ionization gage, an estimate of 5×10^{-9} amperes of positive ion current to the phosphor screen, under normal operating conditions, is arrived at. Independent determination of total ion flux to produce detectable phosphor deterioration (reduced light output) predicts onset of ion burn in a few hours, particularly if ion-focussing is present. Anode coatings of aquadag, platinum, silver, aluminum, metal-cone tubes, and tubes in which most of the anode area was bare glass showed no significant differences in ion deterioration of the phosphor screens, suggesting that residual gas is the major source of positive ions. Since primary electron flux increases rapidly toward the rear of the tube volume, density of positive ion origin is expected to be greater there.

POSITIVE ION FOCUSSING

Where a screen-anode potential difference exists, geometrical configurations of equipotential surfaces in tubes of several geometries are considered. In a round tube—plane and cone electrodes—positive ion focussing to a maximum at the center of the face plate is indicated; this, plus the greater density of positive ions produced at the rear of the tube, and tending to remain near the axis, results in the observed diffuse center spot of ion deterioration. In a rectangular tube, four planes of symmetry through the equipotential surfaces intersect the face plate in the well-known X-like pattern. In a triangular tube, similar reasoning predicts a Y-pattern, which is observed. In the case of underscanning, if the raster area charges to a potential well below that of the unbombarded screen area, four-cornered symmetry of focussing fields again exists and the X-like pattern may occur regardless of the tube geometry.

X-BURN IN COMMERCIAL TUBES

X-burn in cathode-ray tubes is a decrease in electron-induced luminescence as a result of bombardment of the phosphor screen by focussed positive ions travelling at some velocity above a certain minimum. In the case of standard TV picture tubes with settled screens and operated at typical anode voltage, several observations were made:

1. X-burn requires sufficiently high screen-anode potential difference, near 1-2 KV, for the X-burn deterioration pattern to be visible in the region of operating voltage.

2. Sticking of the screen potential does not occur with settled screens because of the field dependence of the effective secondary emission ratio. Sticking is observed only with smooth surfaces.

3. There was no observed instance when a considerable ΔV was present in a rectangular tube that X-burn did not rapidly take place.

4. X-burn is not restricted to rectangular tubes, but occurs wherever four-cornered geometry of focussing fields exists.

5. The X-burn process begins earlier in tube life and proceeds more rapidly, as phosphor coating weight is decreased below the standard weight of about 5 mg/cm^2.

6. X-burn occurrence depends upon three factors:
   a) Positive ion production, b) ion acceleration and focussing, c) phosphor sensitivity to ion bombardment. It appears most feasible to minimize X-burn by elimination of the ion focussing fields in the tube.

7. Maintenance of secondary emission of phosphor screens appears to be the major problem, since typical screens show secondary emission properties that are sufficiently good initially to maintain the tube field-free.

Abstract Number 76

SECONDARY ELECTRON EMISSION IN CATHODE-RAY TUBES

A. B. Laponsky

General Electric Research Laboratory
Schenectady, N. Y.

The process of secondary electron emission is utilized in establishing the screen potential of a number of cathode-ray tubes where electrical contact to the bombarded surface cannot be made. The phenomenon of secondary emission, which is qualitatively similar for all materials, shows a rapid rise in the yield (ratio of secondary to primary current), the attainment of a maximum and a subsequent gradual decline as the energy of the bombarding electrons is increased. The requirement that the effective yield be unity in the steady state determines the screen potential. When the yield is greater than unity, the screen charges to the potential of the secondary electron collector and as this potential varies the screen potential follows. As the electron energy is increased to the region where the yield is less than unity, the screen charges to a potential below that of the collector giving unity yield in the steady state.

For the determination of the secondary emission yield of insulating or floating targets, two pulse methods have been employed. The first, a single gun method, is applicable to commercial tubes. This method establishes the screen potential at that of the secondary electron collector when the bombarding electron energy is in the range to give a yield greater than unity. After establishing the screen potential, secondary current may be drawn to the collector, or suppressed by pulsing the collector positive or negative. Pulse signals corresponding to the difference between the secondary and primary currents and primary current respectively may be obtained from the displacement current to an external conductor on the face of the tube. The yield may be calculated from the corresponding pulse heights observed on a cathode-ray oscilloscope.

The second method establishes the target potential by bombarding the target, by means of an auxiliary gun, with low energy electrons for which the yield is less than unity. The target stabilizes at the potential of the source of these electrons. Pulsed currents which correspond to the difference between the secondary and primary current in the lead to the target plate may be observed on an oscilloscope. The primary current may similarly be determined when the collector and target plate are connected together. This method of determining the yield requires a specially designed tube.

The utilization of these methods has enabled some yield studies to be carried out. It has been found that the secondary electron yield is a function of the past history of the phosphor screen, the yield dropping with increased time of electron bombardment. In addition, the vacuum baking of the phosphor screen influences the yield in a manner that causes it to decrease as higher temperatures are employed. Vacuum baking does not necessarily remove deterioration which occurred under electron bombardment.

While the magnitude of secondary emission might be expected to depend only on the material under investigation and the electron bombarding energy, evidence has been obtained showing a small but definite dependence of yield on collecting potential. On a standard television phosphor in a standard television tube bulb, the variation in yield with respect to collecting potential was found to be $1.78 \cdot 10^{-4}$ volts^{-1} at 14,000 ev bombarding energy. Hence, in the vicinity of unity yield the actual yield could be increased to 1.09 by the occurrence of a collecting potential of 500 volts. The variation of yield with collecting potential is believed to be a consequence, at least in part, of the rough surface presented by a powdered phosphor screen and leads to the absence of "sticking" in the true sense.

While secondary emission is a fundamental process occurring in cathode-ray tubes, both the process and the yield measurements seem sufficiently complex that actual screen potential determinations offer more direct information in evaluating actual tube performance.

Abstract Number 78

INJECTION AND EXTRACTION*

Ralph Bray

Purdue University
Lafayette, Indiana

On both p- and n-type Ge, contacts may be made which have low resistance, but which may greatly enhance minority carrier concentration by injection, or almost completely deplete it by extraction.[1] Ordinary minority carrier injection into germanium from a metal contact is attributed to the existence of a surface inversion layer, i.e. a layer of opposite type to that in the interior. For extraction, we postulate a surface layer of the same type (p or n) but more extrinsic (p+ or n+) than the bulk semiconductor. Here then, the minority carrier concentration is small at the contact. With forward current, a deficit concentration of minority carriers is propagated into the interior. The net result is a depletion of hole-electron pairs in the interior. Complete extraction of hole-electron pairs originating either by thermal or optical generation may be attained if the following two conditions are satisfied: (1) the sweep field in the sample must be high enough so that transit time for minority carriers is much less than the lifetime, and (2) the minority carrier flux across the forward-biased contact must approach zero.

Highly injecting and almost completely extracting contacts to Ge have been made as follows: the Ge surface is first ground, then strongly etched. Soldering at just above the melting point of the solder, gives with pure Sn or In, highly injecting contacts on n-type, and extracting contacts on p-type Ge. Heating the soldered contacts to about 300°C in air for a few minutes usually does not change the In contacts, but just reverses the behaviour of the Sn soldered contacts on both p- and n-type Ge.

The behaviour of the contacts may be tested in several ways.

(1). Photovoltaic test. Observation of polarity of open-circuit photovoltage produced by intense illumination of the contact, shows that the metal side is positive for an injecting contact on n-type, or an extracting contact on p-type Ge. Negative metal polarity is observed for the two opposite cases.

(2). Bulk resistance modulation. Application of forward current decreases bulk resistance for injection, but increases it for extraction. The latter effect is greatly enhanced if the Ge is illuminated, or for moderate rise above room temperature.

*Work supported by Signal Corps Contract.

(3). Collector Contact current modulation. Injection of minority carriers in a sample on which a collector contact is operated, produces an increase in reverse collector current. Extraction, however, produces a decrease in collector current.

We discuss below three ways in which highly injecting or extracting, low resistance contacts may be applied to devices.

(1). Bulk rectification. Considerable bulk rectification may be obtained by using an extracting contact. Such rectification is not due to a high contact resistance, but rather to modulation of the bulk resistance, by sweeping out hole-electron pairs from the bulk for one direction of the current, but not for the other direction. Such rectification is enhanced by illumination or by moderate rise in temperature, contrary to the usual contact rectification. One design for such a rectifier consists of a small area, low resistance, extracting contact on a slab of Ge, and a large area, low resistance, preferably injecting base contact. The Ge should be close to intrinsic. In this design, forward bias on the small area contact depletes the concentration of thermally or optically generated hole-electron pairs from the spreading resistance region, giving enhanced resistance. Reverse bias gives only the normal resistance for given temperature and illumination. Rectification ratios at 10 volts of 10 : 1 have been observed.

(2). Base Contact control of collector response. The injecting or extracting behaviour of a low resistance base contact may be used to greatly influence the properties of a collector contact on a diode or a transistor. When reverse bias is applied to a collector contact, considerable sweep field may exist in the interior especially if the collector reverse resistance is lowered permanently by forming, or temporarily by illumination or heating. This sweep field operates the base contact in the forward direction, which may therefore be producing injection or extraction. The base contact injection may greatly enhance the collector current, thereby decreasing reverse resistance and peak back voltage. Base contact extraction may reduce collector current, thereby increasing collector resistance and peak back voltage. This was demonstrated for given collector contacts by observing their characteristics with respect to separate injecting and extracting base contacts on the Ge slab. A particularly interesting application results from combining a high resistance collector contact with a highly injecting base contact. In the dark, the collector reverse current even at 100 volts may be too low to permit base injection. Illumination, although directly increasing reverse current by a factor of only two or three, opens the gate to base injection which may drop the peak voltage to about 10 volts, and increase the reverse current to several hundred milliamperes. An auxiliary emitter contact may be substituted for the light source, so that an electrical rather than an optical trigger may be used.

(3). Auxiliary Extracting Contact. The properties of a diode or transistor may be modulated with an auxiliary extracting contact, which then needs its own bias supply. In the particular case of a p-type Ge

diode, illumination may greatly enhance the reverse current. Sufficient forward bias on the auxiliary extracting contact may then be used to sweep out the excess carriers and restore and even enhance the initial high reverse resistance of the diode.

In summary, it is apparent that deliberate control of the properties of the base contact, or use of auxiliary injecting and extracting contacts, may be used to extend the degree of control of diodes and transistors.

Reference

1. R. Bray, Bulletin of the Amer. Phys. Soc., Chicago Meeting, Nov. 1954.

THE GERMANIUM-OXYGEN SYSTEM*

Donald Tuomi** and Edward S. Candidus***

Lincoln Laboratory, Massachusetts Institute of Technology
Lexington, Massachusetts

This study of the germanium-oxygen phase diagram was originally initiated to clarify the facts relating to the role of oxygen in the processing of germanium. In all normal operations the oxides of germanium are present to a variable extent.

The phase diagram for pure GeO_2 has been established by Laubengayer and Morton[1]. The water soluble hexagonal form normally encountered is thermodynamically stable from 1035° to 1115° C. The insoluble tetragonal form is stable below 1035° C. At 1115° C. the hexagonal form fuses to a viscous liquid which may be converted to a glass. Above 650°C. the glass devitrifys to hexagonal GeO_2. The transformation to the tetragonal form may be accelerated by a hydrothermal process below 500°C. or by digestion with a LiCl-KCl flux between 500° to 1000° C.

The characteristics of solid GeO are not as well defined. Bues and V. Wartenburg[2] have presented evidence that an amorphous GeO may be prepared which disproportionates above 700° C. to Ge plus GeO_2. Jolly and Latimer[3] concluded from vapor pressure data that solid GeO is thermodynamically unstable at all temperatures below 600° C. In 1954 Hoch and Johnston[4] presented high temperature x-ray data which demonstrated the occurrence of a solid phase reaction between Ge and GeO_2 at elevated temperatures.

The general features of the Ge-O phase diagram were determined by heat treating mixtures of germanium powder with hexagonal and tetragonal GeO_2 at 800 to 960° C. followed by quenching to room temperature. A static nitrogen atmosphere was used to suppress the GeO evaporation. The reaction products were characterized by microscopic examination and x-ray diffraction powder photographs.

As shown in Fig. 1 the phase diagram is characterized by a eutectic at 870 ± 10° C. having a composition corresponding to 61 atomic per cent oxygen. From 870° to 940° C. solid germanium is in equilibrium with a viscous liquid oxide phase containing from 61 to 60 atomic per

*The research in this document was supported jointly by the Army, Navy, and Air Force under contract with the Massachusetts Institute of Technology.

**Present address: Baird Associates Inc., Cambridge, Mass.
***Staff Member

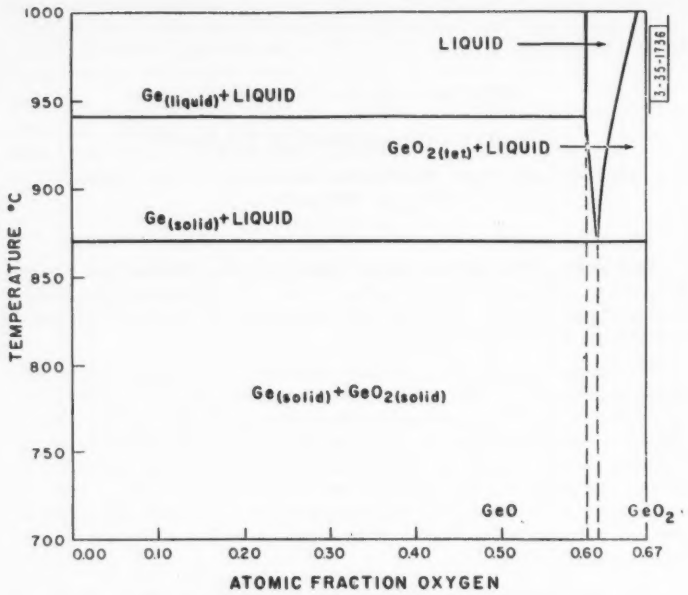

Fig. 1 —Germanium-oxygen phase diagram

cent oxygen. Above the germanium melting point, 940° C, the system consists of two immiscible liquids: Ge and an oxide phase containing 60 atomic per cent oxygen. It is interesting to note that Ge powder in contact with the liquid oxide phase recrystallized to form platelet and needle crystals with well defined crystal faces.

On the GeO_2 rich side of the phase diagram a two phase field exists within which the liquid oxide phase is in equilibrium with tetragonal GeO_2. The heating of a mixture of hex. GeO_2 and Ge containing 63.7 atomic per cent oxygen to 870° C. resulted in fusion to a liquid phase. Prolonged heat treatment of this liquid phase at 900° C. resulted in the precipitation of white tetragonal GeO_2 crystals within the liquid matrix.

The heat treatment of Ge and tetragonal GeO_2 mixtures under similar conditions resulted in products similar to those obtained with the hexagonal form; however, the rates of the reactions were appreciably slower between 870° and 940° C.

The rapid cooling of the liquid oxide from above 870° C. to room temperature resulted in the formation of a black glassy solid. This solid, characterized by a germanium x-ray diffraction pattern, probably consists of precipitated Ge dispersed in a GeO_2 glass. The black glass phase on cooling in a quartz tube consistently caused internal

chipping because of the differential contraction of the glassy phase and the quartz. Limited data suggest that the viscosity of the liquid phase increases on repeated fusions. The heat treatment of the black glass at 800° C. resulted in the formation of hexagonal GeO_2. Amorphous GeO prepared by condensing GeO on a cold surface disproportionated at 800° C. to Ge plus hexagonal GeO_2.

The measurement of the germanium melting point under a variety of conditions was used to determine the phase diagram characteristics at low oxygen concentrations. The melting points were measured using a Pt - Pt 13% Rh. thermocouple calibrated at the silver point with the cold junction at 0° C. The thermocouple EMF was measured with a Leeds Northrup No. 8662 millivolt indicator.

The melting point data are summarized in Table 1. In these experiments the partial pressure of GeO in the system was varied from 10^{-6} to 10-100 mm Hg. without a significant variation in the melting point. Nor was it possible to significantly alter the melting point by repeated vacuum fusion and solidification. Consequently the conclusion is indicated that GeO cannot readily alter the melting point of Ge.

Table I

Germanium Melting Point Data

Sample	Atmosphere	T° C.
N_2 - 12 Pass Zone Refined	Argon	940.2
	Vac. 10^{-5} mm Hg.	940.0
Ge fused under GeO_2	Argon	940.1
N_2 - 12 Pass Zone Refined	Vacuum	939.9
Ge Pwd. + 18% Tet. GeO_2	Nitrogen	339.9
N_2 - 12 Pass Zone Refined	Nitrogen	940.1
H_2 Fused Bar	Nitrogen	939.5
Ave.		940. °C.

In the vacuum fusion experiments an amount of GeO was deposited in the cool portion of the reaction tube which would correspond to 0.1 to 0.01% GeO in the original sample. The observation by R. M. Whaley[5] that a brown smoke is evolved from Ge during vacuum fusion but ceases as soon as fusion is complete suggests that a finite oxygen solid solubility exists.

Several implications of the phase diagram are interesting to note. In the reduction of GeO_2 at temperatures above 750° C the rate of evolution of GeO becomes rapid. This effect may be explained by the rapid increase in the partial pressure of GeO over a Ge - GeO_2 mixture above 700° C. In the heat treatment of germanium samples above 870° C. a viscous liquid oxide film will be formed from the hexagonal or vitrous oxide normally present. Consequently anomalies in the oxidation of Ge at elevated temperatures would be anticipated.

References

1. A. Laubengayer and D. S. Morton, J. Am. Chem. Soc. 54, 2315 (1932).
2. W. Bues and H. V. Wartenberg, Z. Anorg. Allgem. Chem. 266, 281 (1951)
3. W. L. Jolly and W. M. Latimer, J. Am. Chem. Soc. 74, 5757 (1952).
4. M. Hoch and H. L. Johnston, J. Chem. Phys. 22, 1376 (1954).
5. H. C. Torrey and C. A. Whitmer, Crystal Rectifiers, McGraw-Hill Book Co. Inc. N.Y. (1948) p. 368

Abstract Number 80

DONOR ACCEPTOR BALANCE IN SELENIUM RECTIFIERS

H. W. Henkels

Westinghouse Electric Corp.
Pittsburgh, Penna.

The selenium rectifier manufacturing process is quite complex, depending on a number of variables which must be controlled with considerable accuracy and precision. In the development of improved selenium rectifiers having lower forward drops, lower reverse leakages and higher operating temperatures, it is necessary to carefully adjust and control the levels of parameters employed in the process. The proper choice of important process parameters must be made on the basis of the theory of the selenium semiconductor and rectifier or on the basis of rather extensive experimental data.

A model of the selenium semiconductor has been developed[1,2,3]. It was found that halogens form acceptor levels, most metals donor levels. The most effective acceptor element is chlorine; the most effective donor element thallium. The model is used in advancing an n-p or $p\text{-}p^{+}$ theory of the metal-selenium rectifier. The equilibrium theory of W. Schottky of the metal to semiconductor contact is applied with the interpretation that the surface layers of selenium are either n-type or weakly p-type as a result of the diffusion of donor elements from the counterelectrode. The selenium cell then is understood as an effective n-p junction rectifier having the metal electrode applied by spraying and the n layer produced by thermal and electrical diffusion of donor elements from this electrode into the surface of the selenium.

An additional complexity exists in the case of the selenium rectifier beyond that in the germanium and silicon single crystal devices since the selenium is in a microcrystalline form (report _____ discusses the dependence of properties on the microstructure). However, the primary variables determining the properties of the device are the donor and acceptor densities.

The intricacies of the thermal crystallization and electrical forming processes and of initial and ageing properties are understood in terms of the balance of acceptor and donor atoms occasioned by initial doping of materials, the precipitation of acceptors (discussed in report _____), and the diffusion of donors. A factorial experiment was conducted with two parameters (donor density, acceptor density) at four levels each. About one hundred replications were made in each run.

The room temperature properties (forward drop, reverse leakage) of the rectifiers were determined before and during the electrical forming process in order to determine forming rates.

Histograms were prepared showing the ranges of properties of the replications as functions of the two parameters.

All cells were shelf aged at room temperature, for a few months, at 100°C for one month and then aged under full load current (with two-thirds rated voltage) for one month at 100°C ambient temperature.

The units were then aged with full load currents and voltages for one month at 120°C ambient temperature.

The importance of the donor acceptor balance in determining ageing rates was demonstrated.

With careful adjustment of donor and acceptor densities cells can be produced which are easily processed, have low forward drops and reverse leakages, and which will operate (with natural convection) for extended periods of time without derating in an ambient temperature of 120°C.

References

1. H. W. Henkels; J. Appl. Phys. 22, pp. 916-925 (1951).
2. H. W. Henkels; J. Appl. Phys. 22, pp. 1265, 1278 (1951).
3. H. W. Henkels and J. Maczuk; J. Appl. Phys. 25, pp. 1, 11 (1954).

CORRELATION OF ELECTRICAL PROPERTIES OF SELENIUM RECTIFIERS WITH FUNDAMENTAL BULK PROPERTIES

H. W. Henkels

Westinghouse Electric Corp.
Pittsburgh, Penna.

The practical selenium rectifier cell consists in general of the following components:

1. metallic base electrode;
2. semiconducting selenium layer, or layers;
3. artificial barrier;
4. metallic counterelectrode.

In the usual practice the rectifier cell is assembled from the base to the counterelectrode. The base electrode consists of an aluminum or iron plate from about .010" - .040" thick. The base is sandblasted or etched to provide a good mechanical surface for the selenium. The roughened surface is coated with a film of certain metals (most common of which are nickel and bismuth) by vacuum evaporation or electrodeposition to provide a good ohmic contact to the selenium. Next, the base plate is coated with a layer (or layers) of selenium containing halogens (and, in cases, metals) by evaporation or pressing. Next, a barrier layer is usually applied (it may be omitted) consisting of an inorganic or organic insulating film. A counterelectrode of low melting alloy is finally applied by evaporation or spraying.

The electrical properties of the selenium semiconductor have been studied in some detail and a working model of the electronic structure has been developed.[1, 2, 3] A brief review of these properties is essential to a discussion of the properties of rectifiers. The liquid selenium semiconductor has a forbidden band gap of about 2.3 eV. Below 220°C, the liquid can crystallize into the hexagonal crystalline form. However, the crystallization is complicated by five factors:

(1) the nucleation rate is extremely small at room temperature, increases with temperature to about 110°C, then decreases above that temperature;

(2) the crystallization rate increases with temperature to about 217 or 218°C, then decreases somewhat to 220°C;

(3) the crystallization product has a colony structure with needles of selenium extending spherically from nucleation centers;

(4) the colony structure recrystallizes to an equiaxed structure at temperatures above about 80 or 90°C at a rate increasing with temperature to about 218°C;

(5) the rates of nucleation, crystallization and recrystallization depend on traces of impurities including oxygen in the selenium and on the quenching rate to the undercooled liquid.

The individual crystallites have forbidden band gaps of about 1.6 eV and densities of acceptors with low activation energies (probably oxygen or chlorine) of the order of $10^{14}/cm^3$. On crystallizing to the colony structure, the non-metal impurities in the selenium are rather uniformly distributed having been frozen in during crystallization. A large number of levels are present about .27 eV from the full band (presumably lattice defects at grain boundaries). The resistivity of the selenium in this form is independent of concentrations of non-metals. Internal electrostatic barriers between crystallites produce a high resistivity bulk material (which resistivity is thus dependent on frequency).

On recrystallization, the colony structure changes to the equiaxed. During the transition, the excess halogen is assumed to be pushed into grain boundaries. The number of acceptors in the surfaces of the crystallites is determined by a dynamic equilibrium between the diffusion of halogen defects from the crystallite to the grain surface and from the boundary into the crystallite.

The resistance of the internal barriers is decreased by the presence of excess acceptors at the barriers to very small values (with .01 atomic percent chlorine in the selenium the barrier resistance is almost zero). The general effects of donors and acceptors is discussed in report _____.*

On continued heating of selenium at high temperatures the grain size grows and the halogen forms molecules at the grain boundaries which may diffuse to the surface and evaporate. The dynamic equilibrium is upset and the density of acceptors in the surfaces of the crystallites is gradually reduced. Consequently, the resistivity and temperature coefficient of resistivity gradually increases with time.

An experiment was undertaken to correlate the properties of finished commercial rectifiers with the complex properties of the bulk material noted previously. Duplicate samples of 5" x 5" rectifier plates were prepared by two greatly different commercial processes (one employing bromine as acceptor, the other chlorine). Thirty-six different heat treatments were given these duplicate samples. Thus, samples were taken during stages of both the crystallization and recrystallization as well as after recrystallization when grain growth and precipitations of halogen were occurring. Electrical forming periods were varied to produce good cells (in general, periods of forming required depend, as to be expected, on the amount of aggregated acceptors in grain surfaces as described above, i.e., the minimum resistivity material produces rectifiers which are most difficult to form). Static characteristics in both forward and reverse directions were determined at temperatures -55°, 0°, 25°, 50°, 100°, and 150° C.

*To be submitted - donor acceptor balance

REVERSE CHARACTERISTICS

The reverse characteristics of selenium rectifiers depend on the surface properties of the bulk material. Consequently, these characteristics are of interest only insofar as there exists a correlation of bulk and surface properties of the semiconductor. On recrystallization of the bulk selenium, the leakage of rectifiers increases to a maximum at the state corresponding to the minimum bulk resistance. The forming periods required for production of rectifiers and reverse leakages of rectifiers behave qualitatively as expected on the basis of the model of selenium. Further discussion of reverse characteristics, involving treatment of donors, acceptors, and barrier layers in detail is inappropriate in the present report.

FORWARD CHARACTERISTICS

The forward characteristics are more dependent on the bulk properties of the semiconductor. The series resistance in the rectifier consists of contributions from the barrier layer, the bulk semiconductor and the base contact. The series resistance was obtained from the static characteristic by matching the high current portion with the theoretical curve. The following behavior of the series resistance was noted.

(1) It decreased sharply (measured at room temperature) with period of second anneal to a minimum, then increased slowly.

(2) The period of second anneal to the minimum was almost independent of preanneal period.

(3) Its magnitude at the minimum corresponded to that of the bulk selenium.

(4) The relative magnitude of the resistance of the series resistance of rectifiers with material in the colony and equiaxed structures corresponded to the relative magnitudes of the resistances of bulk samples.

(5) The temperature dependences of series resistances throughout the temperature range to 150^{0}C reflected the behavior of bulk semiconductor specimens in the same microcrystalline state.

Since the same correlation of forward characteristics with bulk semiconductor properties was obtained with rectifiers made by two very different processes and, since the properties of the bulk semiconductor are rather uniquely complex, it is felt that the forward properties of selenium rectifiers in their complicated dependence on anneal procedures are understood.

References

1. H. W. Henkels; J. Appl. Phys. 22, pp. 916,925 (1951).
2. H. W. Henkels; J. Appl. Phys. 22, pp. 1265,1278 (1951).
3. H. W. Henkels and J. Maczuk; J. Appl. Phys. 25, pp. 1,11 (1954).

Abstract Number 82

A REVIEW OF THE STATE OF SEMICONDUCTOR SURFACES*

Robert H. Kingston**

Lincoln Laboratory, Massachusetts Institute of Technology
Lexington, Massachusetts

Over the past several years, the bulk properties of semiconductors have been studied in such detail that it is safe to say, at least in the case of germanium, that those transistor and diode properties dependent upon the internal physics and chemistry of the semiconductor are well understood. Such is not the case, however, with the surface properties. Despite its early investigation, the metal-semiconductor contact is still not completely understood, and in addition, such properties as recombination velocity, surface leakage, and noise are only now being explained.

Perhaps the best way to describe a semiconductor surface is to first consider the "ideal" case. The bulk material would have the generally accepted energy-band structure, a valence band, a forbidden gap and a conduction band. In addition one would expect a distribution of donor and acceptor states in the forbidden band, homogeneously distributed throughout the sample. Ideally one would expect the bands to approach and meet the surface with no change in potential energy just as if the semiconductor had been sliced in two and all energies maintained at the same value. What this argument neglects is the creation of new energy states at the exposed surface which apparently overwhelm the contribution of the internal or bulk states. The occurrence of such states was first considered in detail by Bardeen[1] who explained some of the anomalies of point contact rectification in terms of the surface charge present at the interface as a result of the available states. Further work by Brattain and Bardeen[2] presented theory and experiment to explain quantitatively the effect of these surface states both on the surface charge and the recombination velocity. The general picture of the surface in this work was one in which allowed states at the surface acted as intermediate steps for the recombination process and also, in conjunction with adsorbed ionic charge, established the contact potential and shift of the electrostatic potential from its bulk value. More recent work has established a much more detailed idea of the state structure; in particular, at least two if not three distinct types of states seem to be necessary to describe the surface. These are (1) "interface states",

*The research in this document was supported jointly by the Army, Navy, and Air Force under contract with the Massachusetts Institute of Technology.

**Staff Member

occurring at the junction of the germanium with the oxide layer, (2) "adsorption states", associated with foreign species adsorbed on the outside of the oxide, and (3) "oxide states", which could arise from lattice distortion and impurities in the oxide layer. The interface states are similar to those postulated by Brattain and Bardeen[2] and are assumed to be principally involved in the recombination process. Their occurrence seems to depend mainly on the mechanical treatment and oxidation and not on the adsorbed material[3]. The adsorption and oxide states have only recently been considered in the light of surface conductance measurements[4] and the associated transient phenomena.[5,6] In these experiments it is found that the electrostatic potential at the surface and consequently the majority carrier type and density are determined by the amount of oxidation and the adsorbed material. The range of variation of the electrostatic potential is much greater than that predicted by Brattain and Bardeen and it is also found that the states must have capture times of the order of seconds. It is this time dependence which distinguishes these states from the interface states which must have capture times many orders of magnitude smaller to explain recombination velocity. The contribution of the charge in the interface states is now being investigated in the light of these later results.[7,8]

To understand the existence of these states, it is also necessary to consider the chemistry of the surface. The formation and structure of the oxide layer[9,10,11] as well as adsorption data [12,13] should give a clearer picture of the observed behavior. Work on semiconductor-electrolyte contacts[14,15] also shows the importance of adsorbed material, in this case ions in solution. One of the more recent developments, the technique of preparing a clean germanium surface,[16] should yield significant results when used in conjunction with the several types of surface property measurements.

Considering the surface problems of immediate practical interest, surface leakage current has been explained by the occurrence of inversion layers or "channels" due to the adsorbed species[17-21] and also by electrolytic conduction in the presence of water vapor[12]. Recombination velocity is quite well understood experimentally; however, the detailed distribution of the states involved is not known at this time. Excess noise seems to be largely a surface effect[21-23] and its mechanism is postulated to be the electron transfer process to the adsorbed or oxide states.[24] A complicating feature of all the above effects is the possibility of migration of the adsorbed species in high fields at the surface, and such effects are not well understood at this time.

It should be emphasized that the present progress in the study of surfaces is largely due to the great body of knowledge about the bulk properties of semiconductors. Consequently, the above work is largely pertinent to germanium; however, it is hoped that the results may be successfully applied to silicon and the many other known semiconductors.

References

1. J. Bardeen, Phys. Rev., 71, 717, (1947).
2. W. H. Brattain and J. Bardeen, B.S.T.J., 32, 1, (1953).
3. D. T. Stevenson, to be published, Physica
4. S. R. Morrison, J. Phys. Chem., 57, 860, (1953).
5. R. H. Kingston, Phys. Rev., 94, 1416, (1954).
6. R. H. Kingston and A. L. McWhorter, Bull. Am. Phys. Soc., January 27-29, (1955), New York
7. C. G. B. Garrett and W. H. Brattain, to be published
8. J. B. Schrieffer, W. L. Brown, private communications
9. E. N. Clarke, Bull. Am. Phys. Soc., January 27-29, (1955), New York
10. T. H. George, H. E. Farnsworth, and R. E. Schlier, ibid
11. M. Green and J. A. Kafalas, this meeting.
12. J. T. Law, Proc. I.R.E., 42, 1367, (1954).
13. J. T. Law, to be published (J. Phys. Chem.)
14. W. H. Brattain and C. G. B. Garrett, Phys. Rev., 94. 750, (1954).
15. C. G. B. Garrett and W. H. Brattain, Phys. Rev., 95, 1091, (1954).
16. H. E. Farnsworth, R. E. Schlier, and R. M. Burger, Bull. Am. Phys. Soc., Nov. 26-27, (1954), Chicago
17. W. L. Brown, Phys. Rev., 91. 518, (1953).
18. H. Christensen, Proc. I.R.E., 42. 1361, (1954).
19. A. L. McWhorter and R. H. Kingston, Proc. I.R.E., 42, 1376, (1954).
20. R. H. Kingston, to be published (Phys. Rev.)
21. R. N. Noyce, this meeting
22. H. C. Montgomery, B.S.T.J., 31, 950, (1952).
23. T. G. Maple, L. Bess, and H. A. Gebbie, to be published (J.A.P.)
24. A. L. McWhorter, Bull. Am. Phys. Soc., Jan. 27-29, (1955), New York

Abstract Number 83

ULTRA-HIGH VACUUM STUDIES ON GERMANIUM SURFACES

F. G. Allen

Harvard University

Three types of studies are being carried out on single crystal germanium surfaces at vacua on the order of 10^{-9} to 10^{-10} mm Hg: a) Field-emission in a Müller-type tube; b) Relative contact potentials of the various faces of a single crystal; and c) the effect of illumination on contact potential. Results from b) indicate that sputtering the Ge surface with +500-volt argon ions followed by a mild anneal to 300 to $500^{o}C$[1] is more effective than mere heating in producing an atomically clean surface, and this treatment is used for all the studies mentioned.

In the field-emission study, a), small needles of single-crystal Ge are pre-formed by mechanical abrasion, and then sharpened by an a-c electrolytic C.P.4 etch to a tip radius of 10^{-4} to 10^{-5} cm. With this tip as the cold cathode at the center of a 10-cm spherical phosphor-coated anode, field-emission can be observed on the screen at a few thousand volts on the anode. Nearly all the data taken can be represented by the relation $J = Ae^{-b/V}$, where J is the emission current density and V the anode voltage. Hence it is assumed that a field-emission process, analogous to that studied extensively for metals, is taking place. While emitter tips are easily damaged through excessive currents, total currents of 0.04 micro-amps at densities of several hundred amps/cm^2 have been drawn with no change in tip characteristics. Emission becomes appreciable at computed external field strengths considerably below the value 2×10^{7} volts/cm required in the case of a metal. A calculation of the charge distribution at the germanium surface, assuming no surface states, indicates that at field strengths of this magnitude the energy levels may be lowered at the surface till the bottom of the conduction band is at or below the Fermi-level, even for highly doped p-type material. A surface energy state density of 10^{14} to 10^{15} cm^{-2} would be needed to supply the required surface charge with no significant lowering of levels. Two obstacles in obtaining the symmetrical field-emission patterns easily obtained with metals such as tungsten, are i), the difficulty in producing a germanium tip which is both clean and smooth on an atomic scale, and ii) the fact that the work function for Ge, as measured in b), seems to vary much less rapidly with crystal direction than is the case for metals.

In the contact potential study, b), a two-cm single crystal germanium ingot is cut along the (110) axis so that its six sides comprise a pair each of (100), (110) and (111) faces. The crystal can be turned about its

axis manually from outside the pyrex vacuum envelope, presenting, in turn, each face to the vibrating reference electrode,—in this case a single nickel crystal (110) face,—and the contact potential difference measured on each face. A repetition of the contact potential measured for the first face after completing the measurements on the other five faces checks against any relative drift of reference electrode vs. germanium during the course of the run, (about 30 minutes), and a matching of values for like faces of the germanium is an indication of germanium surface regularity. The first germanium sample tested was near intrinsic, and after baking and outgassing at lower temperatures, a few minutes heating at 750°C brought about a "pattern" of face values, with like faces matching, which could be reproduced again and again by cleaning at this or higher temperatures. Only two pairs of faces were available, and these had angular errors in cutting of up to 7°. The results gave the work function of the ~(110) faces as approximately 0.04 volts higher than that of the ~(111) faces. The next germanium sample was heavily doped n-type, (arsenic). Many heatings at 850°C and above caused approximate matching of like faces in some cases, but values were not reproducible. When the argon ion bombardment, followed by annealing,[1] was then tried, good matching of like faces immediately resulted, and the pattern of face values resulting could then be reproduced repeatedly on further cleaning treatments. The values obtained gave the work function of the (100) faces as 0.051 ± 0.005 volts higher than that of the (110) faces and 0.065 ± 0.005 volts higher than that of the (111) faces.

Contamination of the faces could be studied by following their contact potential pattern over many hours of standing at a pressure of $\sim 2 \times 10^{-8}$ mm Hg of residual gases. After such standing the pattern could then be returned to the "clean" condition by a mere heating to above 750°C, and further bombardment was unnecessary except in the case of more drastic contamination. Presumably the mild contamination consisted in a low energy adsorption process of gases such as argon, nitrogen and helium, while the original and later induced "drastic" contaminations were chemisorbed layers of oxygen or oxides.

In study c) on the effect of illumination on the contact potential of a clean germanium surface, light from a W filament is focused through the pyrex walls of the experimental tube into the gap between reference electrode and germanium face. The measured contact potential of the highly doped n-type Ge specimen always shifted, upon illumination, so as to decrease its work function. The magnitude of the shift showed a logarithmic saturation with incident light intensity, and a very strong negative temperature dependence. Thus, for a light intensity causing about half saturation in $(\Delta C.P.)_l$ at 25°C, the value of $(\Delta C.P.)_l$ decreased from 35 millivolts at 25°C to less than 2 millivolts at 65°C. It appears that thermal pair generation, competing with the photogeneration as the temperature is raised, can explain this temperature dependence. If the incident light on the germanium face is now chopped, the electronic null measuring system can be used without alteration to measure the ac signal resulting from the alternating $(\Delta C.P.)_l$ voltage

generated in the germanium. Tests of the frequency response of $(\Delta C. P.)_{\ell}$ for the n-type specimen showed that it was flat from 0 c.p.s to above 17,000 c. p. s. at room temperature. As the temperature is lowered, $(\Delta C. P.)_{\ell}$ falls off at progressively lower frequencies, till at $-50^{o}C$ the signal has dropped by 10 per cent at only 3000 c. p. s. Presumably, this drop-off in the a-c value of $(\Delta C. P.)_{\ell}$ sets in when the time between light pulses approaches the effective recombination time of pairs created by light inside the surface.

Reference

1. Farnsworth, Schlier, and Burger, Bull. Am. Phys. Soc. 29, No. 7, 35(1954)

Abstract Number 84

THEORY OF SURFACE-BARRIER ELECTRODES

W. E. Bradley

Philco Corporation
Philadelphia, Pennsylvania

SURFACE-BARRIER ELECTRODES

The surface-barrier transistor was first described in the Proceedings of the I. R. E. December 1953. This type of transistor employs a semiconducting body which serves as a base electrode with electrodes attached to the surface in such a manner as not to disturb the structure of the semiconducting crystal. The electrodes may consist of electroplated metal deposited upon a freshly etched and chemically prepared surface of the semiconductor. The entire process of shaping the semiconducting body and depositing the metal electrodes can be carried out at room temperature by electrochemical techniques.

Experiments showed that electrodes applied in this way could be excellent rectifiers on N type germanium and also very satisfactory emitter or collector electrodes for transistors. On the other hand, it was found to be possible to adjust the process so as to form a nearly ohmic contact on N type germanium.

The chemical complexity of the interface between the crystal and the electrodes makes a complete theory of surface-barrier electrodes very difficult. On the other hand, experimental results obtained to date suggest strongly that a kind of chemical potential of the electrode determines whether upon contact it injects or extracts electrons from a semiconductor. Even an approximate theory of this sort is useful to guide process development and to interpret results.

ELECTROCHEMICAL POTENTIAL, CHEMICAL POTENTIAL AND ELECTRIC POTENTIAL

The amount of energy required to remove an electron at the fermi level of energy in a solid material to an external reference state is defined as the electrochemical potential of the material. This energy can be resolved into two parts corresponding to the chemical potential and the electric potential of the electron. The chemical potential corresponds to the energy required to remove the electron from the fermi level and place it in a state in the same locality in which it is distributed with equal probability over a very small volume of the material, which is still large enough to contain a substantial number of individual atoms. The electric potential corresponds to the additional amount of energy required to transport the electron from this distributed reference state to the external reference state used in the definition of electrochemical potential.

APPROXIMATE SOLUTION OF THE EQUILIBRIUM CONDITION OF CONTACT

Suppose that for a system of materials to be placed in contact the following initial information is given.

1. The system of electron energy levels is known for each material.
2. The energy of the fermi level when the material is electrically neutral is known.
3. The energy of the chemical energy reference state corresponding to a uniformly distributed stationary electron is known.

Then it is possible to derive the manner in which the electric potential and other properties of the system of substances vary with position at equilibrium when in contact. It is also possible to determine whether or not the contact will be capable of rectification and whether it will be capable of injection of minority carriers into a semiconducting crystal.

Unfortunately the three conditions cited above are difficult to satisfy, since the structure of electron levels is only known approximately for most materials; the location of the fermi level of such a structure of energy levels is only approximately known; and the energy of the chemical potential reference state is only approximately known at best for any material at the present time. For germanium and silicon the energy level structure and the location of the fermi level are, however, relatively familiar and it is with these semiconductors that the discussion is principally concerned.

The difference in electron chemical potential between material when placed in contact causes the displacement of electrons from one material to the other until a counter electric field develops to prevent further flow. As a result the regions near the area of contact tend to become charged. The electric potential obeys the Poisson equation. The displacement of the fermi level in each locality with reference to the electron energy level structure depends upon the amount of charge and the density of energy states near the fermi level at that locality. At equilibrium the electrochemical energy of the fermi level must be constant throughout the system. From these three conditions it is possible to derive the following differential equation which specifies the chemical potential of the fermi level as a function of position throughout the system.

$$\nabla^2 E_f = \frac{q}{e_o} F_n(E_f - e_{fn})$$

In one dimension this reduces to

$$\frac{d^2 E_f}{dx^2} = \frac{q}{e_o} F_n(E_f - E_{fn})$$

where:

E_f is the electron chemical potential in volts of the fermi level at each location.

E_{fn} is the electron chemical potential in volts of the n_{th} material comprising the contact when electrically neutral.

q is the charge on the electron in coulombs.

e_o is the dielectric constant of the material in farads per meter.

$F_{n(E_f - E_{fn})}$ is the effective number of electron states in the energy interval between E_f and E_{fn} for the n_{th} material comprising the contact.

The solution of the differential equation is most conveniently displayed upon a chemical potential diagram in which chemical potential is the ordinate and distance the abscissa. On such a diagram electron energy bands are horizontal for any material while the fermi level is indicated as a curve. The origin of the diagram is taken as the chemical potential reference corresponding to the energy of a uniformly distributed stationary electron and the ordinate may be considered to indicate the binding energy of each electron state. In words the differential equation states that in a one-dimensional system of substances in contact the curvature of the fermi level on a chemical potential diagram equals the effective number of electron states lying between its actual chemical potential and the chemical potential corresponding to charge neutrality multiplied by a constant. The curvature in each locality is such as to be convex toward the neutral chemical potential.

Since the electrochemical potential is constant then the electric potential variations are the negative of those of the chemical potential.

PROPERTIES OF CONTACTS DEDUCIBLE FROM THE SOLUTION

For any region of a material it is possible by inspection of such a diagram to infer many of the electronic properties of the material.

1. If the fermi level passes through a region having a high density of electronic states, then that region is a good conductor of electricity.
2. If the fermi level lies in a forbidden band containing no electron states within approximately 1/4 electron volt of the fermi level, then the material has high electrical resistance in that region.
3. If the fermi level lies near one edge of a forbidden band the material is an N type semiconductor when the fermi level is near the upper edge and a P type semiconductor when near the lower.

It follows that if a material having a large chemical potential in such a sense as to attract electrons is placed in contact with a semiconductor such as germanium the fermi level near the surface will be drawn down toward the filled band of the germanium producing a cloud of holes. Similarly, a material of low chemical potential will tend to produce a cloud of free electrons in the conduction band.

The bonding layer of the contact between the electrode and the semiconductor contains many electron levels not characteristic of either material. These interface states may strongly influence the behavior of the contact even when such a layer is only a few atoms thick. The

chemical potential diagram shows that if such a layer is rich in electron energy states and has a high chemical potential as might be the case for a disorderly P type oxide, then the fermi level of the germanium should be depressed producing a cloud of holes.

If the interface layer is extremely thin so that electrons may tunnel from the metal to the semiconductor, then the chemical potential of the metal becomes the controlling factor. The behavior of such contacts in fact may provide valuable information about the chemical potential of materials placed in contact with them.

EFFECTS OF SURFACE TREATMENTS IN LOW PRESSURE GAS ATMOSPHERES UPON CHARACTERISTICS OF EVAPORATED SURFACE-BARRIER RECTIFIERS

Patricia A. Hartig

Research Division, Philco Corporation
Philadelphia, Pa.

A study of the effect of low energy gas discharges on the surface of freshly etched germanium was undertaken in order to further understand the mechanism leading to large area metal-germanium rectifying contacts.[1,2,3] The effective barrier height at the surface of the germanium directly under the metal can be widely varied by the method to be described.

A nickel tab was soldered to one end of the sample (5 x 2.5 x 0.5 mm) to provide both an ohmic contact and a convenient means of mounting. For most of the work, 5 ohm-cm n-type germanium was used. Each sample was etched in a 7:4 (HNO_3:HF) etch just before being placed in the vacuum system which is schematically shown in Figure 1(a). After an initial evacuation to $\sim 10^{-5}$ mm of Hg., the desired gas was admitted to the pressure of a few millimeters. A glow discharge was set up between the germanium and the collimating shield of the evaporator (see Figure 1(b) using a Tesla coil as the voltage source. When more than one gas was used, the system was re-evacuated and the second gas admitted. After the final gas was pumped out, platinum dots were evaporated onto the bombarded surface from a tungsten wire. Evaporation was done at a pressure of $\sim 5 \times 10^{-5}$ mm of Hg. Platinum was chosen for the metal contact because it consistently produced excellent diodes when no discharge was used. Two dots were evaporated simultaneously onto each sample and many runs of each experiment were made to verify the accuracy of the results.

The characteristics of the diodes were judged by the shape of the current-voltage curves with particular attention paid to the quality and magnitude of the reverse saturation current. It is predicted by metal-semiconductor diode theory[4] that the electron saturation current is

$$J_{ns} = 120\ T^2\ e^{-q\Phi_o/k\ T}$$

where T is the absolute temperature and Φ_o is the height of the barrier at the surface measured from the Fermi level. Since the hole saturation current may be calculated from the bulk properties of the material by[5]

$$J_{ps} = q\ D_p\ \frac{p_n}{L_p}$$

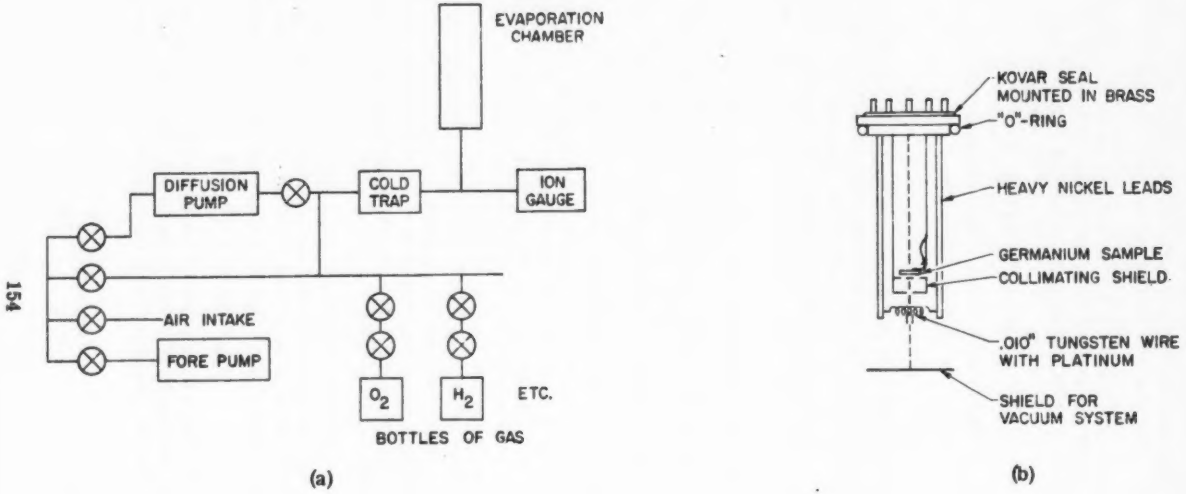

Fig. 1—(a) Schematic diagram of vacuum system. (b) Evaporator.

the electron part of the current is readily determined from the measured total saturation current.

$$J_{sat} = J_{ps} + J_{ns}$$

In most cases the hole current is small so that J_{sat} is itself a direct measure of the effective barrier height. At first, area measurements were made by checking the diode capacitance.[6] Optical methods gave equivalent results so were later adopted.

In each part of the experiment, a comparison was made with the normal platinum diodes. These gave, after a brief clean-up etch, excellent back saturation by -0.1 volt with saturation currents in the range of 3 - 10 μa for a diode diameter of 0.7 mm. This corresponds to a current density of about 1 - 2 x 10^{-3} amps/cm^2 and a Φ_0 of 0.59 ev. Diode breakdown started at anywhere from 50 volts up and was very sharp. This maximum back voltage tended to decrease slightly with time. Before etch the current level was higher by a factor of 10 or so with almost no saturation. Curves a and b of Figure 2 show the typical I - V characteristics of a normal diode before and after etch with forward and reverse currents plotted in the same quadrant.

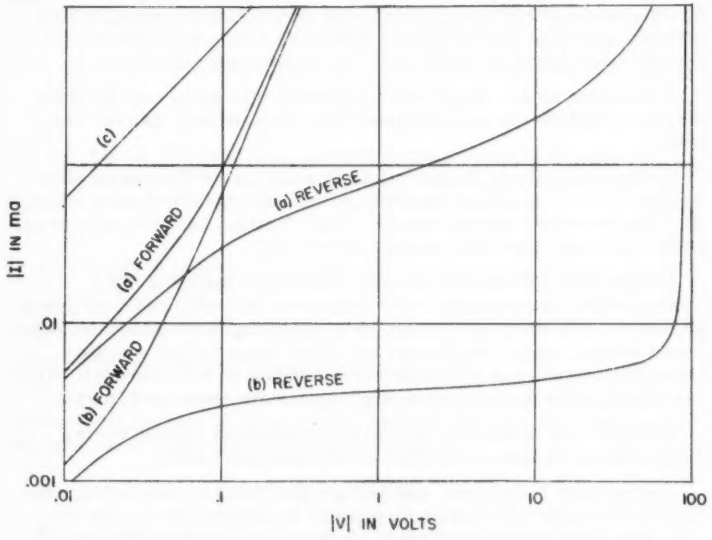

Fig. 2—(a) Forward and reverse characteristics of platinum diode before etching. (b) Forward and reverse characteristics of platinum diode after etching. (c) Ohmic I-V curve.

The results of gas discharges on the germanium surface before depositing platinum are as follows:

1. Hydrogen alone. A discharge for as long as one-half hour resulted in slightly poorer rectifiers than normal. The general shape of the curves was essentially the same as for the normal case, however, and the slightly higher saturation currents were almost within experimental deviation.

2. Oxygen alone. Discharge completely destroyed rectification in less than three minutes. The result was an ohmic contact of the order of 100-200 ohms as shown in curve c of Figure 2. Repeated clean-up etching did not change the result, indicating that the surface directly under the platinum had been altered.

3. Oxygen followed by hydrogen. This shows a result similar to oxygen alone (almost ohmic) before etch. After etch, however, the samples rectified very well—almost comparable with the standard diode. Hence, although the diode was effectively "shorted out" before etching, a condition leading to rectification had been restored under the metal.

4. Hydrogen followed by oxygen. Hydrogen delays the destruction of rectification by the oxygen. Experimentally it was found that more than 15-30 seconds of hydrogen prevents the destruction by oxygen in five minutes, giving an almost normal diode both before and after etch. Oxygen alone destroys rectification in considerably less time.

5. Nitrogen alone. Same result occurred here as for oxygen alone only the rectification was completely destroyed in less than two seconds.

6. Nitrogen followed by hydrogen. A minimum of 20 minutes of hydrogen restores rectification after three minutes of nitrogen in a manner similar to the oxygen-hydrogen case. That is, samples were ohmic before etch and essentially normal afterwards.

7. Hydrogen followed by nitrogen. Nitrogen apparently has a stronger effect than oxygen in the destruction of rectification as it took 30 minutes of hydrogen to prevent destruction by 30 seconds of nitrogen. (See 4 above). As in the oxygen case, those samples that rectified showed almost normal characteristics both before and after etch. Various stages in the destruction of rectification are shown in Figure 3.

8. Argon. Up to one hour of discharge produced slightly poorer diodes than normal as in the case of hydrogen used alone.

The fact that both oxygen and nitrogen discharges each destroy rectification indicates that they both produce an n-type layer on the surface, thus lowering, or completely removing the barrier. This was further substantiated by the fact that slight p-type surface-barrier rectification was induced on p-type material after exposure to these gases, whereas large area metal contacts on this type of germanium are usually ohmic. Hydrogen, although it may raise the already high barrier when used by itself, does

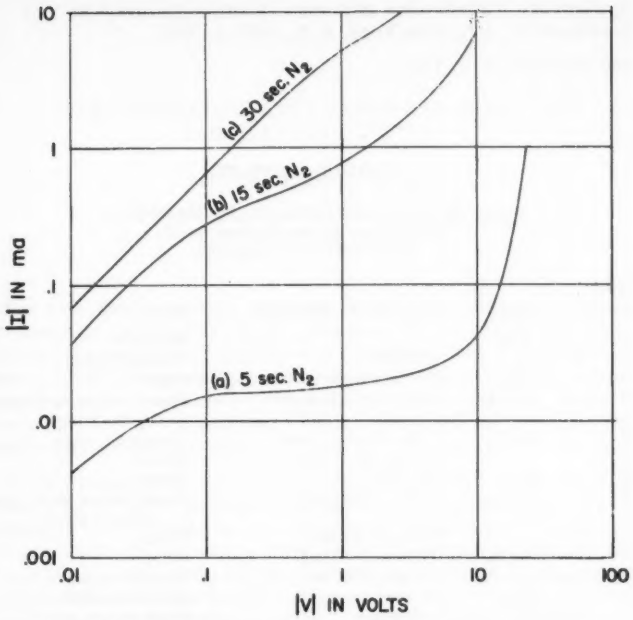

Fig. 3—Reverse characteristics after clean-up etch showing progressive stages in the destruction of rectification by nitrogen following a 30 minute hydrogen discharge.

1) retard the lowering of the barrier by oxygen and nitrogen when used first, and

2) restore its high value when used afterwards.

Thus hydrogen tends to make the surface p-type.

These experiments can be explained by the assumption that the gases enter the lattice during bombardment—nitrogen and oxygen acting as donors, hydrogen acting as an acceptor.

References

1. W.E. Bradley, et al, Proc. IRE, 41, 1702-1720 (1953).

2. J.B. Gunn, Proc. Phys. Soc., 67B, 409 (1954).

3. C.V. Bocciarelli, Physica XX, to be published.

4. H.C. Torrey and C.A. Whitmer, "Crystal Rectifiers," McGraw-Hill Book Co., Inc., New York, N.Y., 1948, p. 77ff.

5. W. Shockley, "Electrons and Holes in Semiconductors," D. Van Nostrand Co., Inc., New York, N.Y., 1950, p. 315.

6. See reference 1, p. 1717.

TABLE OF RESULTS

Quality of Surface-Barrier Rectification on 5 ohm-cm n-type germanium after low energy gas discharges

Type Material	Gas	Duration of Discharge	Result
N	None		Normal*
N	H_2	< 1/2 hour	Almost normal*
N	O_2	<3 minutes**	Ohmic
N	O_2, H_2	3-15 min., 30 min.**	Ohmic before etch, almost normal after.
N	H_2, O_2	>15-30 sec., 5 min.	Almost normal*
		<15-30 sec., 5 min.	Ohmic
N	N_2	>2 sec.	Ohmic
N	N_2, H_2	3 min., >20 min.	Ohmic before etch, almost normal after.
		3 min., <20 min.	Ohmic
N	H_2, N_2	30 min., >30 sec.	Ohmic
		30 min., <30 sec.	Almost normal*
N	A	<1 hour	Almost normal*
P	O_2	40 min.**	Slight p-type rectification
P	N_2	20 min.**	Slight p-type rectification

* Normal ≡ characteristics similar to best platinum diodes both before and after etch.

** Critical times not established.

Abstract Number 87

THE EFFECT OF WATER VAPOR ON GERMANIUM AND SILICON JUNCTIONS

J.T. Law and P.S. Meigs

Bell Telephone Laboratories, Incorporated,
Murray Hill, N.J.

The variation in reverse dark current of germanium np junction units with humidity has been previously discussed[1,2] and it appears that at least two conduction mechanisms are operative. These are, firstly a channel conduction where the carriers are electrons and holes in an inversion region at the surface and secondly an ionic process where the charge carriers are actual ions which move across the surface in the multilayers of adsorbed water.

In the present work, the junction unit was placed in a vacuum system to which water vapor could be admitted at various pressures. This eliminated the necessity of using a carrier gas such as nitrogen. The unit was biased in the reverse direction and a chopped light spot moved across the surface normal to the bulk junction. The A.C. photoresponse could be measured as a function of distance. The presence of a plateau in the photoresponse-distance curve is evidence of the existence of a channel whose length is given by the length of the plateau.

In the early stages of the present work, it was noted that illumination of the surface with steady light caused a marked decrease in the length of the channel and in fact at high light intensities the channel disappeared altogether. This effect is shown in Figure 1. This gives us a means of separating channel and ionic conduction. If one measures reverse current as a function of steady light intensity at a series of humidities one of two things should happen:

(i) If we are only dealing with channel conduction, the current at high light intensities in the wet condition (when the channel no longer exists) should approach the corresponding current observed for the dry state.

(ii) If ionic conduction is the controlling mechanism the increase in current between the dry and wet states should be the same irrespective of the light intensity.

These measurements were carried out and the results are shown in Figure 2. The results shown were taken at 20 volts but similar curves were obtained between 5 and 60 volts. At low humidities the surface recombination rate changes and this accounts for the change in slope between curves 1 and 2. From 30% humidity to saturation, however, the lines are effectively parallel so that the majority of the excess current must be carried by a mechanism that is not affected by the amount of steady light; i.e., ionic conduction.

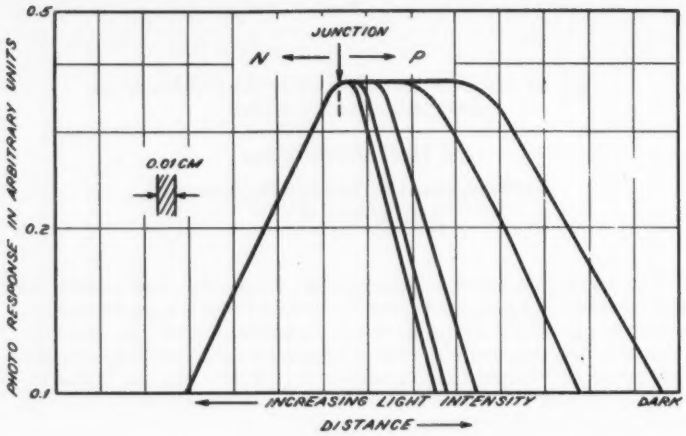

Fig. 1

Attempts were now made to suppress ionic conduction by cooling below the freezing point of the adsorbed water (where the ionic mobilities must be very low) and to measure channel conduction. We placed a p-n junction unit in a high humidity ambient and cooled to 180°K with the bias applied and then warmed slowly to room temperature, measuring the temperature of the bar (with a thermocouple) and the reverse current. The results are shown in Figure 3 where it can be seen that the current is practically zero until temperatures close to 273°K are reached. The current begins to increase rapidly at 263°K but due to the crudeness of the experimental setup this temperature could be in error by several degrees. An accurate measurement of this temperature would be extremely useful as a means of determining the melting point of adsorbed water, which is undoubtedly different from that of the bulk medium. This rapid increase of current near the melting point of ice confirms the previous observation that an ionic conduction mechanism is the important one in increasing reverse currents of n-p junction units in high humidity ambients. A similar curve is shown for the effect of ethyl alcohol. In this case the current increases at 165°K. The melting point of pure ethyl alcohol is 156°K but the material used could easily have been contaminated with water. No normal junction could be expected to show an appreciable current at these low temperatures so that the mechanism must be one involving ions.

In Figure 4, the reverse dark current of a silicon junction unit is plotted as a function of voltage at several humidities. The primary effect of water vapor is to increase the saturation current without markedly affecting the breakdown voltage—except at 100% relative humidity. These changes are what one would expect for the formation of a channel

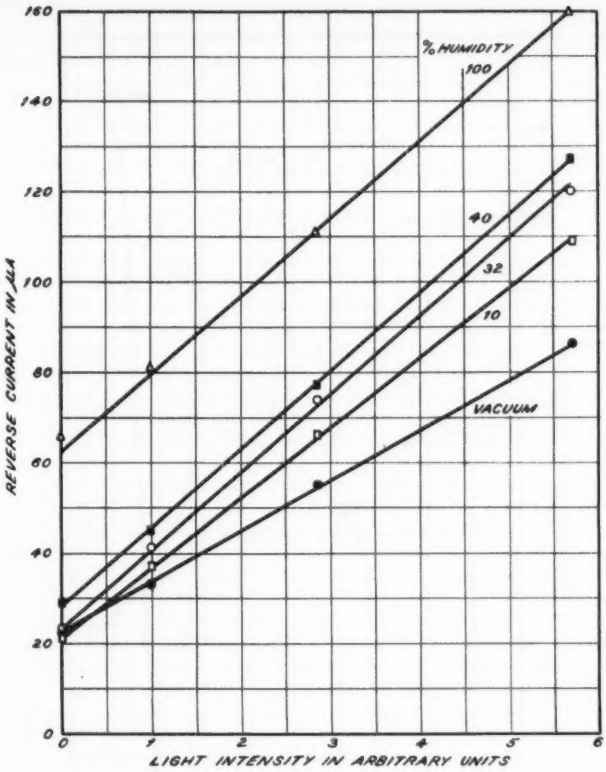

Fig. 2

or surface inversion region. The effective area of the junction was increasing so that the current increased but no marked change was made in the breakdown voltage. As the channel increased in size the current would be expected to saturate at steadily higher voltages and this is what was actually found. In vacuum, it saturated at less than 0.5 volt while at 80% relative humidity it did not saturate until a bias of 2 volts was applied. One might expect to observe the growth of the channel in the photoresponse curve, no change was apparent until the unit was in 100% water vapor. As we could detect a channel of 0.1 mm length, we must conclude that the one existing at humidities below saturation was shorter than this. This means that its saturation current was $>2 \times 10^{-6}$ amps/cm^2 compared with the bulk junction saturation current of 7×10^{-8} amps/cm^2. At saturation, the current was 1×10^{-7} amps/cm^2.

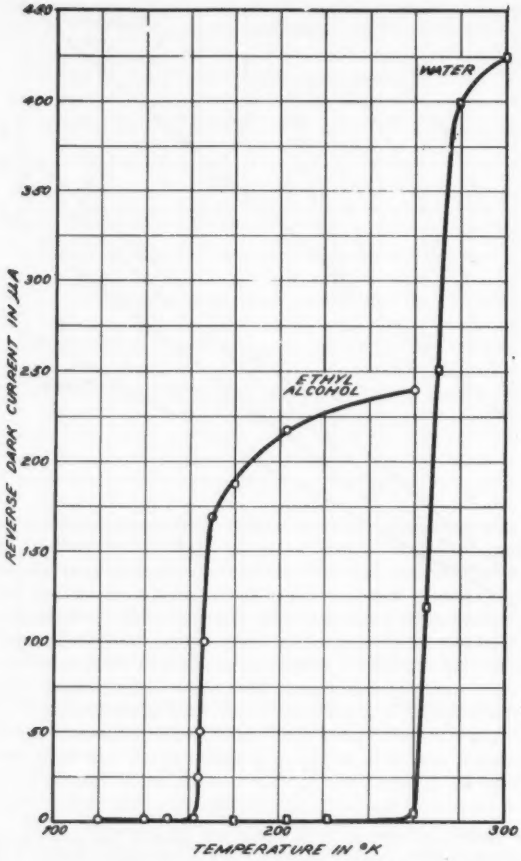

Fig. 3

This formation of channels without the complication of ionic conduction is just what one would expect in the presence of a stable oxide film. The difference between these results and those obtained on germanium is further evidence that in the latter case another conduction mechanism is present.

When a silicon junction on which a channel has been found is exposed to steady light, the channel decreases in approximately the same way as was found for germanium units. However, if the reverse current is

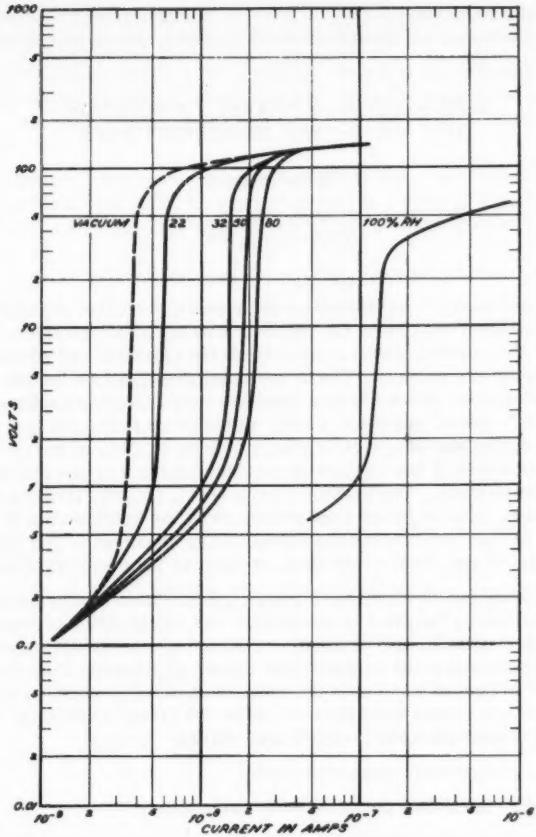

Fig. 4.

plotted as a function of light intensity for various humidities, we do not get a series of parallel straight lines as we did for germanium. As the channel increases in size the lines have a larger initial slope but depart from linearity. This is the same effect that was found for channels on the n-side of a germanium junction and is further proof that the excess current carrying mechanism is electronic in nature.

References

1. A.L. McWhorter and R.H. Kingston, Proc. I.R.E., 42, 1376 (1954).

2. J.T. Law, Proc. I.R.E., 42, 1367 (1954).

Abstract Number 88

OBSERVATION OF CHANNEL FORMATION ON N AND P-TYPE SEMICONDUCTORS

R.N. Noyce

Research Division, Philco Corporation
Philadelphia, Pa.

In recent years it has become widely recognized that the surface of a semiconductor may be of the opposite conductivity type from the interior of the crystal, which results from the chemical and physical properties of the surface. There are many possibilities for the origin of the differences of the surface from the bulk including surface states or "Tamm" levels, interface states, dislocations at the surface caused by creating the surface, high impurity density at the surface due either to the production of the surface or to contamination by the atmosphere around the surface. The surface Fermi level, i.e., the position of the Fermi level relative to the band structure of the semiconductor at the surface, is thus much more dependent on the condition of the surface than on the Fermi level of the bulk, at least in the purer samples.

In general, two methods have been used for the measurements of surface conditions. The first is to examine the rectification characteristics of a surface contact, and imply the existence or non-existence of an inversion layer under the contact from these rectification characteristics[1,2]. The second method is the measurement of properties dependent on the surface Fermi level directly while the "free" surface is exposed to differing ambient conditions. These include:

1) contact potential measurement[3]

2) change in contact potential with illumination[3]

3) "Channel Effect"[4,5,6,7]

4) Surface Conductance[8] or mobility.

This list will probably be expanded in the future. It is the measurement of these last two phenomena which will be discussed here.

The "Channel Effect" was first observed in transistors by Brown, and since, several workers have extended the concepts to diodes. In examining diodes for channel, a plot is made of the photo response of a p-n junction bar as a function of the distance from the junction. When there is no channel present, the response falls exponentially as $\exp^{-x/L_m}$ where L_m is the diffusion length of the minority carrier. If a channel is present, i.e., if an inversion layer exists at the surface, the response will extend further, since the photosensitive junction now extends along the surface. The measurement of channel length suffers lack of

resolution due to the magnitude of the diffusion length. If, however, the high frequency response of the diode is examined, the response now falls as exp $-x/L'_m$ where $L_m' = \sqrt{D_m/\omega}$, which is the effective diffusion length at the frequency ω ($\omega \gg 1/\tau m$). Thus the resolution of the measurement may be increased by a factor of ~20 in using light chopped at 3 mcps.

Apparatus for examining channels at high frequencies which gives a two-dimensional plot of the channel response is shown in Figure 1. The light source is a flying spot scanner which has been modified to give

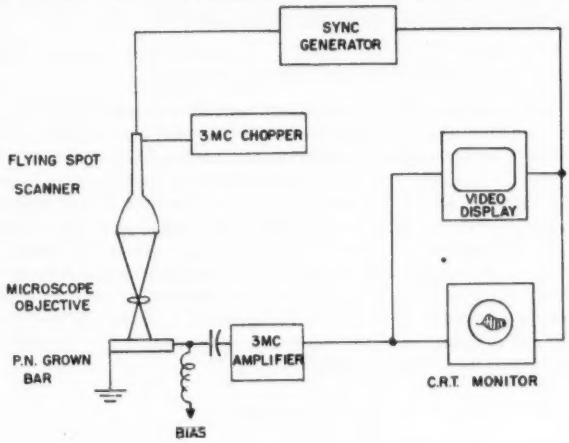

FLYING SPOT SCANNER "CHANNEL" DISPLAY

Fig. 1

light chopped at 3 mcps. This moving light source is focused by a microscope objective on the junction bar. The photovoltage resulting is amplified and displayed on a video display unit which is in synchronism with the scanner. Amplitude data is displayed on an oscilloscope.

This apparatus makes possible the observation of the transient changes in the channel as the ambient gas is changed, or as the voltage applied across the diode is changed. Time constants of the order of 1 second have been found for the channel to come to equilibrium after a step voltage is applied to the junction. This indicates that the states causing the channel are not the centers for surface recombination which must have shorter time constants. As the ambient gases are changed, the channel may be changed from the n to p side of the bar and back, with time constants of the order of a few seconds, which may be entirely due to the amount of time necessary for the change of ambient. The

effects of several gases have been observed. The halogens form a strong channel on the n side of the junction. Oxygen forms a slight channel on the n side, which is not increased appreciably by ozone. A strong channel on the p side was produced by ammonia as well as by water vapor. Channels have been observed within five minutes after etching in HF, which presumably removes most of the oxide from the surface, so channel phenomena are not necessarily dependent upon the existence of a thick oxide layer.

Channels have been observed on silicon grown junction bars, and although the channel lengths are much smaller, they are qualitatively the same in their behavior as channels on germanium.

Motion pictures have been taken of the growth and decay of channels with ambient gas and voltage and will be presented.

The actual surface Fermi level has been determined from the conductance of a thin bar as a function of the ambient atmosphere. Figure 2 shows the change in surface conductance as a function of surface Fermi energy after Schwarz[9]. It can be seen that if the sample may be moved through the minimum conductance, the actual surface Fermi energy may be determined by knowing the magnitude and type of the excess conductance of the bar. Figure 3 shows typical data on the conductance of a thin bar for the wet-dry oxygen cycle. A minimum is observed as the surface changes from n to p—type, and the total change in surface Fermi energy is about .3 volts. It is observed that the surface Fermi energy is not uniquely determined by the atmosphere, but is dependent on the past history of the sample.

References

1. J.B. Gunn, Proc. Phys. Soc., 67B, 409 (1954).
2. P.A. Hartig, this conference.
3. Bardeen and Brattain, Bell System Tech. Journal, 32, 1 (1953).
4. Brown, Phys. Rev., 91, 518 (1953).
5. R.H. Kingston, Phys. Rev., 94, 1416 (1954),
6. A.L. McWhorter and R.H. Kingston, Proc. Inst. Rad. Engrs., 42, 1376 (1954).
7. H. Christenson, Proc. Inst. Rad. Engrs., 42, 1371 (1954).
8. S.R. Morrison, Jour, Phys. Chem 57, 109 (1953).
9. R.F. Schwarz, private communication.

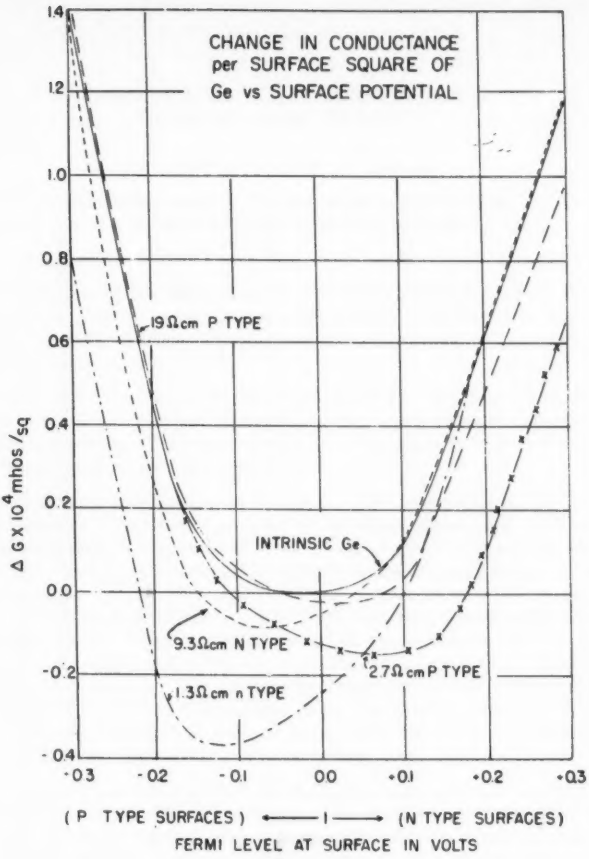
CHANGE IN CONDUCTANCE
per SURFACE SQUARE OF
Ge vs SURFACE POTENTIAL
1.4
1.2
1.0
0.8
0.6
0.4
0.2
0.0
-0.2
-0.4
Δ G X 10⁻⁴ mhos /sq
19Ωcm P TYPE
INTRINSIC Ge
9.3Ωcm N TYPE
2.7Ωcm P TYPE
1.3Ωcm n TYPE
-0.3
-0.2
-0.1
0.0
+0.1
+0.2
+0.3
(P TYPE SURFACES) ← I → (N TYPE SURFACES)
FERMI LEVEL AT SURFACE IN VOLTS

Fig. 2

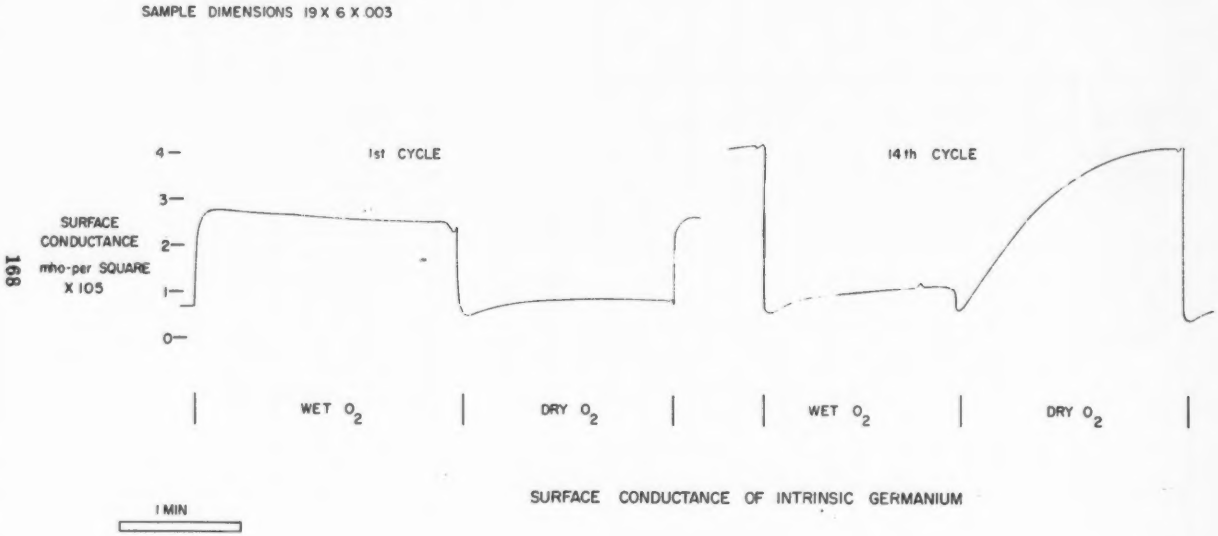
SAMPLE DIMENSIONS 19 X 6 X 003
SURFACE CONDUCTANCE mho-per SQUARE X 105
4
3
2
1
0
1st CYCLE
14th CYCLE
WET O_2
DRY O_2
WET O_2
DRY O_2
1 MIN
SURFACE CONDUCTANCE OF INTRINSIC GERMANIUM

Fig. 3

OXIDATION OF CLEAN SURFACES OF GERMANIUM BELOW 25°C*

Mino Green** and James A. Kafalas**

Lincoln Laboratory, Massachusetts Institute of Technology Lexington, Massachusetts

The oxidation of germanium is of particular interest because there appears to be a relationship between the surface sensitive electrical properties and the nature and extent of the oxide layer on the germanium surface.

One region of interest is in the oxide layer formed on a clean surface. A method was devised to study a truly fresh surface exposed to an oxygen atmosphere. This is achieved by crushing a sample in the presence of oxygen in an all-glass system.

The apparatus used is shown in Fig. 1. The experimental procedure was as follows: The sample, a germanium disc, about 1 cm in diameter and 0.62 mm thick was placed at the bottom of a cylindrical tube about 12 mm I.D. The Pyrex encased iron core hammer was placed on top of the sample, the system was evacuated and outgassed and then filled with oxygen to the desired pressure. The pressure was determined using a thermistor gauge. The d.c. signal from the gauge circuit was fed to a Brush d.c. amplifier and recorder, thus the pressure in the system was recorded continuously. The adsorption system was then sealed off from the vacuum and gas handling apparatus so that in use, the former was simply a Pyrex tube with no stopcocks, grease, or other components which might interfere with the measurement.

The hammer was then raised and dropped several times by the use of a permanent magnet. The sample was thus crushed, exposing a truly fresh surface to the oxygen atmosphere. The change in oxygen pressure in the system due to crushing of the germanium was measured, and the amount of oxygen adsorbed by the freshly exposed surface determined. After the adsorption measurements were made, the sample was carefully transferred to a set of sieves. This transfer process was carried out using methyl alcohol; the use of the liquid in transferring the fine germanium particles insured that no dust was left behind in the glass system. These samples were then subjected to a partial size analysis, by collecting the various sieve fractions and weighing them. The data

* The research in this document was supported jointly by the Army, Navy, and Air Force under contract with the Massachusetts Institute of Technology.

** Staff Members

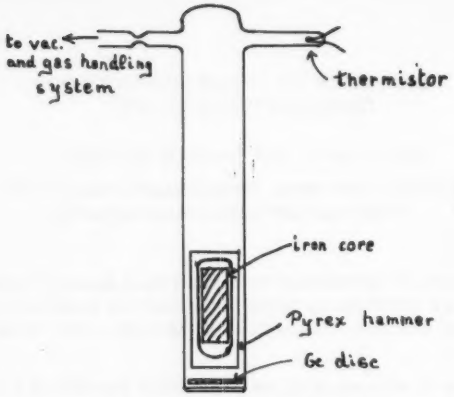

Fig. 1—Ge crushing apparatus

for surface area was calculated on the assumption that the particles were smooth and spherical in shape. Such a calculation necessarily will yield a surface area somewhat on the low side. The true surface area was probably about a factor of two greater than the calculated area.

It was not possible to determine a time constant for the oxidation process with this apparatus because the response time of the vacuum gauge was too slow. However, in all samples treated, an immediate uptake of oxygen was observed upon crushing, and no further uptake was observed even after four days. It can be stated that for the pressure range studied, (2 - 200 microns of oxygen) the oxidation process stops within five seconds of exposure of the surface to oxygen.

A side tube was added to the adsorption vessel to serve as a cold trap. Oxygen saturated with water vapor was then added and the system sealed off. The side tube was then cooled to liquid nitrogen temperature to condense out water. The sample was crushed in this dry oxygen atmosphere and the final pressure recorded. The side trap was then warmed to room temperature and allowed to stand for an hour. The trap was again cooled to liquid nitrogen temperature and the pressure again recorded. There was no additional oxygen take-up during the period of exposure to the oxygen-water vapor system, indicating that water vapor has no effect on the extent of oxidation of germanium surfaces.

The effect of temperature on the extent of oxidation was studied in the following manner. The sample was cooled to -65°C, then crushed and the amount of oxygen adsorbed was recorded. The sample was then brought by stages to +90°C and at each stage the final pressure was recorded. The amount of oxygen adsorbed was about 15 per cent greater at +90°C than at -65°C.

There was no detectable difference in the extent of oxidation between n-type and p-type samples.

Oxidation of etched germanium surfaces was studied in the following manner. A freshly etched sample of germanium, with surface area of about 100 cm sq. was placed in one limb of a mercury manometer and the pressure of oxygen adjusted to 65 cm Hg. The differential pressure in the manometer was then measured with a cathotometer over a period of two weeks. These measurements were taken using both wet and dry oxygen, and in both cases there was no measurable change in pressure during this time. Since the first measurement was taken thirty minutes after etching, it was concluded that no measurable amount of oxidation took place after this time, and that if the germanium had oxidized this must have occurred within thirty minutes after etching.

Several conclusions can be drawn from this work:

For truly clean Ge surfaces

(1) The extent of oxidation is small, equivalent to about two layers of GeO_2. This is probably the sort of oxide that we get on sandblasting a surface.

(2) The extent of oxidation is not sensitive to changes in the bulk properties of the germanium; n- or p-type, high (+90°C) or low (-65°C) temperatures, indicating that the bands must be "clamped" at the surface probably due to Tamm states.

(3) The extent of oxidation is not affected by water vapor, indicating that a germanium hydroxide-germanium oxide cycle of the type found in the rusting of iron does not occur.

Etched Surfaces

(1) Since no long-time oxidation occurs with these surfaces when exposed to wet or dry 0_2, we can conclude that the long-time changes formed in such measurements as contact potential (Brattain and Bardeen) or other measurements of surface sensitive properties made in our laboratory cannot be explained in terms of simple oxidation.

(2) It is quite possible that the oxide layer that we have on germanium as a result of etching is quite different from that produced on a fresh Ge surface, and in fact experiments that have been carried out would indicate the existence of a considerably thicker oxide.

(3) The changes on going from wet to dry 0_2 may be associated with a reaction on the oxide/gas interface of the type $0 = + H_20 \gtrless 20H^-$, which would give rise to new levels of a different energy. The long-time drift might be due, in the case of a CP4 etched surface, to the slow description of bromine. Thus H. Kolm of our Laboratory has found that a CP4 etched sample which has been boiled in water gives much more stable readings in measurements of contact potential than a CP4 etched sample which has merely been washed with distilled water.

Abstract Number 90

ETCHES FOR IMPERFECTIONS IN SI AND GE

J.W. Faust, Jr.

Westinghouse Research Laboratories,
East Pittsburgh, Pa.

A knowledge of the degree of perfection of a crystal is vital not only in the production of semiconducting devices but also in many fundamental investigations. Imperfections decrease the lifetime, give rise to resistivity fluctuations, and in fused junction devices decrease the breakdown voltage, increase leakage, and sometimes cause shorts due to the increased diffusion rate of the alloying element in the imperfections. X-ray analysis is often used in imperfection studies, but this has certain obvious objections—one being the time usually involved in getting a report. Etching is a convenient method for revealing imperfections, and when used in conjunction with an optical goniometer will furnish all the information usually required.

Etches for semiconducting materials can be considered to fall into one of two general classifications—namely, preferential and non-preferential. A preferential etch is one that attacks a certain crystallographic plane thus giving a characteristic etch pattern on the surface, while a non-preferential etch gives a smooth surface. Actually all etches show a preferential nature under carefully controlled conditions, but in the way etching is usually done certain etches appear non-preferential. Imperfections are attacked much more vigorously by the etchant giving pits or lines which are easily seen on the smooth surface formed by a non-preferential etch but are difficult, and sometimes impossible, to distinguish in the pattern produced by the preferential etch. Although the non-preferential etch is used for most imperfection determinations, the preferential etch gives valuable information as to the crystallographic direction of imperfection lines and also what the lines are.

Slices of the semiconductor are lapped with 600 mesh alundum to give a uniform matte surface free of scratches. The sample is then etched with the desired etchant and washed in water and alcohol. A few of the etches found useful for germanium and silicon are listed below.

	Preferential	Non-Preferential
Ge	WAg	CP4
	H_2O_2	Cu
		Mixed Acids
Si	CP4	Hg
	NaOH	Mixed Acids
		CP4

For silicon, the CP4 etch has been listed under both classifications because it gives characteristic pyramids on a (111) surface and a non-preferential appearance on a (100) surface. The etched surfaces are viewed under a metallurgical microscope employing bright field vertical illumination. Magnifications from 150 to 500 are used, although occasionally magnifications of 1000 are necessary.

Individual etch pits, believed to be single edge dislocations, show up distinctly with the CP4 and Cu etches on germanium as conical etch pits. Thermal etching also produces etch pits of this nature. The pits on a (100) surface are found to have a four fold symmetry while those on a (111) surface show a 3 fold symmetry. On silicon, the Hg etch gives pyramidal type pits while the mixed acids etch gives hemispherical pits. These dislocations are found not only in slices cut perpendicular to the growth axis but also in slices cut along many of the common crystallographic planes parallel to the growth axis.

Lineage lines of the type proposed by Burgers[1] and found by Vogel et al[2] have been found on (100) and (111) slices of germanium and silicon. These show up with the CP4 and Cu etches on germanium and with the Hg etch on silicon as a row of etch pits of the type mentioned above. As the angular difference increases, the etch pits become closer together until they merge into a solid line at an angular difference of a few degrees. Lineage lines in germanium of the order of a degree angular difference on (111) and (110) slices show up as a row of pyramids or "mountains" when the surface is etched with the WAg etch.

Twin boundaries and grain boundaries also show up as thin solid lines with a non-preferential etch. In order to determine the type of line exposed by the non-preferential etch, the surface is relapped and etched with a preferential etch. A lineage boundary will show the same etch pattern on both sides of the boundary while a twin or grain boundary will have a different etch pattern on each side of the boundary. The etch pattern on each side of the boundary will differentiate between the twin and grain boundary.

Dislocations and lineage lines have been observed on indium antimoide using the CP4 and the mixed acids etches. The H_2O_2 etch is found to be preferential.

References

1. J.M. Burgers, Proc. Phys. Soc. (London) 52, 23 (1940).

2. F.L. Vogel, W.G. Pfann, H.E. Corey, and E.E. Thomas, Phys. Rev. 90, 489 (1953).

Abstract Number 91

ELECTROLYTIC ETCHING OF SEMICONDUCTORS

W.E. Bradley

Philco Corporation
Philadelphia, Pennsylvania

Electrolytic etching is a convenient process for shaping the semiconducting bodies employed in the manufacture of surface-barrier transistors and rectifiers. The fact that potential differences may exist within various regions of a semiconductor which affect the nature and the rate of electrolytic action cause this process to have several peculiarities which must be taken into account

While it is possible to limit the etching action to the specific areas desired by means of surface coatings which protect those areas which it is desired to leave undistrubed, this practice is not always desirable since it may unfavorably affect the chemical potential of the semiconductor surface which should preferably be kept in a clean condition. It has proved convenient to define the area to be etched by means of fine jets of electrolyte expelled from glass nozzles. One of the electrodes is attached to the semiconductor through an ohmic contact while the other is placed in the liquid reservoir supplying the jet. A very large variety of electrolytes will satisfactorily etch germanium and a somewhat smaller group, silicon.

With some N type semiconductors of which germanium is an example, a surface barrier forms during the etching process which tends to greatly increase the resistance of the semiconductor adjacent to the electrolyte. This effect can be usefully controlled by exposing the region to be etched to strong illumination with visible light. The illumination produces electronhole pairs in the material causing a controlled flow of current.

The potential in the interior of a piece of N type semiconductor can be displaced in the negative direction by a nearby rectifying electrode. If such an electrode is attached to the opposite side of a specimen of N type germanium during electrolytic etching then the etching action will stop abruptly when the jet has penetrated to the region of negative interior potential. Additional etching merely serves to expose more of the equipotential surface within the material. The remaining stratum of germanium extending from the exposed surface to the electrode has a thickness approximately equal to $1.1 \sqrt{rV}$ microns where r is the resistivity of the N type germanium and V is the potential with respect to the semiconductor applied to the rectifier electrode on the reverse side. This structure provides a convenient means of thickness control for semiconducting devices. Using this process a precaution is often

useful: The electrolyte should preferably contain no metal which when electroplated upon the germanium surface will cause strong emission of positive charge carriers or "holes" since such a metal would be deposited upon the exposed equipotential surface, the very large electric currents then passing to the rectifying electrode from the electrodeposited metal, resulting in possible damage of the specimen or disturbance of the rectifying electrode potential. A dilute solution of sodium nitrite has proved satisfactory with N type germanium for most purposes.

If after the equipotential surface has been exposed, the rectifying electrode potential is increased in the negative direction, etching continues at a different equipotential causing a step in the surface. A prescribed variation of rectifying electrode potential can control the contour of the excavation subject to the limitation that no portion of the bottom of the pit can be convex toward the jet.

Abstract Number 92

THE PURIFICATION OF GERMANIUM THE GERMANIUM TETRACHLORIDE—ARSENIC TRICHLORIDE SYSTEM*

Mino Green** and James A. Kafalas**

Lincoln Laboratory, Massachusetts Institute of Technology Lexington, Massachusetts

The purification of $GeCl_4$ has attracted attention because of its importance as a stage in the preparation of pure germanium.[1] The anhydrous system $GeCl_4$—$AsCl_3$ has been investigated by Sebba,[2] who found that the vapour-liquid equilibrium curve showed no azeotropes, and so concluded that the two compounds could be separated by fractional distillation. The system was also studied in a packed fractionating column by Cluley and Chirnside.[3] They reported high overall separation when the mole fraction of $AsCl_3$ was 10^{-5} or greater, but comment that ". . . . .when the starting material contained only a few parts per million of arsenic, the purification factor achieved was very small and this work showed that redistillation was of little value. . . . ." The experimental investigation reported here was undertaken with a two-fold object in view: to test the practicality of fractional distillation as a method for obtaining pure $GeCl_4$ (i.e. $[AsCl_3] / [GeCl_4] < 10^{-8}$, and, at the same time, if possible, to explain the data obtained by Cluley and Chirnside. In particular it seemed difficult to understand the rapid decrease in fractionation at low $AsCl_3$ concentrations.

The re-examination of the $GeCl_4$—$AsCl_3$ vapour-liquid system has given results in substantial agreement with Sebba's data. In addition, a more detailed study of the system in the region poor in $AsCl_3$ shows that the relative volatility is constant from 5×10^{-2} mole fraction $AsCl_3$ in the liquid down to 6×10^{-10}. This is not surprising since every $AsCl_3$ molecule must be entirely surrounded by $GeCl_4$ molecules and so mutual interactions between $AsCl_3$ molecules are negligible. In the part of the system which is poor in $GeCl_4$, the same reasoning applies and the relative volatility becomes constant at about 5×10^{-2} mole fraction $GeCl_4$. This is not obvious from Fig. 1 because of the use of a log scale for mole fractions. There was no evidence of azeotrope formation in this system.

The distillation studies showed that the $GeCl_4$—$AsCl_3$ mixtures behave in a perfectly normal manner if concentration changes were followed by a radiotracer method. However, the results of absolute

* The research in this document was supported jointly by the Army, Navy, and Air Force under contract with the Massachusetts Institute of Technology.

** Staff Members

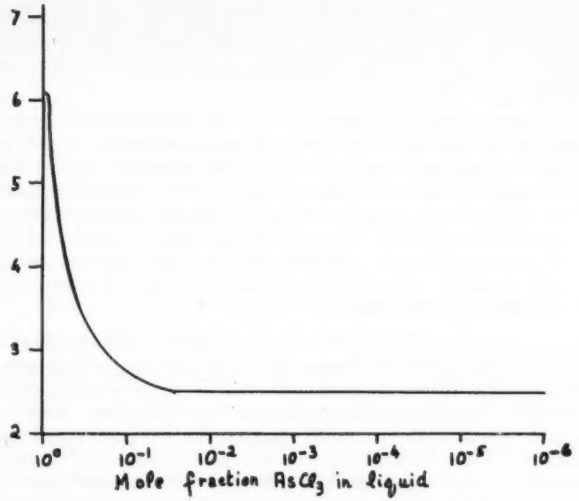

Fig. 1—Variation of alpha α with composition.

arsenic analyses indicate that there is a source of arsenic in the closed distillation assembly. Since an increase in arsenic concentration was detected in a Pyrex distillation assembly and not detected in a quartz assembly it was concluded that the additional arsenic was obtained as a result of the leaching action of $GeCl_4$ on the Pyrex glass. To confirm this hypothesis, $GeCl_4$ of high purity was refluxed in a Soxhlet extractor and the material reanalysed, whereupon an increase in $AsCl_3$ concentration was detected. The level of $AsCl_3$ contamination as a result of exposure to Pyrex glass was not always the same. This would be expected since the amount of leachable arsenic might well be related to the history of the glassware—e.g. how much previous leaching had occurred; how the glass had been treated, such as the extent of fire polishing or whether it has been cleaned with detergents or a dilute solution of HF. The temperature at which exposure of $GeCl_4$ to Pyrex glass occurred would also appear to be important. The species of arsenic leached from the glass is not known. These studies would help to explain the results reported by Cluley and Chirnside.

Finally it may be said that $GeCl_4$ can be obtained in an extremely pure state if a quartz distillation column is used. The relative volatility is sufficiently large so that a column of small platage at total reflux can be used at large take-off rates to give a product sufficiently pure for germanium semiconductor needs.

The experimental work described involved the measurement of $AsCl_3$—$GeCl_4$ concentration ratios in the boiler liquid and the vapour condensate of an equilibrium still, and in the still-pot and still-head of a fractionating column.

As^{74} was used as a tracer in some of the experiments described. Carrier free As^{74} was obtained by bombarding germanium samples with 16-Mev deutrons in the M.I.T. cyclotron. A method of isolation was that due to Green and Kafalas.[4]

Absolute arsenic concentrations, in the low concentration range, were determined by the method of neutronic activation analysis.[5] The lower limit of arsenic detection was 3.6×10^{-10} mole fraction $AsCl_3$.[6] Higher arsenic concentrations were determined using the following procedure. 1 ml of the mixture was transferred from a pipette into a weighing bottle and the sample weighed. The mixture was then placed in a dilute solution of sodium hydroxide and finally neutralized with sodium bicarbonate. The weight of arsenic present was determined by titration against a standard iodine solution.

Vapour-Liquid Equilibrium.—The vapour-liquid equilibrium still used was a slightly modified version of the design due to Gillespie.[7] The apparatus was throughly dried before charging it with the mixture to be studied in order to avoid hydrolysis of the chlorides. Mixtures containing a known amount of $AsCl_3$, tagged with As^{74}, were distilled into the apparatus. After equilibrium was reached (in about 1-1/2 hours) 1 ml samples of the boiler liquid and the vapour condensate were drawn off. In the region from 0.09 mole fraction $AsCl_3$ in the starting material to the maximum $AsCl_3$ concentration used, the mole fraction of $AsCl_3$ was determined by iodine titration. For lower arsenic concentrations, the solutions were assayed by comparing ratios of arsenic activities. The variation of the relative volatility with concentration $AsCl_3$ is shown in Fig. 1. It can be seen from Fig. 1 that α, that is the relative volatility, is approximately constant for concentrations below 0.05 mole fraction $AsCl_3$ in the liquid. The average α in this range is 2.52 ± 0.035.

Distillation Studies.—The distillation studies were made with very dilute solutions of $AsCl_3$, where α is essentially invarient with composition. It was possible to use the Fenske equation and similar relations in interpreting the experimental results obtained in these packed fractionating columns. A Pyrex fractionating assembly of a plate equivalence of 10.6 ± 0.24 at total reflux and boil-up rate 3.42 moles per hour at atmospheric pressure was used in the first study. The fractionation obtained in these columns at various take-off rates was measured by two methods. First, the ratio of As^{74} in the still-head and still-pot was determined; and secondly, the ratio of arsenic in the still-head and still-pot was determined by radio-activation analysis. Table I shows the results obtained.

A similar study was repeated using a quartz fractionating column and this time absolute arsenic analyses gave fractionations which would be expected from measurements of the platage of the column. These results are also shown in Table I.

Since the above studies pointed to the possible existence of leaching of arsenic from Pyrex, the following experimental test was carried out. $GeCl_4$ previously purified in a quartz column was refluxed for 24 hours in a Soxhlet extractor which was packed with Fenske helices. The $GeCl_4$

was analysed for arsenic and the results showed a marked increase in arsenic concentration. $GeCl_4$ before refluxing contained $< 6.3 \times 10^{-10}$ mole fraction $AsCl_3$ and after refluxing it contained 2.52×10^{-9} mole fraction $AsCl_3$. This increased arsenic concentration, while being significant, is somewhat lower than the values obtained in the distillation assembly. However, the two systems are not entirely comparable, in particular the temperature of the liquid contacting the Fenskie helices in the distillation column was 83°C while the temperature of the contacting liquid in the extractor was about 40°C. Further we expect leaching to be a somewhat erratic process.

References

1. A.P. Thompson and J.R. Musgrave, J. of Metals, 4, 3 (1952).
2. F. Sebba, J. Chem. Soc. (London), 1975 (1951).
3. H.J. Cluley and R.C. Chirnside, J. Chem. Soc. (London), 2275 (1952).
4. M. Green, and J.A. Kafalas, J. Chem. Phys. 22, 760 (1954).
5. A.A. Smales and B.D. Pote, Anal. Chem. 24, 717 (1952).
6. G.W. Leddicotte, private communication).
7. D.T.C. Gillespie, Ind. Eng. Chem., Anal. Ed., 18, 575 (1946).

TABLE I

FRACTION, RADIOACTIVE AND ABSOLUTE ASSAY
FOR PYREX AND QUARTZ STILLS AT TOTAL REFLEX

Distillation Apparatus	No.	Absolute Arsenic Concentration		Fractionation, Absolute	Fractionation, As^{74}
		Mole fraction $AsCl_3$ Still-pot	Mole Fraction $AsCl_3$ Still-head		
Pyrex	1	2.98×10^{-7}	3.08×10^{-8}	9.7	2×10^4
	2	3.27×10^{-7}	2.90×10^{-8}	11.3	2×10^4
Quartz	3	1.64×10^{-7}	$< 6.30 \times 10^{-10}$	>260	300
	4	1.64×10^{-7}	$< 6.30 \times 10^{-10}$	>260	600

Abstract Number 94

DEPTH OF SURFACE DAMAGE DUE TO ABRASION ON GERMANIUM

T.M. Buck and F.S. McKim

Bell Telephone Laboratories, Incorporated
Murray Hill, N.J.

INTRODUCTION

The drastic effects of surface damage on Ge produced by mechanical abrasion, e.g. sandblasting, was one of the earliest surface effects recognized in semiconductor and transistor research; various chemical etching treatments were developed for removing mechanically damaged material.

The aim of the present work was to make a quantitative evaluation of the depth of damage, as manifested in surface recombination velocity, produced by various abrasion techniques on a germanium surface. Such information will perhaps be useful in device fabrication, as smaller and more critical physical dimensions are required. It should also contribute toward a more complete description and definition of surface effects on semiconductors. The principal method employed in the work was the photoelectromagnetic[1,2] method of investigating surface recombination velocity, which seemed particularly suitable because of geometry considerations. The depth of material removed by etching was computed from weight loss.

Some work along this line has been published recently. Clarke and Hopkins[3] found that sandblasting a thin rod of germanium produced a high conductivity surface layer and, by successive etching with a calibrated etchant and measurement of effective resistivity, estimated that this high conductivity layer was about 0.7×10^{-4} cm. thick.

Camp[4] found from etching rate experiments that the depth of the disturbed layer was about 6 microns when a (100) germanium face was ground on No. 305 abrasive.

McKelvey and Longini[5] found that a surface lapped with 800 grit Alundum required removal of Ge corresponding to a depth of 5μ to bring S (surface recombination velocity) down to the order of magnitude associated with etched surfaces.

EXPERIMENTAL

Photo-electromagnetic Measurements

In the procedure originally proposed for measuring surface recombination velocity, S, and the only one for which even an approximate

quantitative treatment has been published,[1] the front, illuminated, surface is assumed to remain constant at a low value of S while the back surface is given treatments to be tested for their effect on recombination velocity. However, as has been shown previously[2] just as large a range of response can be obtained if the back surface is held constant at a high value of S, produced by sandblasting, for example, while the front surface is given treatments to be tested.

In the present work it was more convenient to apply the abrasive treatment to the front surface where there were no leads to interfere, while the back surface remained constant in a sandblasted condition to provide a "sink" for the carriers created by the light. After an abrasive treatment on the front surface a very low value of the photoelectromagnetic voltage, V_X, a fraction of a millivolt, is obtained, since in this situation most of the carriers created by the light recombine at the front surface and there is little or no concentration gradient or diffusion current. As the front surface is given a series of etching treatments V_X will increase and finally saturate, and in this region we assume that the disturbed material has been removed.

The two germanium specimens used were p-type, 5.5 ohm cm. slabs 1.25" long, 0.25" wide and about 0.05" thick initially. The back surface was sandblasted, leads were soldered about 1.8 cm. apart and the whole assembly was then cast in Araldite resin with a glass backing leaving only the front face of the slab and the ends of the leads exposed. The specimen could then be cemented with wax to a holder for lapping or polishing.

Etching of the front surface after an abrasive treatment was performed by dipping it into CP-4 diluted by adding 15 ml. of distilled water to the usual formula.* The slab was moved about gently in the acid to obtain uniform etching. The specimen was then rinsed thoroughly in a stream of distilled water and blotted dry on filter paper. The photoelectromagnetic measurements were made quickly, the balance on the Type K-2 potentiometer being reached by trial and error, in order to prevent heating of the sample by the light. These measurements were made in an atmosphere of dry nitrogen.

Weight Loss Measurement

The depth of material removed was computed from weight loss assuming uniform etching over the surface. For the specimens used, 1 mg. weight loss corresponded to about 1 micron change in thickness. Sufficiently small weight losses could be measured quite accurately, and rapidly, on an analytical balance. This procedure may be open to the objection that uneven etching, for example tapering toward the edges, would cause faulty estimates of the depth of material lost at the most important region which is on a line between the projected contacts on the illuminated face of the slab. However, weight loss seemed the quickest

*The usual formula is 25 ml. conc. HNO_3, 15 ml. conc. HF, 2-3 drops bromine, 15 ml. glacial acetic acid.

and most precise method with the large specimens involved. Checks with a micrometer at various times during the series agreed fairly well with the weight loss values.

Results

Some of the results are given in Table I. All of the abrasive treatments tested caused high surface recombination velocities (low V_X) initially but the amount of etching required

TABLE I

Treatment	Depth of Damage (Microns)	Nominal Particle Size of Abrasive (Microns)
Linde Fine Abrasive "B" Polish	1	0.1
Ultrasonic Abrasion (600 mesh SiC in water, ultrasonically agitated)	1-2	
Diamond Polish	1-2	0.5
No. 305 Lap	6-7	5
Diamond Saw Cut	12-13	
600 Mesh Silicon Carbide Lap	17-18	25
180 Mesh Sandblast	32-34	125

varied widely and in quite a reproducible manner with the type of abrasive treatment. Thus, a surface which was sandblasted with 180 mesh SiC required removal of about 32-34 microns, computed from weight loss, while a diamond polished surface required only 1-2 microns. (Details of these treatments will be given.) The fine polishes were developed and administered by Messrs. W.L. Bond, J. Andrus, and E.B. Berry of Bell Telephone Laboratories.

Several times the freshly lapped or polished surfaces were carefully washed in alcohol, toluene, water, etc. to determine whether any cleaning action short of actual removal of material would raise V_X, especially in the case of the fine polishes. None of these attempts was successful; it appeared that the high recombination velocities were indeed due to mechanical damage even with the very finest abrasive treatment.

The 600 mesh SiC was slurried in water and the lapping done by hand on a glass plate with moderate pressure. Anywhere from 0.7 to 5 mils were removed in five separate treatments of this type, and practically the same depth of damage was measured for all.

The depth of damage for the No. 305 Lap is in good agreement with the 6 micron value obtained by Camp[4] from etching rates for the same abrasive material on the same crystal face (100).

Since in the photoelectromagnetic method of investigating surface recombination velocity, the light is assumed to be absorbed and the hole-electron pairs created at the illuminated surface it would be

reasonable to ask whether penetration of the water-filtered light a small distance into the material has any influence on the apparent depth of damaged material. Evidently it does not. Substitution of a 2%$CuCl_2$ solution in water for the water filter in two experiments lowered V_X because of the decrease in intensity but did not change the position where the maximum was reached.

Diode Studies

Three of the abrasive treatments—diamond polish, No. 305 lap, and 600 mesh silicon carbide lap—were given to two large grown junction p-n diodes in order to determine whether the differences shown by the P.E.M. method would appear also in treatment of a junction device. The diodes were lapped or polished on all four sides and were then put through the etching and weighing procedure. After each etching and washing a diode was allowed to stand over silica gel in a bottle for 24 hours before measurement of the reverse characteristic. The recovery of the reverse characteristic as a function of depth of material removed agreed quite closely with P.E.M. measurements for the three treatments. However, the behaviour of the reverse characteristics after abrasion—i.e. failure to saturate, cannot be explained on the basis of recombination velocity alone by existing theoretical treatments of p-n junctions. These effects may be caused by a conductive layer across the junction of the type found by Clarke and Hopkins[3] on a sandblasted filament.

References

1. T.S. Moss, L. Pincherle, and A.M. Woodward. Proc. Phys. Soc. 66, (London), B 743-752 (1953).
2. T.M. Buck, W.H. Brattain, paper delivered at Chicago meeting of the Electrochemical Society, May 6, 1954. To be published.
3. E.N. Clarke and R.L. Hopkins, Phys. Rev. 91, 1566 (1953)
4. P.R. Camp, Printed abstract of paper delivered at Chicago meeting of the Electrochemical Society, May 2-6, 1954.
5. J.P. McKelvey and R.L. Longini, J. Appl. Phys. 25, 634-641 (1954).

Abstract Number 95

THE ELECTROCHEMICAL PREPARATION OF GERMANE *

Mino Green** and Paul H. Robinson**

Lincoln Laboratory, Massachusetts Institute of Technology Lexington, Massachusetts

Paneth and Rabinowitsch[1] first described the electrochemical preparation of monogermane: the yields that they obtained were about 0.1% in current efficiency. No attempts to improve the yield of GeH_4 have been reported. A study of the electrochemical preparation of GeH_4 was undertaken with a view to improving the yield of GeH_4, to the point where it might be considered as a suitable alternative step in the preparation of pure germanium.

A number of systems were investigated and the system, cathode Na(Hg) | NaOH, GeO_2 (aqueous) | Pt anode, was found to give by far the best yields of GeH_4. We shall, therefore, concern ourselves with reporting in detail on the reduction of GeO_2 at a sodium amalgam cathode.

EXPERIMENTAL

Estimation of GeH_4-H_2 ratios—The gaseous product from the cathode was a moist mixture of GeH_4 and H_2; no other gaseous species were detected nor were there any other volatile hydrides of germanium. The GeH_4-H_2 ratio was determined using a Rayleigh-Zeiss interferometer. The essentials of the analytical method have been reported elsewhere.[2]

The cell assembly—The electrolysis cell is shown in Fig. 1. The mercury cathode, A, was in the form of a cup, and electrical contact was made to it by means of a platinum wire passing down the shaft, E. D, was a conventional mercury seal. The gases produced at A were collected in the gas trap, B. F was a fritted disc which separated anolyte from catolyte. The cell assembly was placed in a trough and cooled by means of rapidly flowing tap water.

The electrolysis current was measured continuously on a recording ammeter, and the number of coulombs determined by integrating the current-time curve obtained.

A typical run was performed as follows: The trap, B, was completely filled with liquid. The current was allowed to flow and the trap, B, filled

* The research in this document was supported jointly by the Army, Navy, and Air Force under contract with the Massachusetts Institute of Technology.

** Staff Members

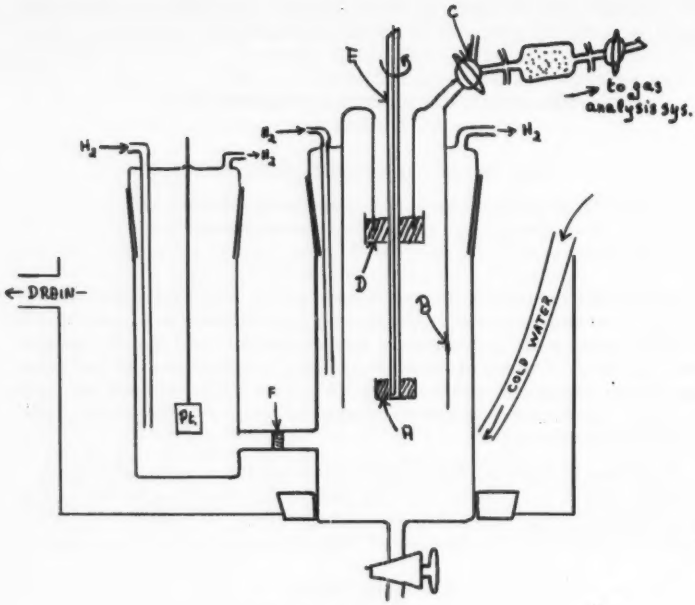

Fig. 1—Cell assembly

with gas, displacing liquid as it filled. The current cut off automatically when there was no longer a current path between the cathode and anode. This served to "run-in" the electrode. The gas was discarded and the experiment repeated, only this time the gas trapped in B was collected and analyzed. The volume of liquid displaced was known and since the pressure of gas was known (corrected for water vapor pressure) it was possible to determine the quantity of gas produced by a given number of coulombs.

Results

The information that we have from each run is: the composition of the catolyte, the current density at the cathode, the amount of gas collected its GeH_4-H_2 ratio and the number of coulombs passed. There are three main products of electrolysis, GeH_4, H_2 and Ge. The yield from the cathode can be defined in several ways: a) The mole fraction, x, of GeH_4 in the GeH_4-H_2 mixture. b) The current efficiency for GeH_4 production, $Y_C = \frac{4x \text{ no. of moles of } GeH_4}{\text{no. of moles of } (4GeH_4, H_2, 2Ge)}$ c) The mass conversion efficiency, $Ym = \frac{\text{no. of moles of } GeH_4}{\text{no. of moles of } (GeH_4, Ge)}$

Figures 2, 3 and 4 give a typical NaOH, GeO_2 composition-yield contour diagram for a fixed current density.

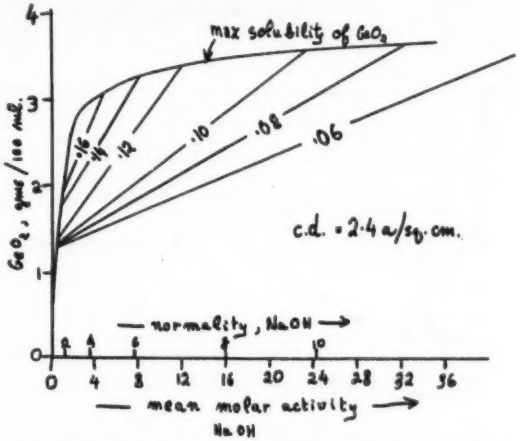

Fig. 2—Contour yield diagram (mole fraction) for [GeO_2], [$N_2$0H] coordinates.

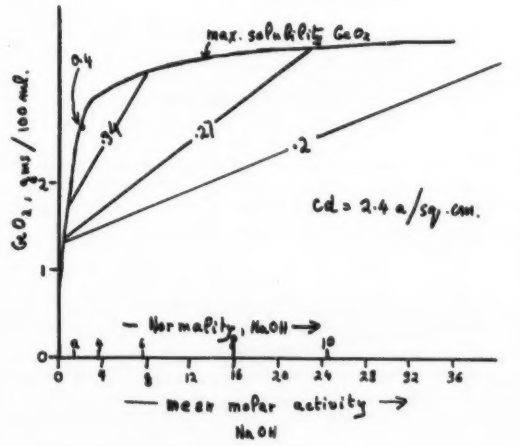

Fig. 3—Contour yield (Y_C) diagram for [GeO_2], [NaOH] coordinates.

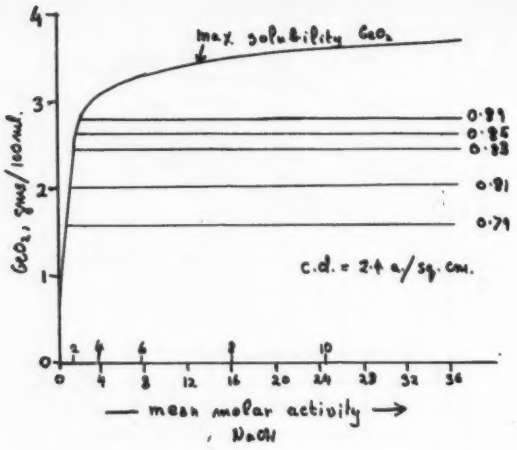

Fig. 4—Contour yield (Ym) diagram for [GeO_2], [NaOH] coordinates.

Figure 5 shows the variation of yield with current density for a catolyte of a particular composition.

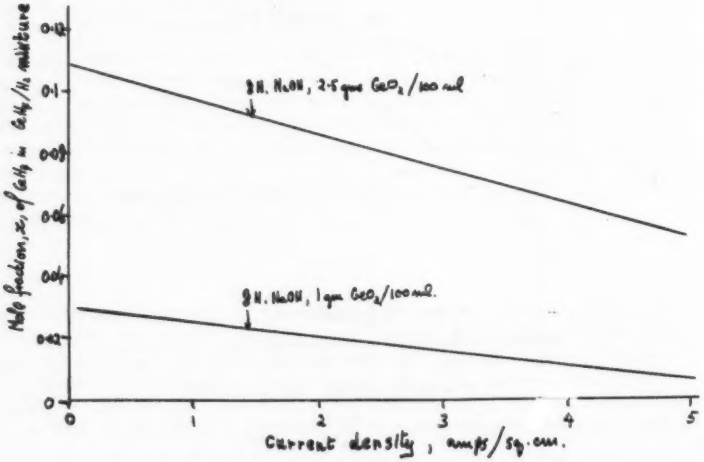

Fig. 5—Yield (x) as a function of current density.

The effect of stirring is shown in Fig. 6.

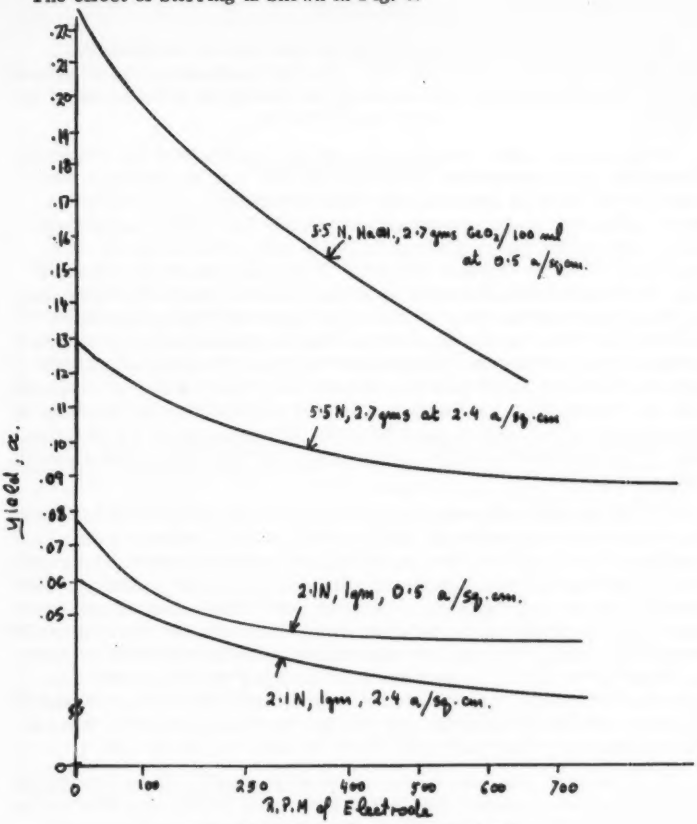

Fig. 6—Effect of stirring on yield.

The following experiments were performed to find out if a highly reducing intermediate product was present in the catolyte as a result of the partial reduction of GeO_2. It was necessary that the reagent to be reduced had a stronger reduction potential at the pH used than the omnipresent Ge. For this reason an acid solution containing V^{+++} was used. A sample of catolyte was taken and rapidly added to the reagent, there was a color change indicating the presence of a strong reduction agent. If the same experiment was repeated with a pure NaOH solution, no color change was observed. Also if a NaOH/GeO_2 solution was electrolyzed and the sample of catolyte which was removed was allowed to stand for several minutes and then added to the V^{+++} solution, no color change was observed.

Discussion

No serious attempt has been made in this work to elucidate the mechanism of GeH_4 production. But a partial explanation can be offered for the variation of yield with changes of some of the parameters of the system.

In the system under consideration we are dealing with the reduction (hereafter called secondary reduction) of $GeO_3^=$ ions by hydrogen produced at the cathode (probably the discharge of Na^+ to give Na which then reacts with water to produce hydrogen). That $GeO_3^=$ is the form which GeO_2 takes when dissolved in highly alkaline solution has been concluded from the work of Carpeni.[3] It has been generally assumed[4] that secondary reduction at a cathode goes more easily with increasing hydrogen overvoltage but such is not the case with the system under discussion. Thus we see from Fig. 5 that the yield decreases with increasing current density, yet we know that the overvoltage increases with increasing current density. In fact our measurements of overvoltage in a 2N·NaOH–2.1 gm GeO_2 per 100 ml solution show an increase of overvoltage of ~1 volt on going from 0.5 amps/sq. cm to 5.0 amps/sq. cm. It is quite possible then that the electrode process is under partial diffusion control.

An examination of the conditions of diffusion at the cathode following the treatment of Wagner[4] and others shows that the concentration changes of Na^+ and $GeO_3^=$ at the cathode as compared with the bulk electrolyte will not be very significant. Thus the Na^+ concentration at the cathode will be slightly enhanced and the $GeO_3^=$ concentration will be near to zero but not completely exhausted. The effect of stirring can be explained if one postulates the existence of some intermediate product produced at the cathode which has a lifetime of say a few seconds in solution. Then when one rotates the cathode the hydrodynamic boundary layer is reduced in thickness and this intermediate produce is thrown out into solution where it decays either to $GeO_2 + H_2$ or $Ge + H_2$.

It can be seen from the results reported that GeH_4 can be obtained at high current efficiencies >50% and at good mass conversion efficiencies ~90%. Since one can start with crude sodium germinate and obtain pure GeH_4, there being no production of the hydrides of As, Sb, B or Si, it is suggested that this might be an economical method for going from crude germanium extracts to a pure germanium compound which has the further property that it decomposes at low temperatures (<400° C) into Ge and H_2.

References

1. Paneth, F. and Rabinowitsch, E., Ber., 1138a, 58B, (1925).
2. Green, M. and Robinson, P.H., Anal. Chem. 1913, 25, (1953).
3. Carpeni, G., Bull. Soc. Chim., France, 629, 15, (1948).
4. Hickling, Quart. Revs. (London), 122, 3, (1949).
5. Wagner, C., J. Electrochem. Soc., 181, 101, (1954).

Abstract Number 96

THE PRESENT STATUS OF INTERMETALLIC SEMICONDUCTORS

R. G. Breckenridge

National Bureau of Standards
Washington, D. C.

Since the recent concentration of attention on the intermetallic semiconducting compounds, a considerable amount of information has been obtained on a variety of these compounds, giving an overall picture of their properties. More recently, some of these compounds have been prepared in a highly purified state allowing a detailed study of many of their more interesting features.

The group of compounds most widely investigated in recent years is that based on the zincblende structure, composed of elements from the 3rd and 5th columns of the periodic table.[1,2] An example of this group is InSb. Historically, the semiconducting compounds Mg_2Si, Mg_2Ge and Mg_2Sn were the first to be studied. These materials possess the fluorite structure with an average of 8/3 ϵ per atom. Apparently Mg_2Pb is metallic, although it has not been investigated in sufficient detail to make this certain. The energy gaps in this series range from 0.3 ev for Mg_2Sn to 0.7 ev for Mg_2Si. The mobilities reported for rather impure materials are low, but this apparently is due to impurity scattering. Of these compounds, only Mg_2Sn has been prepared in a state of high purity. This high purity (ca. $2.1 \times 10^{16}/cm^3$ impurity centers) material has an activation energy at T = 0° of 0.31 ev and rather high mobility; μ_e = 3500 cm^2/volt sec at 100°K. Photoconduction and photovoltaic effects in the infrared have been observed as well, with a maximum response at about 4.1 μ.[3]

The first group mentioned, based on the zincblende structure, has an average of 4 ϵ per atom. There is a wide range of activation energies in these compounds, from 0.23 at T = 0°K for InSb to 1.6 ev for AlSb. The compounds in general are characterized by high electron mobilities, particularly for combinations of heavy elements. Recent studies on high-purity InSb give μ_e of ca. 2.1×10^5 cm^2/volt sec at liquid air temperatures, and μ_e = 30,000 and 17,000 cm^2/volt sec at room temperatures have been reported for InAs and HgTe respectively. These remarkable properties are strongly indicative of an unusual electronic structure in the compounds and both theoretical and experimental studies are being carried on to clarify the situation. It is found that the conduction band, at least in InSb, has a very low density of states near the bottom of the band, and as a result the conduction electrons have an unusually low effective mass. This model satisfactorily explains a number of striking observations on the absorption spectra and also on

the unusually large magneto-resistance and magneto-Hall effects. It has, however, made the precise interpretation of many of the results very difficult since the generally used formulae for these effects are only approximations and lose their validity when the effective masses are extremely low.

InSb has also shown itself to be a very interesting material as an infrared photoconductor. The small energy gap provides a response with peak sensitivity at ca. 5.3 μ (T = 80°K) and the high charge carrier mobility gives an unusually high photoresponse.

In addition to these simple binary compounds, it has been recently reported[4] that a similar series of ternary compounds based on the chalcopyrite structure of the type $A^{I}B^{III}C_2^{VI}$, such as $CuInSe_2$, are also semiconductors. This structure is a close relative of the zincblende structure and again the average number of electrons per atom is 4. No precise data are available for these compounds, but it might be expected that their properties would be rather similar to the $A^{II}B^{VI}$ compounds.

There are also a number of other binary types of semiconducting intermetallic compounds including the well-known series of lead compounds PbS, PbSe and PbTe with the simple cubic structure[5,6] and the $A^{II}B^{V}$ compounds CdSb and ZnSb which crystallize in the orthorhombic system[7,8].

Both CdSb and ZnSb have energy gaps near 0.5 ev and charge carrier mobilities of the order of a few hundred cm^2/volt sec. Similar mobilities are observed in the lead compounds whose energy gaps range from 0.25 to 0.4 ev. The lead compounds have shown at least a partial ionic character and it has proven possible to vary the stoichiometry and use controlled valence techniques to vary their properties. The infrared photoconducting properties of films of the lead compounds have been studied in great detail since, as indicated by their energy gaps, they respond quite far into the infrared region and they have been shown to have a high sensitivity when activated.

Still other series of intermetallics are compounds like Ca_2Si (tetragonal lattice) and Mg_3Sb_2. Measurements of the conductivity of the Ca-compounds[6] show the following energy gaps: 1.9 ev for Ca_2Si, 0.9 ev for Ca_2Ge, and 0.46 ev for Ca_2Pb. The compound Mg_3Sb_2 has a very complicated structure; several workers have reported on the electrical, thermal and optical properties of this material.[9] Their results indicate an energy gap of about 0.8 ev.

It is thus becoming clear that, instead of being restricted to a very small number of elementary semiconductors, there are actually available a wealth of semiconducting materials and, as technology advances, it will become possible to "tailor-make" semiconductors for particular applications.

References

1. H. Welker, Z. Naturforsch 7a, 744 (1952); 8a, 248 (1953).
2. R. G. Breckenridge et. al., Phys. Rev. 96, 571, 576 and 578 (1954).
3. H. P. R. Frederikse and R. F. Blunt, Paper presented at Atlantic City Conference on Photoconductivity, Nov. 1954, to be published (Wiley).
4. C. H. L. Goodman and R. W. Douglas, Amsterdam Conference on Semiconductors (1954).
5. T. S. Moss, Proc. Phys. Soc. (London) B62, 741 (1949); B63, 167 (1950).
6. R. F. Brebrick and W. W. Scanlon, Phys. Rev. 96, 598 (1954).
7. E. Justi and G. Lautz, Z. f. Naturforsch. 7a, 602 (1952).
8. G. Busch et. al., Helv. Phys. Acta 27, 193 (1954).
9. T. S. Moss, Proc. Phys. Soc. (London) B63, 982 (1950).

Abstract Number 97

EFFECT OF ZONE REFINING VARIABLES ON THE SEGREGATION OF IMPURITIES IN InSb

T. C. Harman, R. K. Willardson, H. L. Goering, and A. C. Beer

Battelle Memorial Institute

Ultra-pure indium-antimonide specimens, whose uncompensated n-type impurity concentration is 1×10^{14} cm^{-3}, have been prepared by utilizing the following techniques: (1) additional purification of chemically pure indium, (2) extensive zone-melting of the indium antimonide, and (3) the selection of the specimens from uncompensated regions of optimum purity in the zone-refined InSb ingots.

InSb ingots were prepared using indium of three different purities and zone-refined antimony. The starting materials were placed in a Vycor tube under a partial pressure (approximately 2/3 atmosphere) of pure, dry hydrogen. All zone-melt passes were made with a 2 kw high-frequency induction heater. Initially, the ratio of zone length to ingot length and the rate of travel of the molten zone were large. These quantities were gradually decreased until the zone-length was 2.0 cm -2.5 cm and the rate of pass was 1 cm/hr. The final 10-15 zone-melt passes were made under these conditions.

During the course of the zone-refining passes, specimens were removed for electrical measurements. In addition, the ingot was periodically probed for thermal emf at room temperature and at 80°K. These measurements indicated that initially, the ingot was p-type. However, upon subsequent zone-passing, the region at the rear of the ingot became n-type. Subsequent passes increased the length of this n-type region and after 30 passes, it extended over half the length of the ingot. After a total of 30 or more zone passes, thin slices, cut perpendicular to the direction of travel of the molten zone, were removed from the ingot. Hall coefficient and resistivity measurements were carried out on specimens prepared from these slices. Calculations of carrier concentrations and mobilities showed that as the ingot is traversed from rear to front, regions of the following characteristics are distinguishable: (1) the carriers are n-type and decreasing in concentration; the mobility is increasing, (2) the carriers are n-type but per unit fractional distance along the ingot, they are decreasing at a faster rate; the mobility is decreasing, (3) an inhomogeneous p-n region, (4) the carriers are p-type of low concentration; the mobility is quite low, and (5) the carriers are p-type and increasing in concentration. In those regions of complete ionization of the impurities and negligible compensation, the carrier concentration will be approximately equivalent to the impurity concentration. Compensation effects in material of regions 1 and 5 are believed negligible. The above observations indicate that

the most slowly segregating impurity is n-type, and that it lowers the melting point. The second most slowly segregating impurity is p-type and it raises the melting point. In order to determine the identity of the two unknown impurities, spectrographic and activation analyses were carried out. Spectrographic analyses on front and rear regions of an InSb ingot after five and nine passes showed that zinc segregates to the front while copper, lead, tin, and nickel segregate to the rear. These results suggest that the p-type impurity, which segregates slowly to the front of zone-melted InSb ingots, is zinc.

Impure ends were periodically clipped off during the extensive zone refining of an InSb ingot. After removal of the fast-segregating impurities, spectrographic and electrical analyses were carried out. The electrical data indicated the presence of 8 ppm of the unknown n-type impurity. No impurity was detected by spectrographic analyses. Therefore, the impurity is either indium, antimony, or a foreign element whose spectrographic detection limit is at rather high concentration. A possibility which was considered is selenium since it has a relatively high detection limit and is known to be an n-type impurity in InSb. In view of these facts, activation analyses for selenium were obtained on specimens with known concentrations (calculated from Hall coefficient data) of the unknown n-type impurity. However, results did not confirm selenium to be the impurity in question.

Spectrographic analyses on the indium of 99.97+ per cent purity revealed zinc, copper, lead, and tin as the major impurities. Since no zinc had been detected in the antimony, indium purification was studied.

As-received indium of 99.97+ per cent purity, indium further refined by electroplating, and indium further refined by zone-melting were used in the preparation of InSb ingots. The effects of the indium purification on the concentration of zinc in zone-refined InSb ingots are shown in Figure 1. These results indicate that either indium purification technique is effective in removing zinc from indium. The effect of indium purification on the concentration of the n-type impurity is shown in Figure 2. It is seen that further purification of indium either by electroplating or by zone-melting results in a considerable reduction in the concentration of the n-type impurity. All data reported in Figure 2 are from region 1 of extensively zone-refined ingots. The mobilities at 80°K of the specimens in Figure 2 vary from 500,000 $\frac{cm^2}{volt\text{-}sec}$ to 40,000 $\frac{cm^2}{volt\text{-}sec}$ in a consistent manner with increasing impurity concentration. The distribution of the n-type impurity after 40 zone-melt passes does not differ greatly from the distribution after 50 zone-melt passes.

An ingot of high-purity InSb (total impurity concentration 10^{15} cm^{-3}) was doped with 2.6×10^{18} cm^{-3} zinc atoms. After five zone-leveling passes, the distribution was as shown in Figure 3. The carrier concentration varied from 1.7×10^{18} cm^{-3} to 3.1×10^{18} cm^{-3}, indicating that each zinc atom had contributed one hole. The distribution of the zinc atoms after five zone-melt passes is shown in Figure 3. Thus, it

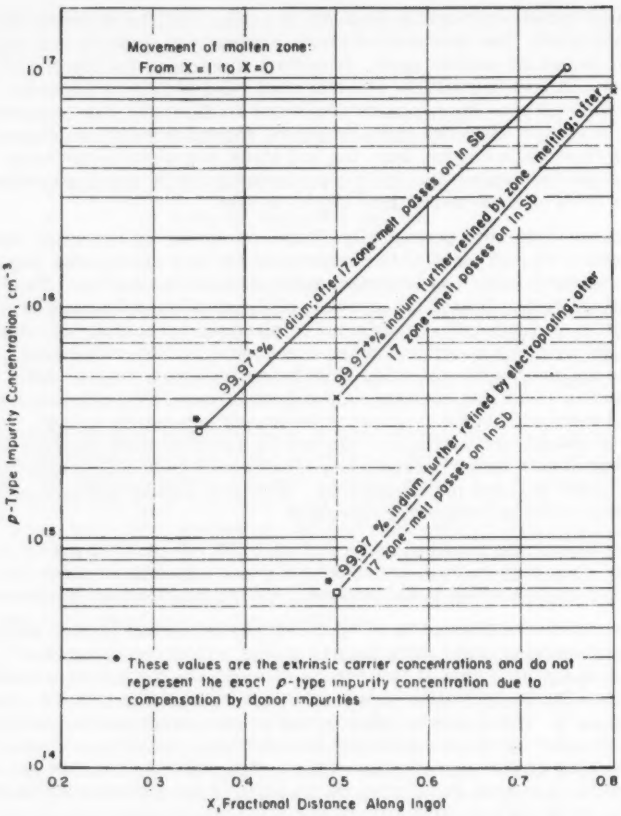
Movement of molten zone:
From X=1 to X=0
99.97 % indium; after 17 zone-melt passes on In Sb
99.97 % indium further refined by zone melting; after 17 zone-melt passes on In Sb
99.97 % indium further refined by electroplating; after 17 zone-melt passes on InSb
These values are the extrinsic carrier concentrations and do not represent the exact p-type impurity concentration due to compensation by donor impurities
p-Type Impurity Concentration, cm⁻³
X, Fractional Distance Along Ingot

Fig. 1—Effect of indium purification on the concentration of the second most-slowly segregating impurity found in In Sb.

is further verified that zinc is the slowly segregating p-type impurity in InSb, with segregation coefficient greater than one.

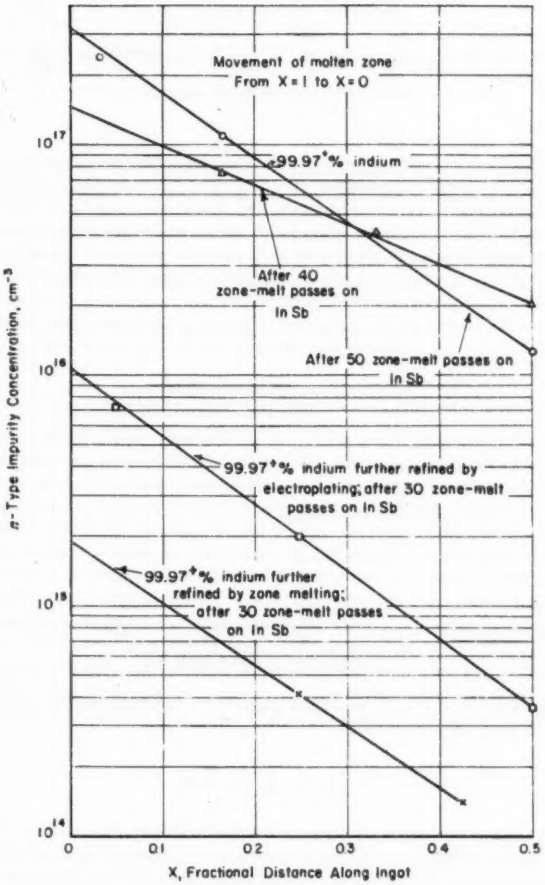

Fig. 2—Effect of indium purification on the concentration of the most slowly segregating impurity found in In Sb.

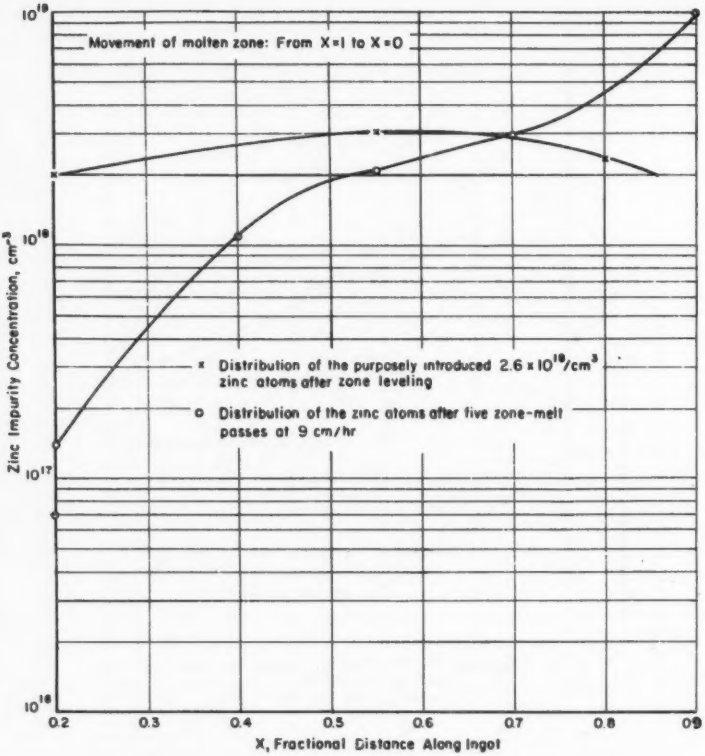

Fig. 3—Effect of five zone-melt passes on the distribution of zinc atoms in In Sb.

PHOTOEFFECTS IN InSb*

S. W. Kurnick, A. E. Goldberg, G. M. Mitchell, and R. N. Zitter
Chicago Midway Laboratories

InSb, when prepared in pure form and single crystal state, has appreciable injected carrier lifetimes. In addition, its photoresponses from liquid nitrogen to ambient temperature extend sufficiently far into the infra-red (5.5 to 7μ) to make it a useful detector material. A group of experiments revolving around P-N junctions, photoelectromagnetic (PEM) effects and photoconductivity will be described in this paper, evaluating such properties of this material as wavelength cut-off, surface recombination speeds, bulk recombination time and minority carrier mobilities at liquid nitrogen temperature.

PREPARATION OF MATERIAL

Indium and antimony used in the preparation of this compound were obtained from the American Smelting and Refining Company and the Bradley Mining Company respectively. The antimony was further purified by repeated vacuum distillation and zone melting. After reaction of the constituents the compound was zone melted to the extent of some fifty zone passes. Zone melting acts to establish stoichiometry and also further segregate impurities. The number of passes seems high compared to those required for the purification of germanium but this is because the effective distribution coefficient is closer to unity. Acceptor impurities segregate with k = 1.2 and donors with k = 0.6. For purposes of crystal growth, zone-refined ingots were cropped and only the central portions were used. In the study of all photoeffects, single crystal material was used and was obtained by the Czochralski method.

P-N JUNCTIONS

P-N junctions are readily formed by pulling from the melt. Because of the normal segregation of acceptors toward the crystal being pulled, and the segregation of n-type impurities toward the melt, natural junctions may be formed. Although such junctions (when cooled to liquid nitrogen temperatures) display photovoltaic responses, the transition zone is not sharp and the rectification characteristics are weak. Sharper junctions are formed by selecting p-type crystals and n-type crystals, melting the former and dipping the n-type crystal into the

*This work was supported in whole by the United States Air Force under Contract #33 (038)-25913.

melt. The crystal is then pulled from the melt. When such a junction is cooled to about 77°K, it shows good rectification characteristics, (Fig. 1) and operated as a photovoltaic cell its spectral distribution (shown in Fig. 2) agrees well with the transmittancy data reported for InSb.[1] Photovoltaic cells such as these show a sensitivity of some 10 volts/watt/cm².

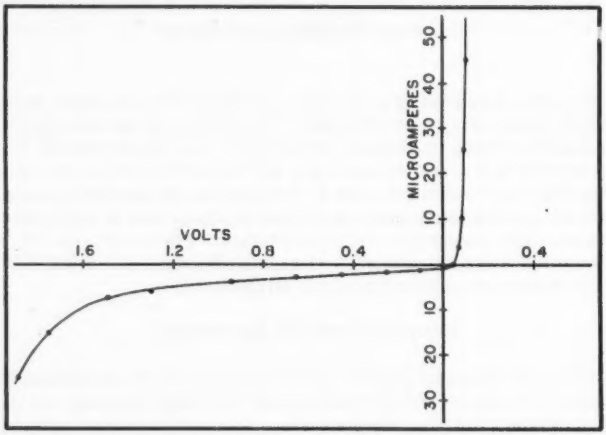

Fig. 1—Voltage-current characteristic of InSb p-n junction at 77°K.

PEM AND PC RESPONSE

Studies of the PEM effect have been made previously on Cu_2O, PbS, Si and Ge.[2-7] Measurement of this effect in p-type and intrinsic InSb with their large electron mobilities permits the determination of both the bulk lifetime and the surface recombination speed, which is dependent on the state of the surface. In p-type material, furthermore, the PEM effect may be used to estimate the bulk minority carrier mobility.

To interpret the PEM effect in p-type InSb (at liquid nitrogen temperatures) and the different behavior of electropolished from "mechanically" polished surfaces, a simple theory based on constant relaxation time is first derived. This theory differs from previous developments[8,9] in that an attempt is made to account for the PEM response in which μB is no longer restricted to values smaller than unity. To evaluate the PEM short-circuit current, the current generated with no electric field along the sample length, only the electrons will be considered because of the high ratio of electron to hole mobilities. The following relations are assumed to hold for the electron current in the bulk:

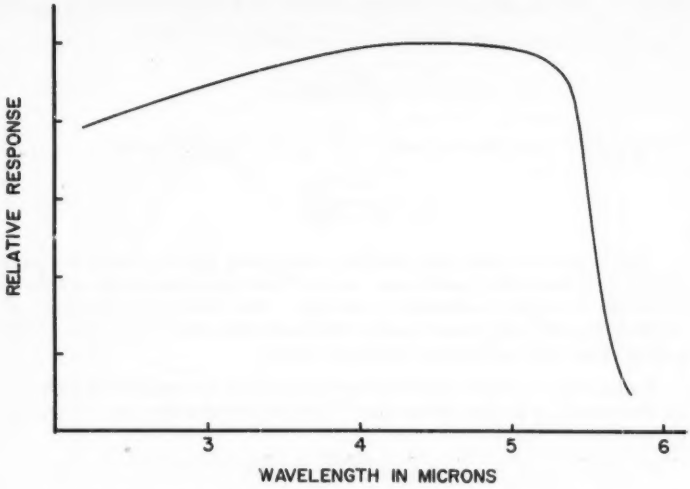

Fig. 2—Spectral response of p-n junction as a photovoltaic cell at 77°K. Relative response for given number of quanta at different wavelengths.

$$\vec{J}_e = eD\nabla n - \mu \vec{J}_e \times \vec{B} \qquad (1a)$$

$$\nabla \cdot \vec{J}_e = \frac{en}{\tau} \qquad (1b)$$

where $\vec{J}_e$ is the electron current density, $\vec{B}$ is the magnetic flux density, μ, τ, and D are the electron mobility, lifetime and diffusion constant respectively. The system of units used throughout is M.K.S. The following boundary conditions for the normal component of the current density are assumed to hold at the illuminated and non-illuminated surfaces respectively:

$$J_{e\perp} = -eI + esn \qquad (2a)$$

$$J_{e\perp} = -esn \qquad (2b)$$

where I is the illumination in quanta per second per unit area and ,s is the surface recombination speed. With both sample-length and -width large compared to the diffusion length, with the recombination speed s assumed independent of magnetic field, and with the production of hole-electron pairs by the light limited to the illuminated surface, the short-circuit current per unit sample-width, i_s, reduces to:

$$i_s = \frac{eI\mu B}{\sqrt{1+\mu^2B^2}} \cdot \frac{1}{1+\frac{\tau s}{L_D}\sqrt{1+\mu^2B^2}} \qquad (3)$$

where L_D is the electron diffusion length. If s is sufficiently large so that $\frac{\tau s}{L_D} >> 1$, the expression for i_s reduces to:

$$i_s = \frac{eI\mu B}{1 + \mu^2 B^2} \frac{D}{s} \tag{3a}$$

and if $\frac{\tau s}{L_D} << 1$ and the magnetic field is not unusually large,

$$i_s = \frac{eI\mu B L_D}{\sqrt{1 + \mu^2 B^2}} \tag{3b}$$

The behavior of (3a) with varying B suggests that i_s reaches a peak and is then reduced as more and more of the photo-electrons are turned back into the high recombination surface. With little or no surface recombination (3b) suggests that the short-circuit current reaches a saturation value with increasing magnetic field.

It is useful to carry out the PEM experiment in conjunction with a measurement of photoconductivity. The photoconductive short-circuit current is

$$i_{pc} = \frac{eI\mu E\tau}{1 + \frac{\tau s}{L_D}} \tag{4}$$

where E is the electric field. To determine the lifetime τ, the quantities $(\frac{B}{i_s})_o$ extrapolated to sufficiently small magnetic fields and $(\frac{i_{pc}}{E})$ are used.

$$\tau = D(\frac{i_{pc}}{E})^2 (\frac{B}{i_s})_o^2 \tag{5}$$

It is seen that this ratio-determination of τ does not depend on the exact evaluation of the light flux intensity. The PEM and PC currents from p-type samples at liquid nitrogen temperature which have been first "mechanically" polished and then electrochemically polished are shown in Fig. 3. For the "mechanically" polished samples, the variation of $\frac{B}{i_s}$ with B^2 is shown in Fig. 4. The plot is consistent with equation (3a). Similarly, the data for an electropolished sample is plotted $(\frac{B}{i_s})^2$ vs. B^2 consistent with equation (3b) (see Fig. 5). The following table gives a resume of the derived values for the different polished surfaces.

The consistent data above derived from a constant relaxation model, is not to be construed as verification of such a model for p-type InSb. The short circuit current may be derived using Rutherford scattering[10] for describing impurity ion scattering. The relaxation time varies as $\tau \propto v^3$ and the PEM current for $\frac{\tau s}{L_D} << 1$,

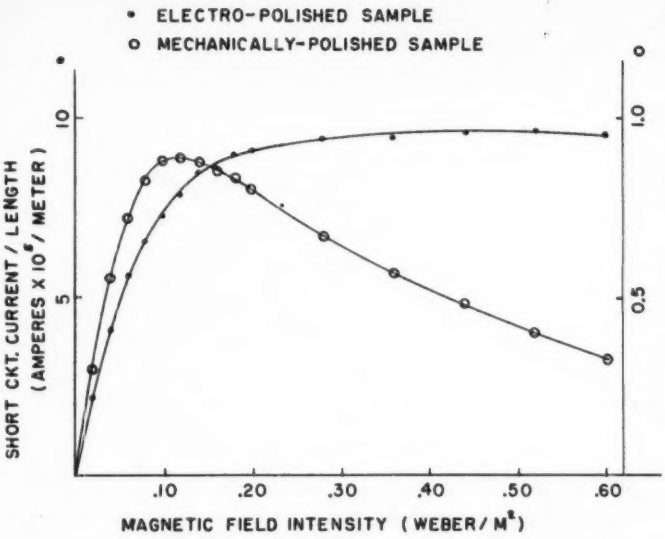

Fig. 3—PEM response vs magnetic field intensity for p-type InSb first mechanically, the electrolytically polished. Electropolished sample current approximately ten times greater than mechanico-polished sample current.

$$i_S = \frac{eIL_D}{\sqrt{6}} \gamma^{\frac{1}{2}} \frac{K_4}{K_1^{\frac{4}{3}}} \tag{6}$$

where $\gamma = \frac{\pi}{64} \mu^2 B^2$

and $$K_1 = \int_0^\infty \frac{x^3 e^{-x} dx}{1 + \gamma x^3} \tag{7}$$

$$K_4 = \int_0^\infty \frac{x^{\frac{9}{2}} e^{-x} dx}{1 + \gamma x^3} \tag{8}$$

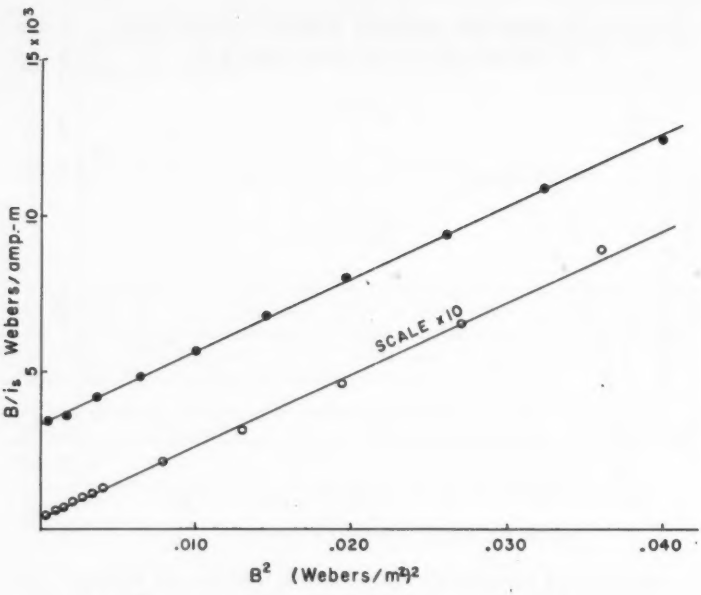

Fig. 4— $\frac{B}{i_s}$ vs B^2 for mechanically polished surface for both large and small magnetic fields; upper line for smaller magnetic fields.

TABLE 1

P-TYPE SAMPLE AT 77°K

$P_0 = 4 \times 10^{15}\,cm^{-3}$

	Mechanically Polished	Electro-polished
lifetime τ (sec)	9×10^{-8}	9×10^{-8}
minority mobility m^2/volt-sec	9	11
$\frac{\tau s}{L_D}$	10	<1
s m/sec	$\sim 10^4$	<100

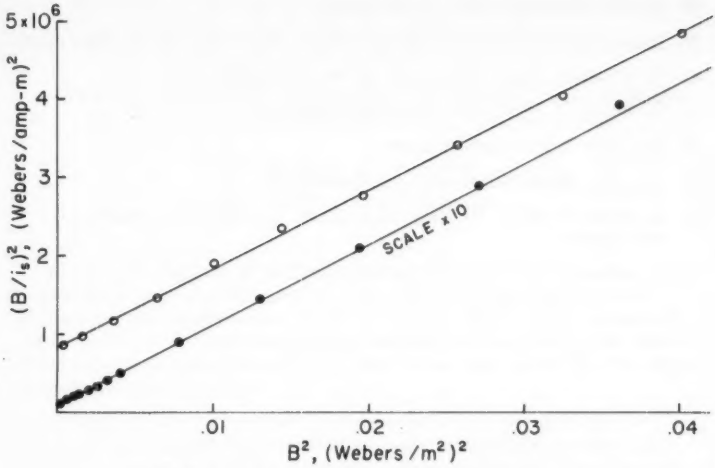

Fig. 5—$\left(\frac{B}{i_s}\right)^2$ vs B^2 for electrolytically polished surface for both large and small magnetic fields; upper line for smaller magnetic fields.

SUMMARY

Surface conditions in p-type InSb at liquid nitrogen temperatures influence the magnitude of photoconductive and PEM responses and strongly alter the variation of the PEM response with magnetic field; the response of "mechanically" polished samples exhibit a peak-value with increasing magnetic field, while the response of electrolytically polished samples reaches a saturation value.

A simple theory using the concept of surface recombination speeds has been developed to analyze these effects. Values of minority carrier (bulk) lifetimes and mobilities obtained from "mechanically" polished samples are consistent with the values from the same samples after electropolishing. In addition, the theory may be used to estimate surface recombination speeds.

References

1. Avery, Goodwin, Lawson and Moss, Proc. Phys. Soc. B, 67, 761 (1954)

2. I. K. Kikoin and M. Naskov, Phys. Zeit. fur Sov. Union, 5, 586 (1934)

3. P. Agrain and H. Bulliard, Comptes Rendus, 236, 595, 672, (1953)

4. H. Bulliard, Ann. Phys. 9, 52 (1954)
5. Moss, Pincherle and Woodward, Proc. Phys. Soc. B, 66, 743 (1953)
6. T. S. Moss, Proc. Phys. Soc. B, 66, 993 (1953)
7. H. Bulliard, Phys. Rev. 94, 1564 (1954)
8. loc. cit., Agrain and Bulliard
9. loc. cit., Moss, Pincherle and Woodward
10. E. Conwell and V. F. Weisskopf, Phys. Rev. 69, 258, (1946), 77, 388 (1950)

Abstract Number 99

EFFECT OF IMPURITIES ON PHOTO-CONDUCTIVE CADMIUM SULFIDE, CADMIUM SELENIDE AND LEAD SULFIDE

W. B. Hugle and F. Hugle

The Baldwin Piano Company

Films and crystals of cadmium sulfide and cadmium selenide were prepared in order to demonstrate the effect of impurities on their photo-sensitive properties. Photo-conducting films prepared according to the chemical and evaporative techniques described in the literature for the preparation of lead sulfide were also tested for the effect of impurity concentration.

PbS films* were prepared by the method of Gensel and Müser[1] in which a 4 Molar sodium hydroxide solution is added drop-wise to a solution composed of equal parts of a 0.35M lead acetate solution and a 0.20M thiourea solution. Carefully controlled temperature, stirring and concentration conditions must be used throughout.

Films of cadmium sulfide and cadmium selenide were prepared in three different ways. In the first method hydrogen selenide and hydrogen sulfide are reacted with cadmium to produce cadmium sulfide and cadmium selenide vapor which then condenses to form the photo-conducting films. This method is very similar to the Frerichs[2] vapor phase method of single crystal production except that the substrate temperature is adjusted so as to favor the formation of films rather than monocrystals.

In the second method cadmium sulfide and cadmium selenide films are formed by sublimation of the materials themselves.

Thirdly, cadmium selenide is produced by evaporating cadmium on a glass substrate. Subsequently, the cadmium metal film on the substrate is converted to cadmium selenide or by the passage of hydrogen selenide thru a heated tube in which the cadmium coating has been placed.

Single crystals of cadmium sulfide and cadmium selenide have been prepared by the method of Frerich's, by sublimation and by higher than atmospheric pressure bombs. Crystals of the latter type show a definite habit modification favoring the production of thicker crystals.

Our own X-ray diffraction data indicates the presence of a surface layer of some compound other than PbS but still within the Pb-O-S system.

IMPURITIES

Impurities were introduced into the photo-conductive films and crystals to determine their effect upon photo-sensitivities, time constants, and spectral sensitivities.

In the film method of Genzel and Müser, the cation impurities Tl, As, Sb, Al, Ce, Cr, Sn, Mn, Ag, Cu were introduced into the chemical solutions in the form of the soluble salts $TlNO_3$, As_2O_5, $SbK(C_4H_4O_6)_2$, $Al_2(SO_4)_3$, $Cr_2(SO_4)_3$, $SnCl_2$, $Mn(C_2H_3O_2)_2$, $AgNO_3$, $Cu(C_2H_3O_2)_2$, $Ce(NO_3)_3$.

Several alternative methods for the introduction of impurities into cadmium sulfide and cadmium selenide were used. Basically these methods involve the direct introduction into the sample of weighed quantities of impurities or careful control of the impurity vapor pressure during the film formation.

TEST METHODS

Samples were tested from -190°C to 100°C Electrodes of silver, gold, platinum and aquadag were used on the films.

Chopper frequencies of between 30 and 150 cycles per second were employed in the time constant measurements.

Noise measurements were carried out on all samples using a band pass filter with a band width of 4750 cycles/sec. (between 250 and 5000). All photo-sensitivity measurements (except where specified otherwise) were made with a 2500°K Tungsten light source at 8 inches.

RESULTS

The results of these measurements on cadmium sulfide and cadmium selenide showed that any one of the following "activators" Zn, Cu, In, Ag, As, Mn, Cl, Br, I and O may act to enhance photosensitivity and in addition non-stoichiometic ratios may themselves produce "self-activation." But, the impurity "activators" in cadmium sulfide and cadmium selenide produce different results, e.g. CdS:Mn gives the shortest time constants, CdS:In has high dark current characteristics. Light to dark ratios of more than 100,000 to 1 have been observed in CdSe:As using a Tungsten light source with 800 ft. candles of illumination on the sample. Light resistances as low as 10,000 ohms per square for CdSe:As have been obtained under similar test conditions.

The results with the "lead sulfide" method of Müser & Gensel were of an entirely different nature namely practically none of the ten elements tested enhanced the photo-conductivity. One of the elements definitely "poisoned" the photo-conductivity in all cases, namely, Thallium. This corroborates the evidence of Bruckman,[3] although he states that only a 10% decrease in detector action occurred whereas ours was complete over a wide range of concentrations. Manganese was shown to increase the resistance of the photocells and antimony

inhibited the deposition of the films.[4]

Stirring of the solutions reduced the resistance, but also the sensitivity.

Additional platings reduced the sensitivity indicating that with our films and with the light spectrum we used, the photosensitivity was primarily a surface phenomena. Photo-sensitivity was inversely proportional to the time in the bath after the completion of the reaction indicating excessive oxidation may have occurred under these circumstances.

After treatments with heat ammonium poly-sulfide and hydrogen peroxide did not improve the sensitivity of the better films (30-1, light to dark ratios at 1000 ft. candles and at ambient temperature) although heating at 100-400°C and hydrogen peroxide treatments did improve sensitivity of the poorer films (2-1 light to dark ratios at room temperature). Light to dark ratios of 30-1 were about maximum obtained for PbS at room temperature with light resistances ranging from 100 megohms to 100K per square.

References

1. Z Physik 134, 419-24, (1953)
2. R. Frerichs Phys. Rev. 72, 594-601 (1947)
3. Gerhard Bruckman Kolloid Z 65, 148-161 (1933)
4. Bruckman, ibid, states Antimony improves the film deposition.

Abstract Number 100

EXPERIMENTS ON THE FORMATION OF ANODE FILMS ON InSb

J. F. Dewald

Bell Telephone Laboratories, Inc.
Murray Hill, N. J.

In the course of some other experiments with the semiconducting compound, InSb, we have recently found that tightly adherent, highly colored anode films can be formed on this material which have properties quite similar to those which may be formed on metals such as tantalum and aluminum. In the past few years a sizable effort has been made by many workers, to achieve a detailed understanding of the mechanism of formation of anode films generally. Several ambiguities have arisen in the theoretical interpretation of the experimental observations which seem unresolvable by further study of simple metal systems. The present study was undertaken as an attempt to resolve some of these ambiguities by use of the additional degree of freedom implicit in the binary nature of the indium antimonide system. This system seemed to be a particularly appropriate one since we had available to us single crystals of high purity material and since the crystal structure of the compound was such as to high-light the effects under investigation.

One of the principal ambiguities in the interpretation of the results of the work on simple metal systems is the location of the rate determining step in the process. The theory of the high-field formation process was first proposed by Cabrera & Mott. They considered that the rate determining step in the process occurs at the metal-oxide interface. This would imply that rate of film formation on any given metal should depend upon the crystallographic orientation of the surface being oxidized. Charlesby and his co-workers have looked for such an orientation effect in the formation of films on aluminum; their apparently negative result implies either that the potential energy parameters do not differ much from face to face on aluminum or that the rate determining step in the process is located somewhere else than at the metal-oxide interface.

The structure of aluminum makes it difficult to choose between the above alternatives, since the energy differences between faces are not expected to be very large. In the InSb system on the other hand we anticipate fairly sizable differences between faces in view of the largely directional and chemical character of the forces holding the surface atoms to the crystal. We have studied the kinetics of formation on three faces; 110, and two others which we believe to be 332 and $\bar{3}32$.

The assignment of the 332 and $\bar{3}32$ faces is ambiguous in two

respects. In the first place the two faces differ only in the chemical bonding of the surface atoms, not in their location. Thus standard x-ray techniques cannot distinguish between the two. One may visualize these faces as "stepped" 111 and $\bar{1}11$ faces. They differ essentially in that on one of them all surface antimony atoms are singly bonded, all indium atoms triply bonded, while on the other, just the reverse type of bonding exists. In going from the diamond to the zinc blende structure the four-fold 100 axis is transformed to a four-fold inversion axis. A second difficulty arises from the fact that the goniometric data yield information only on the microscopic surface condition not on the submicroscopic condition which determines the kinetic behavior. The assignment 332 is to be taken as a tentative one. The problem is discussed in some detail.

The indium antimodide specimens were in the form of single crystals grown from zone refined material. The normal habit of crystals pulled in the 100 direction shows principally the 110 and 332 faces. When an entire crystal is oxidized anodically the variation of the interference colors from face to face gives immediate demonstration of the positive orientation effect. For the systematic study of the process the single faces were prepared by cleavage in the case of the 110 face and by crystallographic etches for the other faces. Capacitance, colorimetric, and analytical measurements were employed for the determination of relative film thickness.

The results are in striking accord with the theory of space charge effects previously presented by the author. The Tafel plots (E vs ln i) are linear at low current density and the rate of formation (at constant field) is strongly dependent on the crystallographic orientation of the face. One of the 332 faces (presumably the one with antimony atoms 3 bonded) forms at a rate some hundred-fold greater than the other two faces. This then implies quite strongly that at low current density the rate determining step is located at the metal-oxide interface.

At high rates of formation we find that the Tafel plot exhibits a very sizable upward curvature of a magnitude comparable to that predicted on the assumption of a significant space charge in the film. Coincident with this, as the current density is raised the crystallographic orientation of the face being oxidized becomes progressively less important until eventually at the highest current density all faces form at the same rate. We conclude that the rate determining barrier at high current density is no longer at the metal-oxide interface. If we retain the hypothesis of interstitial ion migration, we are forced to conclude that the rate determining barrier at high current density is located <u>inside</u> the film and that thus space charge effects are significant.

Microchemical analyses of films formed under a variety of conditions are reported. The films are found to dissolve slowly and uniformly (as determined by interference color) in dilute tartaric acid. Use has been made of this fact to obtain the layer by layer distribution of indium and antimony thru the film. The analytical results give additional insight into the mechanism of film formation. The electrolyte

employed in all the work reported here, (KOH), was one which would dissolve any antimony arriving at the oxide-electrolyte interface unless the rate of dissolution were so slow compared to the rate of oxidation that the antimony could be covered up by a subsequent indium atom. In this same electrolyte pure antimony will not "form up" at all. The experimental result is that at any current density the molar antimony-indium ratio is constant in the body of the film with a value approaching unity at very high rates of formation. At intermediate current density the ratio drops off in accordance with the interstitial ion mechanism. However, at very low current density the antimony to indium ratio appears to rise again. This very definitely is not in accord with the simple interstitial ion model. Some hypotheses regarding this behavior are discussed.